ASSESSING THE NATURE OF RAINFALL VARIABILITY ON HYDROLOGICAL RESPONSE IN MAYURAKSHI RIVER BASIN UNDER CHANGED CLIMATE SCENARIO

A thesis submitted towards partial fulfillment of the requirements for the degree of

Master of Engineering in

Water Resources and Hydraulic Engineering Course affiliated to

Faculty of Engineering & Technology, Jadavpur University

Submitted By

SANKALITA ROY

Examination Roll No.: **M4WRE22023**

Registration No.: **154663 of 2020-2021**

Under the guidance of

Prof. Dr. PANKAJ KUMAR ROY

Director & Professor

School of Water Resources Engineering,

Jadavpur University

School of Water Resources Engineering

M.E. (Water Resources and Hydraulic Engineering)

Course affiliated to

Faculty of Engineering and Technology,

Jadavpur University

Kolkata – 700032, India

M.E. (Water Resources and Hydraulic Engineering) Course affiliated to

Faculty of Engineering and Technology

Jadavpur University

Kolkata – 700032, India

CERTIFICATE OF RECOMMENDATION

This is to certify that the thesis entitled "**ASSESSING THE NATURE OF RAINFALL VARIABILITY ON HYDROLOGICAL RESPONSE IN MAYURAKSHI RIVER BASIN UNDER CHANGED CLIMATE SCENARIO"** is bonafide work carried out by Sankalita Roy under our supervision and guidance for partial fulfillment of the requirements for the Post Graduate degree of Master of Engineering in Water Resources & Hydraulic Engineering during the academic session 2020-2022 in the department of School of Water Resources Engineering, Jadavpur University, Kolkata – 700032.

DIRECTOR
Prof. (Dr.) Pankaj Kumar Roy
School of Water Resources Engineering
Jadavpur University
Kolkata – 700032

THESIS ADVISOR
Prof. (Dr.) Pankaj Kumar Roy
School of Water Resources Engineering
Jadavpur University
Kolkata – 700032

DEAN
Faculty of Interdisciplinary Studies, Law & Management
Jadavpur University
Kolkata – 700032

M.E. (Water Resources and Hydraulic Engineering) Course affiliated to
Faculty of Engineering and Technology

Jadavpur University

Kolkata – 700032, India

CERTIFICATE OF APPROVAL**

This foregoing thesis is hereby approved as a credible study of an Engineering subject carried out and presented in a manner satisfactorily to warranty its acceptance as a prerequisite to the degree for which it has been submitted. It is understood that by this approval the undersigned do not endorse or approve any statement made or opinion expressed or conclusion drawn therein but approve the thesis only for the purpose for which it has been submitted.

Committee of final examination for theevaluation of the thesis

_____

_____

_____

** Only in case the thesis is approved.

Declaration of Originality and Compliance of Academic Ethics

I hereby declare that this thesis contains literature survey and original research work by the undersigned candidate, as part of my Master of Engineering degree in Water Resources & Hydraulic Engineering , Jadavpur University during the academic session 2020-22.

All information in this document has been obtained and presented in accordance with academic rules and ethical conduct.

I also declare that, as required by these rules and conduct, I have fully cited and referred all materials and results that are not original to this work.

Name : **SANKALITA ROY**

Roll No : **M4WRE22023**

Thesis Title : Assessing the nature of rainfall variability on hydrological response in mayurakshi river basin under changed climate scenario.

Date:

Place: S.W.R.E, Jadavpur University

SANKALITA ROY

ACKNOWLEDGEMENT

I express my sincere gratitude to my supervisor Prof. (Dr.) Pankaj Kumar Roy, Director & Professor, School of Water Resources Engineering, Jadavpur University under whose supervision and guidance this work has been carried out. I am deeply indebted to him for his valuable suggestions, inspiring guidance and continuous help, which made possible the completion of the present work. It would have been impossible to carry out this thesis work with confidence without his wholehearted involvement, advice, support and constant encouragement throughout.

I also express my sincere gratitude.Prof. (Dr.) Asis Majumdar,SWRE, Jadavpur University;Prof. (Dr.) Arunabha Majumder,Professor- Emeritus, SWRE, Jadavpur University;Dr. Rajib Das, Assistant professor, SWRE, Jadavpur University,Dr. Subhasish Das, Assistant Professor, SWRE, Jadavpur University; Dr. Gourab Banerjee, Assistant Professor, SWRE, Jadavpur University for their valuable suggestions.

I would like to express my special thanks my lab seniors Swetasree Nag,Sudipa Halder,Arnab Ghosh for their care,affection and encouragement,throughout my research work.

I wish to express my gratefulness to my batch mates Sayak and Pratik for their constant and meticulous encouragement.

Thanks are also due to all the faculties and staffs of School of Water Resources Engineering Jadavpur University for their direct and indirect help and support.

_____

Date: SANKALITA ROY

Place: JADAVPUR UNIVERSITY Roll No.: **M4WRE22023**

DEDICATION

This thesis is dedicated to my parents and my respected teachers, who never stopped encouraging me throughout this endeavor and constantly inspired me for keeping me on my toes and encouraged me to never stop learning.

ABSTRACT

Climate Change has become a widely discussed topic world wise. The adverse effects of changing climate on hydrological processes and water resources have received much attention. During the period 2000-2015, there have been significant changes in precipitation in India compared to the last 100 years. This is a sign of climate change in India. A comprehensive and detailed understanding and clear assessment of the impact of climate change on India's water resources is important to reach definitive conclusions. In this present study, spatial-temporal rainfall trends & variability assessment as well as hydrological modelling was done to assess the rainfall variability on hydrological response under change climate scenario. The rainfall variability was analysed by Coefficient of variation(CV),Precipitation concentration index(PCI) & Standard anomaly index(SAI). The rainfall trends were evaluated using the Mann-Kendall(MK),Sen's slope estimator(SSE)and the ITA method which is a latest technique to detect trends and for hydrological modelling arc SWAT had been used with SUFI 2 algorithm. Highest rainfall was found in monsoon in all rainfall stations and high variability of rainfall was seen in the winter season. The ITA approach is more accurate in recognizing several hidden significant rainfall trends. The hydrological model was calibrated with observed river discharge data for 2011-2013 and validated for 2014-2016,2008-2013 was the warm up period. the values of statistical parameters(R^2, NSE, and PBIAS) which had been used for evaluating the SWAT model performance analysis where are 0.56,0.61 and -7.9 respectively and in the case of validation, the values are 0.63,0.66, and -14.2 respectively. Based on the calibration and validation findings, the model satisfactorily simulated the streamflow which was observed in the Mayurakshi River Basin. The calibrated model might be used to assess the impact of climate change as well as LULC on water resources in the upcoming days. the findings of this study may be used to plan and manage water resources, as well as analyse and manage the effects of climatic risks such as floods & droughts.

TABLE OF CONTENT

CHAPTER 1: INTRODUCTION

There is a substantial increase in the climatic extremities,including heavy rainfall events and extreme hot days in the past few decades(Alexander,2006;Vose,2005).Climate Change has become a widely discussed topic worldwise.Unusual rainfall pattern has significant effect on water resources, agricultural output and hence economy (Oza M.,2014). The adverse effects of changing climate on hydrological processes and water resources have also received much attention (Gleick, 1986; Burn,1994).Assessment of water availability and its evolution in river basins is important to allocate limited water supplies to different sectors and developing strategies for sustainability of water usage. (Abeysingha,2015).In addition, to frame appropriate policies for the fair and efficient use of limited water resources,the water resources of river basins / small basins should be estimated in a spatially and temporally explicit manner(Abeysingha,2015).The IPCC predicted a temperature rise of 2.7-4.3°C across India by the 2080s(IPCC 2007). It is predicted that average temperatures may rise by 3-5°C by the end of this century.During a short time span, not only hydrological systems are expected to experience changes in average water availability, but also extreme event changes (Grillakis,2016; Jiang,2007; Modrick,2015; Piras,2016). Rainfall in India is expected to increase by about 20% by the end of this century. (IPCC 2014).Many studies focused on the analysis of climate change and the impact of change on various elements of the water cycle (Sonali P.,2012).By recent studies, it has been observed that significant warming in the second half of the 20th century resulted in a drastic shift in the hydrology of an agrarian country like India (Sonali P.,2012). The past thirty years have experienced most increase in temperature during pre monsoon months (March to May) while heavy rainfall events have increased by 50% in central parts of India (Goswami,2006).The Indian monsoon rain simulation is very sensitive to initial conditions, so some integration methods suitable for seasonal forecasts need to be developed (World Climate Research Program,1992).The effects of climate change are expected to have varied range of national and international impacts (Arora,2005).Information on these changes is very crucial for a variety of purposes at the global, regional and watershed level (Arora,2005).India in the 20th century has clear adverse evidences of climate change that will worsen in the 21st century(Goswami,2006).

1.1 Climate

Climate is a characteristic state of the atmosphere surrounding the surface of the earth. Temperature and precipitation are the main deciding factors that determine the climate of a region. However, the IPCC defined climate as long-term average weather (IPCC 1992). This includes precipitation, temperature, pressure, humidity, wind, and various other meteorological factors in a particular region (IPCC – 2007b) over a long period of time.

1.2 Climate change

Climate change is an unavoidable consequence of the Earth's evolution from ice.Natural and artificial factors determine climate change in a place or region. Natural factors such as the atmosphere, hydrosphere, geosphere, and biosphere, as well as human factors such as land and its use cause local, regional, and even global climate change. This is a pervasive crisis in terms of health and safety, economy and food security.

1.2.1 Impact of Climate change

Much research has been going around the world to assess the impact of climate change on our future world. Many a times, it is associated with identifying and assessing the potential for human allostasis to climate change. The most affected are people directly involved in agriculture and the use of water resources. Climate change has a direct impact on people's lives, especially people residing in rural areas.The impact of climate change on different areas of society is interrelated. Drought can affect both food production and human health. Floods can spread illness along with harming the ecosystems and infrastructure. Human health problems may increase mortality, affect

food availability and limit productivity of the manpower. The effects of climate change can be seen in every sphere of the world.

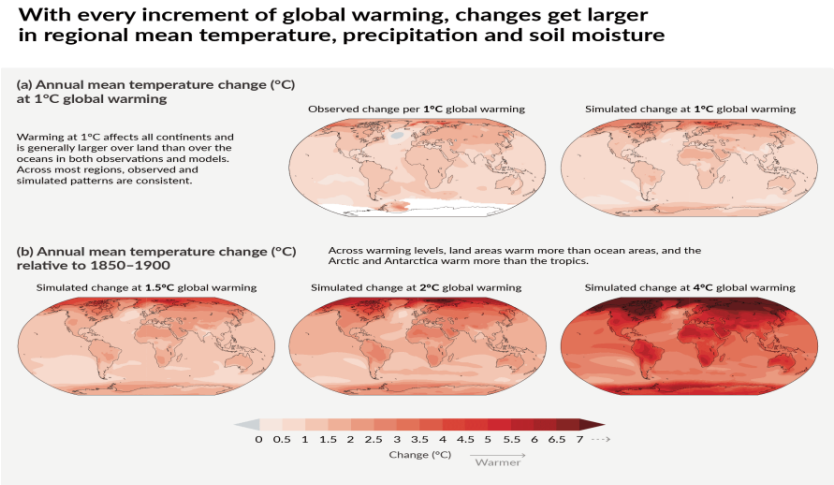

Fig 1.1 Impact of climate change(IPCC,2022)

1.2.2 Impact of climate change on water resources

Climate change can no longer be denied as its effects have become increasingly evident worldwide. Rising temperatures, melting of glacial ice at an alarming rate, farmlevel concerns on groundwater depletion and consequent water scarcity emerge from rising intersegment on deepening of tube wells, increasing the cost of irrigation due to the use of diesel, unexpected yield and income losses translating into food and livelihoods insecurity are clear evidences of global warming.

1.2.3 Impacts of climate change on water resources of India

The direct and indirect impacts of climate change adversely affect water resources, human systems, local agriculture and food security.Precipitation is highly skewed over space and time, with the highest precipitation areas in North-Eastern India (NE), in contrast to the Thar Desert in

western India. In India, there have been considerable variations in rainfall and temperature between 2000 and 2015, compared to the previous 100 years.

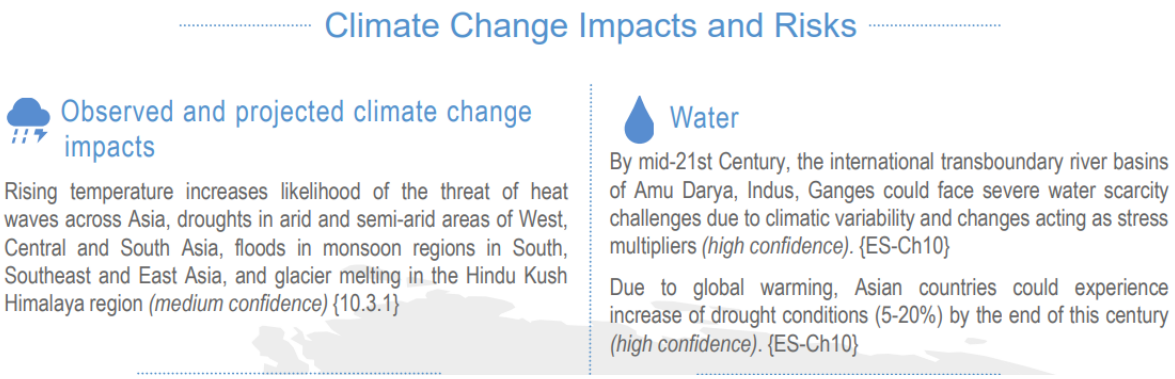

Fig 1.2 Climate Change Impact and Risks(IPCC,2022)

In India, this is an indication of changing climate. To establish conclusive findings, it is necessary to have a complete and detailed understanding of the impact of climate change on India's water resources, as well as a clear assessment of the impact of climate change on India's water resources.

The present study estimates the impact of climate change on rainfall through the hydrological modelling.The analysis has been performed to evaluate the impact of climate change on Mayurakshi River Basin. Evaluation procedures can be generated in the near future utilising simulation models, long-term projections, and early warning.Climate change impacts have direct consequences for water security and conflict.

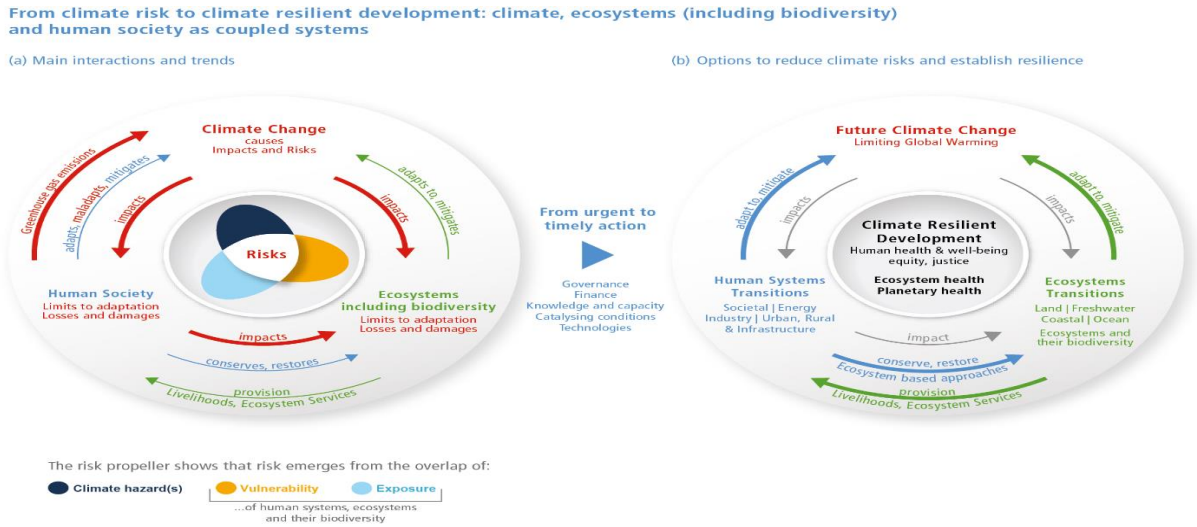

Fig 1.3 From climate risk to climate resilient development(IPCC 2022)

In order to achieve the Sustainable Development Goals, climate change adaptation may lead to climate resilience and it can be achieved through healthy ecosystem services that rely on well functioning of river basins.Effective country driven climate change adaptation should reflect the importance of water management in reducing vulnerability and building climate resilience.

In this regard, the research objectives are summarized as follows:

1.3 Objectives

- Spatial-temporal rainfall trend and variability assessment.
- To assess impact of climate change on the watershed by using arcSWAT model

CHAPTER 2: LITERATURE REVIEW

2.1 Literature review on spatial-temporal assessment

Arus Edo Harka, Nura Boru Jilo, and Fiseha Behulu (2021) investigated spatial-temporal rainfall trends and variability in Ethiopia's Upper Wabe Shebelle River Basin. They looked at seasonal and yearly rainfall patterns and trends, as well as the spatial distribution and variability of rainfall**.** The CV, PCI, and SAI were used to evaluate precipitation variability. They also used the Mann-Kendall test (MK) and the Sen Slope estimator to look at spatiotemporal trends (SSE). They applied the latest technology of ITA method for analyzing the rainfall clusters. They also discovered that the ITA approach is superior to the MK test in terms of detecting monotonic and non-monotonic trends that the MK method cannot identify. This study's findings are beneficial to UWSRB's water resource planning and management.

Alemu, M.M., Bawoke, G.T., (2019) studied on spatial variability and temporal trends of rainfall in the Amhara region, Ethiopia. Using time series rainfall data from the Climate Hazards Group Infrared Precipitation with Stations (CHIRPS) for the period 1981–2017, this study studied the regional distribution and temporal patterns of rainfall in the Amhara region. Rainfall variability and seasonality were assessed using the coefficient of variation, standardised anomaly index (SAI), precipitation concentration index (PCI), and seasonality index (SI). The Mann–Kendall test was also used to analyse rainfall trends. The findings revealed that the region has seen varying rainfall events, resulting in droughts and floods in different years. Inter-annual variability of rainfall with negative and positive anomalies was also observed in 59.46 percent and 40.54 percent of the investigated years, respectively. The PCI and SI data indicated that the rainfall distribution in the area was erratic and intense. During the research period, trend analysis revealed an overall rise in annual and seasonal rainfall (excluding winter). This study's findings could be used as a proxy for

rainfall variability and trend in the study area. The Mann–Kendall trend test and novel trend analysis were utilised in the analysis, with Sen's slope being used to quantify the magnitude of the changes.

Ali, R., Kuriqi, A., Abubaker, S., Kisi, O., (2019) investigated the long-term trends and seasonality detection of the observed flow in Yangtze River Using Mann-Kendall and sen's innovative trend method. The goal of this research is to see if there are any probable trends in the Yangtze River's annual, seasonal, maximum, and lowest flows at Cuntan and Zhutuo stations in China from 1980 to 2015. The study's findings revealed that at Cuntan and Zhutuo stations, there were increasing and decreasing tendencies in different months.

Indrani Pal (2009) dealt with the socio-economic impacts of discrete random extreme events due to climate change. According to Pal (2009) the risk of extreme events impact could be severe to extreme but these are difficult to predict. During the monsoon season in central India, an increase in extreme events has been documented. Kerala has experienced rainfall with return periods ranging from 10 to 50 years, according to the study.

Dave H. K. (2012) stated that annual rainfall is the only source of water in the targeted basin. This rainfall causes runoff and ground water recharge. The catchment Characteristics vary across the basinThe rainfall co-efficient of variance ranged from 41 to 63 percent. Drought conditions are present for an average of 40% of the time, with severe drought occurring for 10% or less of the time. This suggests that the area's odd hydrological behaviour is due to the non-uniform distribution and unpredictable nature of rainfall rather than a lack of rainfall.

Malik & Kumar (2019) Using an innovative trend analysis approach with a significance test, researchers analyzed at the spatio temporal trend analysis of seasonal and annual rainfall from 1966 to 2015. The spatial and temporal patterns of seasonal (pre-monsoon, monsoon, post-monsoon, and winter) and annual rainfall time series data (1966–2015) at 13 locations in Uttarakhand, India, are explored in this study. The temporal trend was examined utilising the newly suggested innovative trend analysis (ITA) method, which included a significance test. At a

significance level of 5%, the ITA method's results were compared to the Mann-Kendall (MK) test. In the ArcGIS 10.2 environment, the spatial variation of the trends in seasonal and yearly rainfall series was interpolated using the Thiessen polygon (TP) method. The comparison demonstrated that the trend recognised by the MK test can be efficiently identified using the ITA approach, and that the ITA method can detect several trends that the MK test cannot detect.

Khare, D., Tripathi, S.K., (2018) conducted a study on Spatiotemporal trend analysis of rainfall and temperature, and its implications for crop production. The goal of this work was to conduct a spatiotemporal analysis of seasonal and annual rainfall and temperature, as well as their consequences. The MK test, Sen's slope, and the precipitation concentration index (PCI) were used, as well as a Pearson correlation study of crop production and climate factors. The annual and seasonal rainfall trends were highly varied, and the minimum and maximum temperatures climbed by 0.8 and 1.1 degrees Celsius per year, according to the Mann–Kendall test results. In comparison to annual and winter season rainfall, the PCI result demonstrates that rainfall throughout the summer and spring seasons is moderately scattered. The area's rainfall pattern and distribution might be categorised as irregular and erratic based on these findings.

2.2 Literature review on hydrological modelling

The study by **Lakshmanan (2011)** aims to assess the impacts of climate change on hydrology and rice yield in the Bhavani Basin of India using the SWAT model. SWAT can be used as a decision support tool for structuring adaptation strategies such as changing agricultural methods by adjusting water and fertiliser management in a changing environment, according to the research. For an A1B scenario, the RegCM3 model using EH5OM GCM output was used to create climate change scenarios. The maximum and minimum temperatures in the RegCM3 model were slightly underestimated. The SWAT model was used to examine the impact on the river basin's hydrology and rice productivity for a continuous time span of 130 years using the daily climatic data obtained (1971-2100). Predicted rice yields for the Bhavani Basin were compared to observed rice yields in

Erode district, where the Bhavani Basin is located, over an 11-year period (1999-2009), and the results showed that the model performed well.

Boini Narsimlu,et al(2015) studied SWAT Model Calibration and Uncertainty Analysis for Streamflow Prediction in the Kunwari River Basin, India, Using Sequential Uncertainty Fitting. For hydrologic modelling, the KRB built up the Soil and Water Assessment Tool (SWAT), a semi-distributed physically based model. SWAT-CUP was utilised for model calibration, sensitivity, and uncertainty analysis using the Sequential Uncertainty Fitting (SUFI-2) technique. The model was calibrated for the years 1987–1999. After a three-year warm-up period (1987–89), the model was verified over the next six years of data (2000–2005). Two indices, the p-factor and the r-factor, were used to evaluate the model calibration and uncertainty competency. The p-factor and the r-factor were 0.82 and 0.76 after SWAT simulations, respectively, while the p-factor and the r-factor were 0.71 and 0.72 during validation. The goodness of fit was further tested using the coefficient of determination (R2) and the Nash–Sutcliffe efficiency (NS) between observed and validated values after a thorough calibration and validation. R2 and NS values found during calibration were 0.77 and 0.74, respectively, while verified values were R2 0.71 and NS 0.69, indicating satisfactory performance. The findings will be beneficial to the hydrological community, water resource managers active in agricultural water management and soil conservation, as well as those working to mitigate natural disasters like droughts and floods.

Tao Can *et al* (2015) assessed the impacts of different land use scenarios on water budget of Fuhe River, China. The Soil and Water Assessment Tool (SWAT) model was used to examine the effects of alternative land use scenarios on hydrological processes in the Fuhe watershed in the Poyang Lake Basin, East China. A total of 12 model parameters were calibrated and validated for baseline conditions using observed monthly runoff data from 1982 to 1988. Throughout the calibration and validation periods, baseline R2 and Nash-Sutcliffe model efficiency (NSE) values varied from 0.88 to 0.94, suggesting that SWAT accurately duplicated the Fuhe watershed streamflow.

Ashish Pandey *et al*(2021) studied on SWAT modeling approach to prioritize soil conservation management in river basin critical areas coupled with future climate scenario. The soil and water assessment tool (SWAT) model was used in their study to priorities crucial sites in the Tons river basin in central Indian states.

Sharlene L. Beharry *et al*(2021) estimated reservoir volume in the Upper Navet watershed in Trinidad using SWAT model. The model was built using the soil water assessment tool (SWAT). Using sequential uncertainty ftting, the sensitivity analysis, calibration, and validation were carried out in the SWAT calibration and uncertainty programme (SWAT-CUP) (SUFI-2). The anticipated volume of water flowing into the reservoir had six sensitive characteristics, according to the results. After validation, the model's performance for the Flow was adequate(R^2=0.91 and NSE=0.81). Validation results for Res Vol suggested satisfactory values (R^2=0.72 and NSE=0.70), with P- and R-factors of 0.80 and 0.64, respectively. The uncertainty for the Res Vol was deemed fair based on statistical measures. However, caution should be exercised while using the model during the dry season, as the simulated Flow In was frequently underestimated.

Das (2019) investigated the multisite performance of the SWAT model in India's Gomti River Basin. The basin was calibrated using monthly discharge data from 2002 to 2008, including a 2-year warm-up period from 2000 to 2001. The model was then verified using 5-year hydrometeorological datasets from 2009 to 2013 at two gauge sites.The initial curve number was discovered to be the most sensitive characteristic for moisture condition II (CN2). The p-factor and r-factor were 0.73 and 0.58 in the calibration period at Neemsar, respectively, while they were 0.79 and 0.51 at Lucknow, and 0.61, 0.45 and 1.22, 0.75 in the validation period.The performance of the SWAT model was evaluated using three statistical parameters: coefficient of determination (R2), Nash–Sutcliff efficiency (NSE), and percent bias (PBIAS). At two of the above-mentioned gauging stations, the NSE and R2 values were 0.85, 0.84, and 0.87, 0.86, respectively, during the calibration period, and 0.76, 0.76, and 0.79, 0.83, respectively, during the validation period. At the

same gauge location, the PBIAS values throughout the calibration & validation periods are -13.3, -14.7, and -4.0, -15.7 indicating good model performance.

Patil, Gaurav & Reddy (2019) Using a hydrological model, researchers assessed the impact of climate change on a watershed.This research employed the Soil and Water Assessment Tool (SWAT) to look at climate change in the Malaprabha sub-Basin.Due to insufficient R2 and NSE values, the model was implemented and calibration was performed from 1988 to 1998, followed by validation from 1999 to 2002. SWAT-CUP (SUFI-2) is a semi-automated programme that is used for calibration and validation. This research provides an idea of the magnitude of change that may occur in the study area in the following years, and these data can be utilised to construct water structures, watershed management, and crop pattern adaptability.

CHAPTER 3: STUDY AREA

The demonstration of the assessment is done on one of the major rivers which is in India, with a long history of devastating floods,the name Mayurakshi River.Mayurakshi literally means "peacock eyes". Mayurakshi floods the valley during the monsoons, even though it is named after the crystal-clear water of the dry season. It is a 5^{th}-order rainfed tributary of Bhagirathi. The Mayurakshi Basin forms the transition zone between the two geographically large provinces on the edge of the Chota Nagpur Plateau and the Bengal Basin is a well-known name in the West Bengal flood scenarios.Fig 3.1 shows the location map of the Mayurakshi River produced from Arc GIS.

3.1 Study Area

Mayurakshi River Basin (MRB) stretches from 23˚15′03″N to 24˚34′36″N latitude and 86˚ 58′17″E to 88˚15′52″E longitude spanning an area of 5154 km² in the states of Jharkhand and West Bengal (Fig. 3.1). Chotonagpur Plateau runs across the western half of the basin, which is mostly in the Dumka district of Jharkhand, while the Ganges Plain runs through the eastern section, which is mostly in the Birbum and Murshidabad districts of West Bengal.There are 16 rain raingauge stations in the study area as shown in the table 3.1.

LOCATION MAP

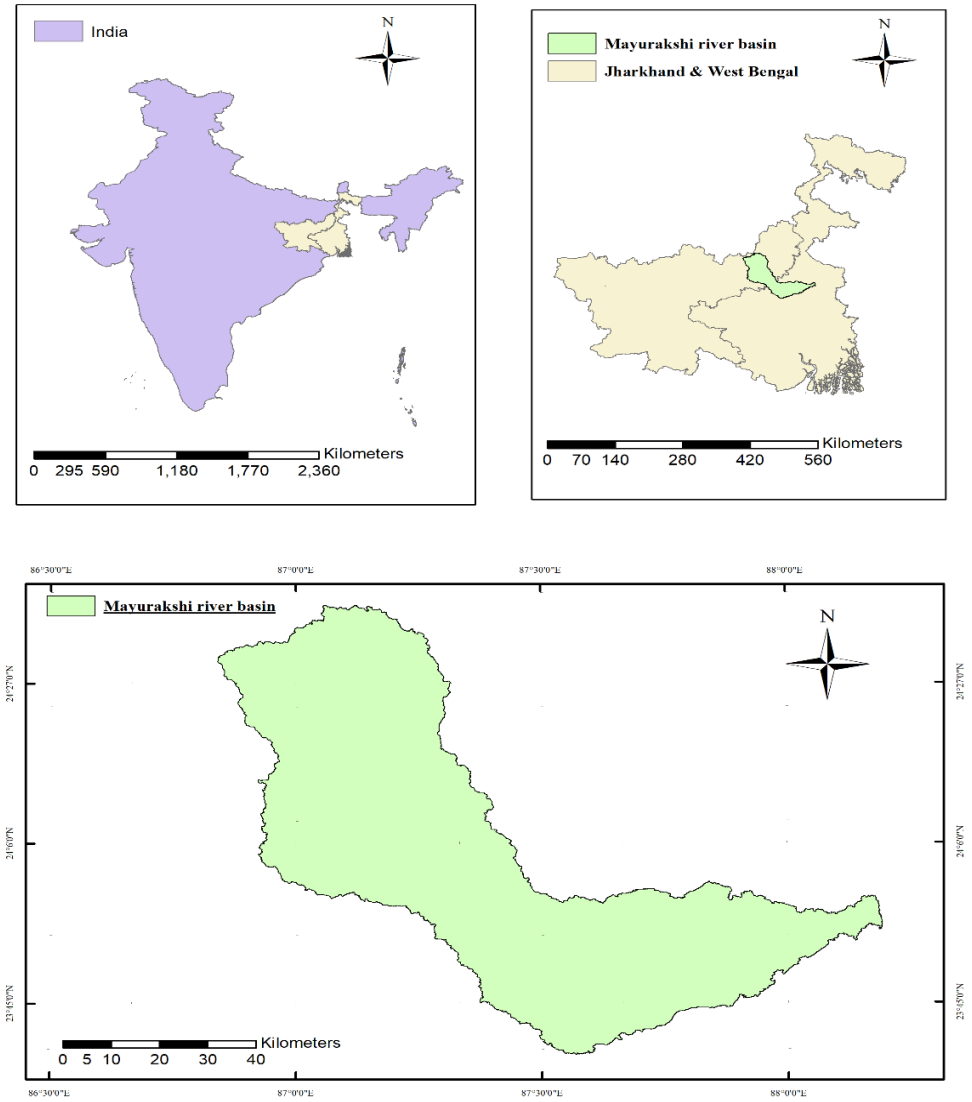

Fig 3.1 Location map of Mayurakshi River Basin, India

The average annual rainfall is recorded as 1428 mm. The coefficient of variation of annual rainfall over the basin is low and ranges between 13-15% and the average maximum and minimum temperatures reach about 32°C & 17°C. The data for the study includes various spatial data like DEM, LULC, Soil Map generated from SENTINEL 2 and prepared in ArcGIS on 1:12500 scale with the resolution of 30 m and several collateral data like weather files (from 1982 to 2021) from rain gauge stations & climate stations have been collected.

Table 3.1 Raingauge Staions and their location

Station	Latitude	Longitude
Tilpara barrage	23°55'18"N	87°30'48"E
Suri	23°53'33"N	87°30'04"E
Shyambati	23°41'20"N	87°40'54"E
Shekhampur	23°45'05"N	87°44'51"E
Sainthia	23°56'47"N	87°39'24"E
Narayanpur	24°01'35"N	86°36'39"E
Massanjore	24°06'19"N	87°18'34"E
Maharo	24°20'09"N	87°12'44"E
Kundahit	23°58'37"N	87°10'37"E
Kultore	23°22'27"N	86°46'12"E
Kirnahar	23°45'50"N	87°52'35"E
Kandi	23°57'23"N	88°03'32"E
Jama	24°21′58″N	87°15′53″E
Dumka	24°16'57"N	87°14'57"E
Bharatpur	23°53'03"N	88°05'01"E
Kuli	23°58'18"N	87°57'44"E

3.2.1 Physiography

The MRB contains a variety of topographic characteristics, with elevations ranging from 3 to 663 meters above the sea level.Physiographically, Mayurakshi river basin can be (broadly) divided into three units.

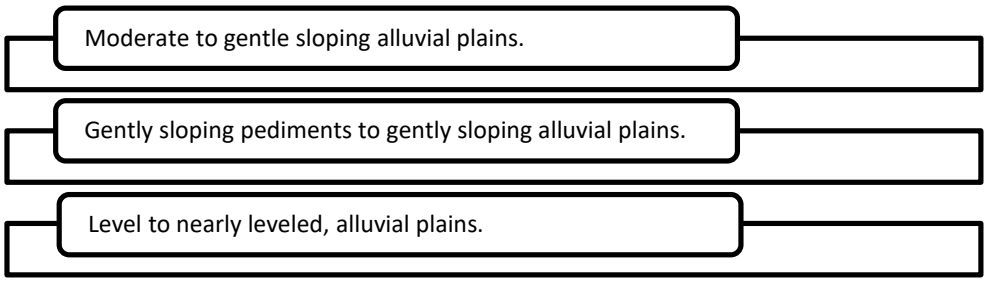

Table 3.2 Slope Classification

Slope (%)	Area (% of Watershed Area)
0-3	16.07
3-15	74.97
15-99	8.96

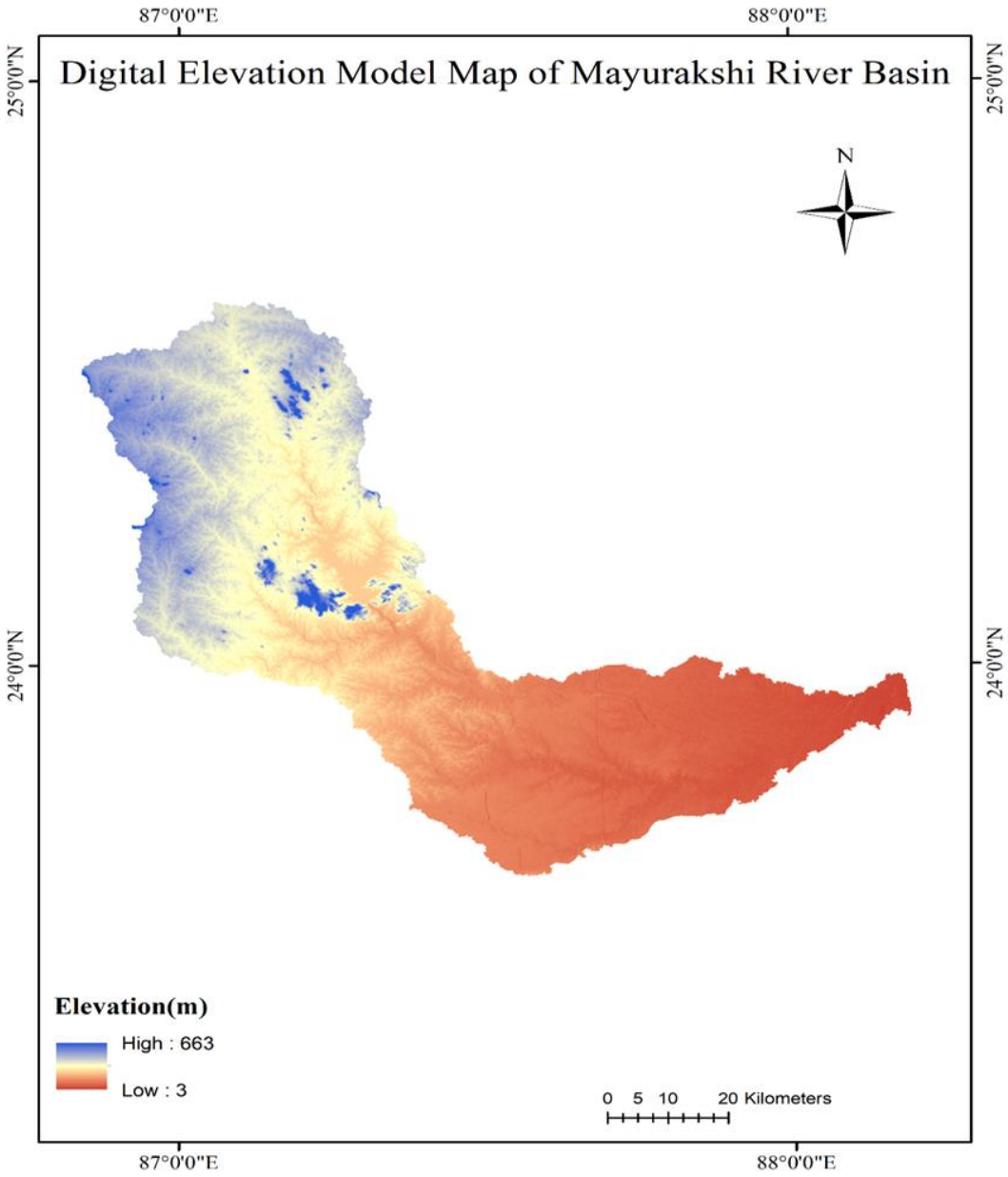

Fig 3.2 Digital Elevation Model of the study area

3.2.2 Hydrometeorology

Mayurakshi river basin has a Sub-tropical monsoon climate with 4 seasons, the monsoon (June to September), the Post monsoon (October to December), The winter (January, February), and The Pre-monsoon (March to May). The rainfall occurs mostly in the monsoon months (June to September).The average annual rainfall of Mayurakshi River Basin is 1428 mm.

3.2.3 Temperature

The average monthly temperature in the study area is shown in fig 3.3 The temperature normally fluctuates during pre-monsoon to post-monsoon periods.

After February,the temperature progressively rises and by the month of May and June it reaches maximum before the onset of the monsoon. On average maximum and minimum temperature reaches about 32°C & 18°C. The winter period is very pleasant with an average temperature of about 17°C in the month of December/January.

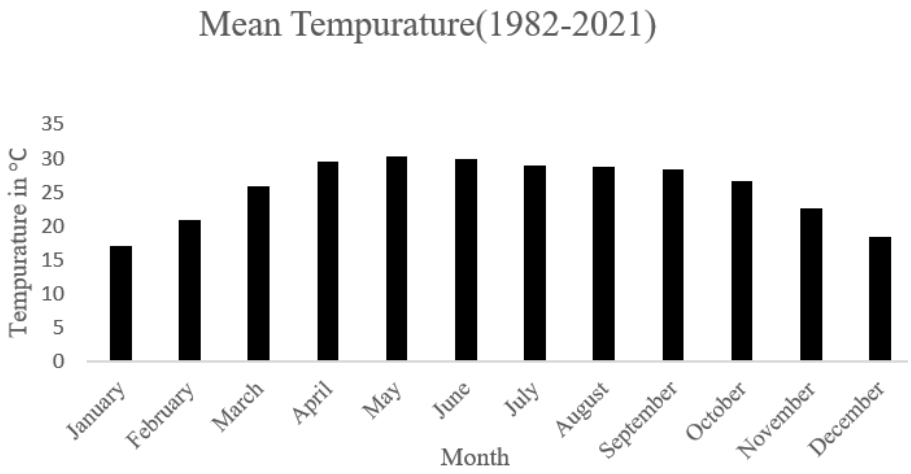

Fig 3.3 Average monthly temperature (°C) in the study area

3.2.4 Wind

In upper part of basin winds are generally light to moderate throughout the year.In the post monsoon, winter and summer season winds mainly blow from westerly direction. Towards the end of summer season winds blow from the easterly direction and this wind strengthens and predominates during monsoon season.

From April onwards, a southerly breeze blows in the middle of the basin. From May through September, the wind is mostly from the south or southeast. Winds blow primarily from the north or northeast between October and November. Westerly winds can also be found in February and March.

Winds are normally modest in the lower basin, with a minor increment during the summer and south-west monsoon seasons.

3.2.5 Relative Humidity

In the upper part of basin in the southwest monsoon months, air is generally humid with the relative humidity well above 80%. Air is generally mildly humid in post monsoon and winter season. The rest of the year, the relative humidity in the afternoon is generally lower than value in the morning. Summer is the driest season of the year, with relative humidity ranging around 40% in the afternoons. During the southwest monsoon season, the air in the middle and lower parts of the basin is extremely humid. The relative humidity measurements gradually decline after that. During the pre-monsoon season, relative humidity averages around 45 percent in the afternoons and 59 percent in the mornings. The average humidity in this location is 64 percent during the summer and 78 percent during the monsoon season.

3.2.6 Rainfall

Both seasonal and yearly variations may be seen in the rainfall data. The average annual rainfall for the current study region is estimated to be around 1428 mm based on available rainfall data. Figure 3.3 depicts the average monthly rainfall.

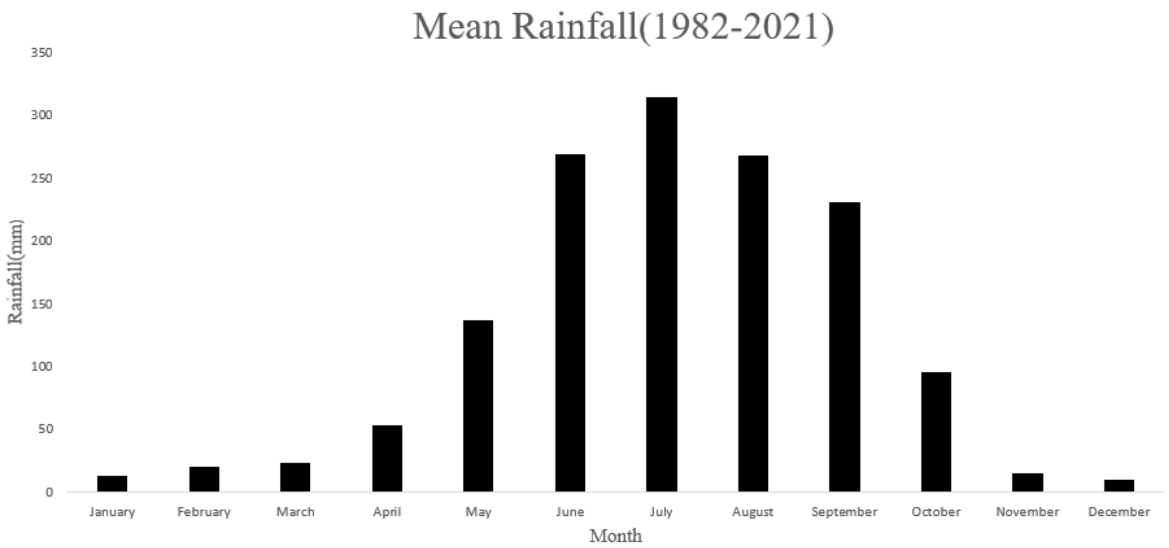

Fig 3.4 Average monthly precipitation(mm) in the study area

3.2.7 Soil Type

Many types of soils are present in the Mayurakshi River Basin. The soil series found in the area are given in in table 3.3.

Table 3.3: Soil type in the Mayurakshi River Basin

Soil	Area (% Of Watershed Area)
Loam	14.64
Sandy Loam	9.30
Clay loam	20.57
Sandy clay loam	55.49

3.2.8 Landuse/Land Cover

The land-use data was collected from the sentinel 2 satellite imageries. Forest, agricultural, and barren terrain are the most common land uses in the Mayurakshi River Basin basins. The extent of the Mayurakshi basin watershed under various land uses is depicted in table 3.3

Table 3.4 Landuse/Land cover in the Mayurakshi River Basin

Landuse/Land Cover	Area (% of watershed area)
Water	1.79
Forest-deciduous	9.17
Agricultural land-generic	72.46
Residential	7.18
Barren	9.39

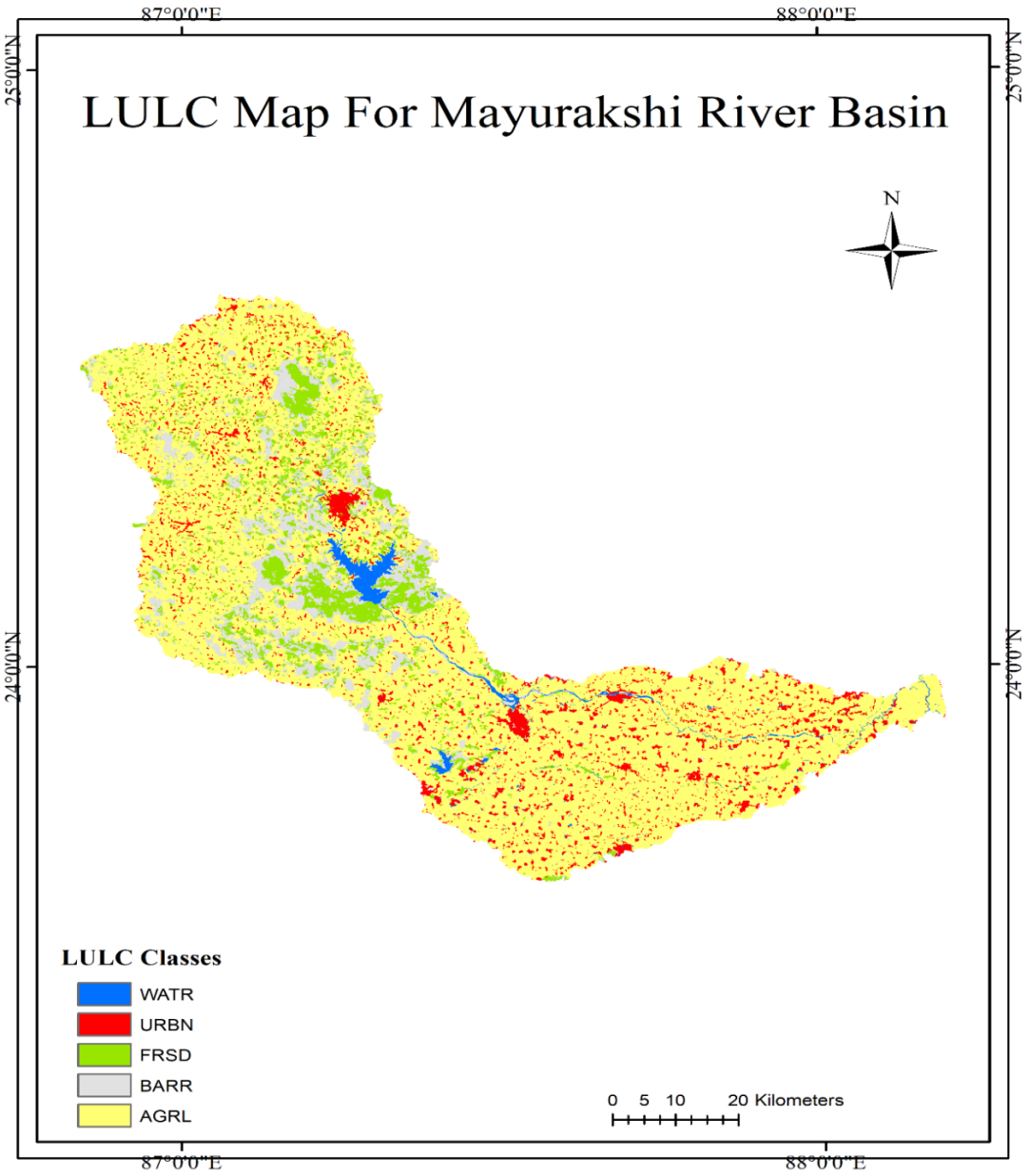

Fig 3.5 Landuse Map of the study area

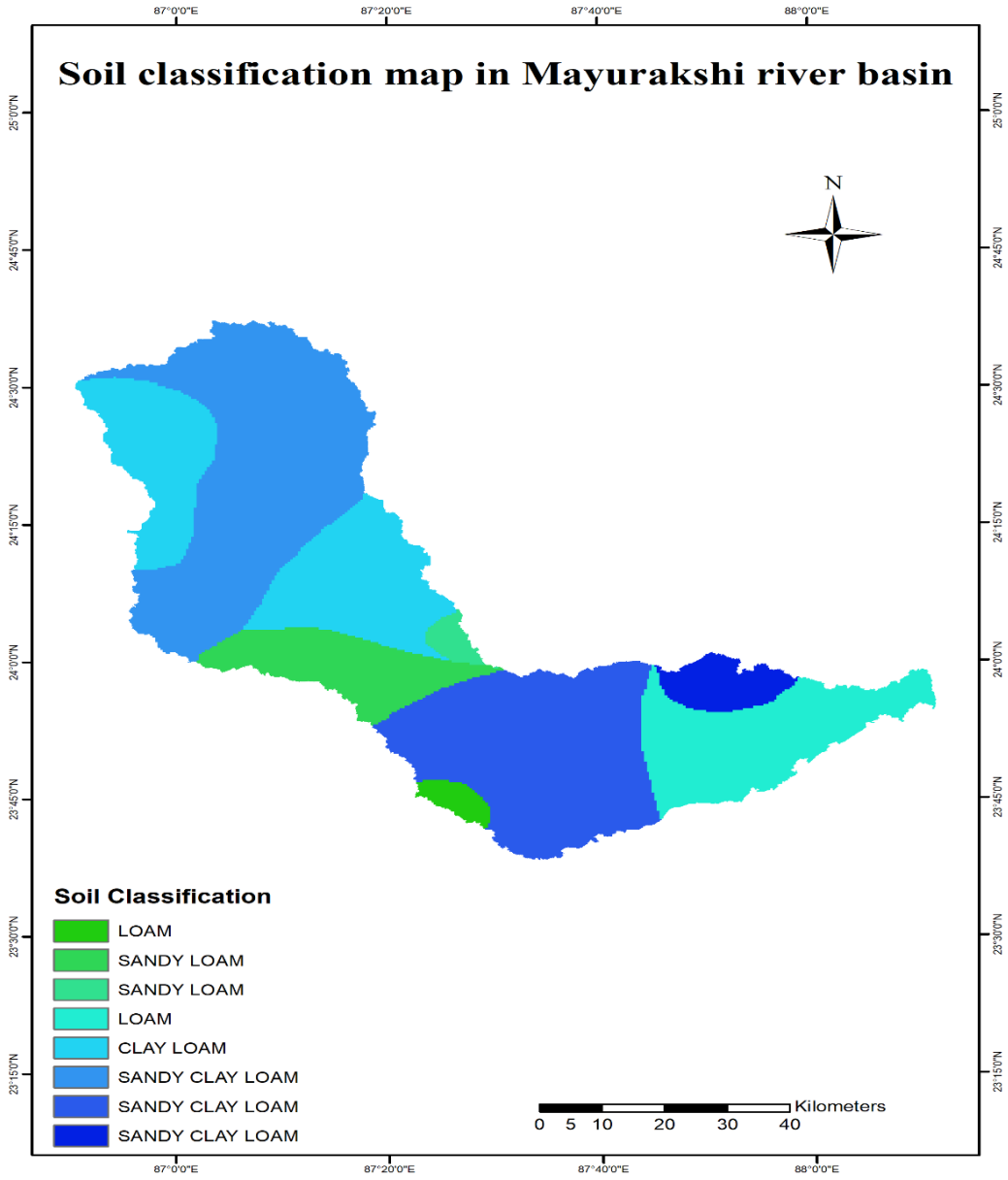

Fig 3.6 Soil Map of the study area

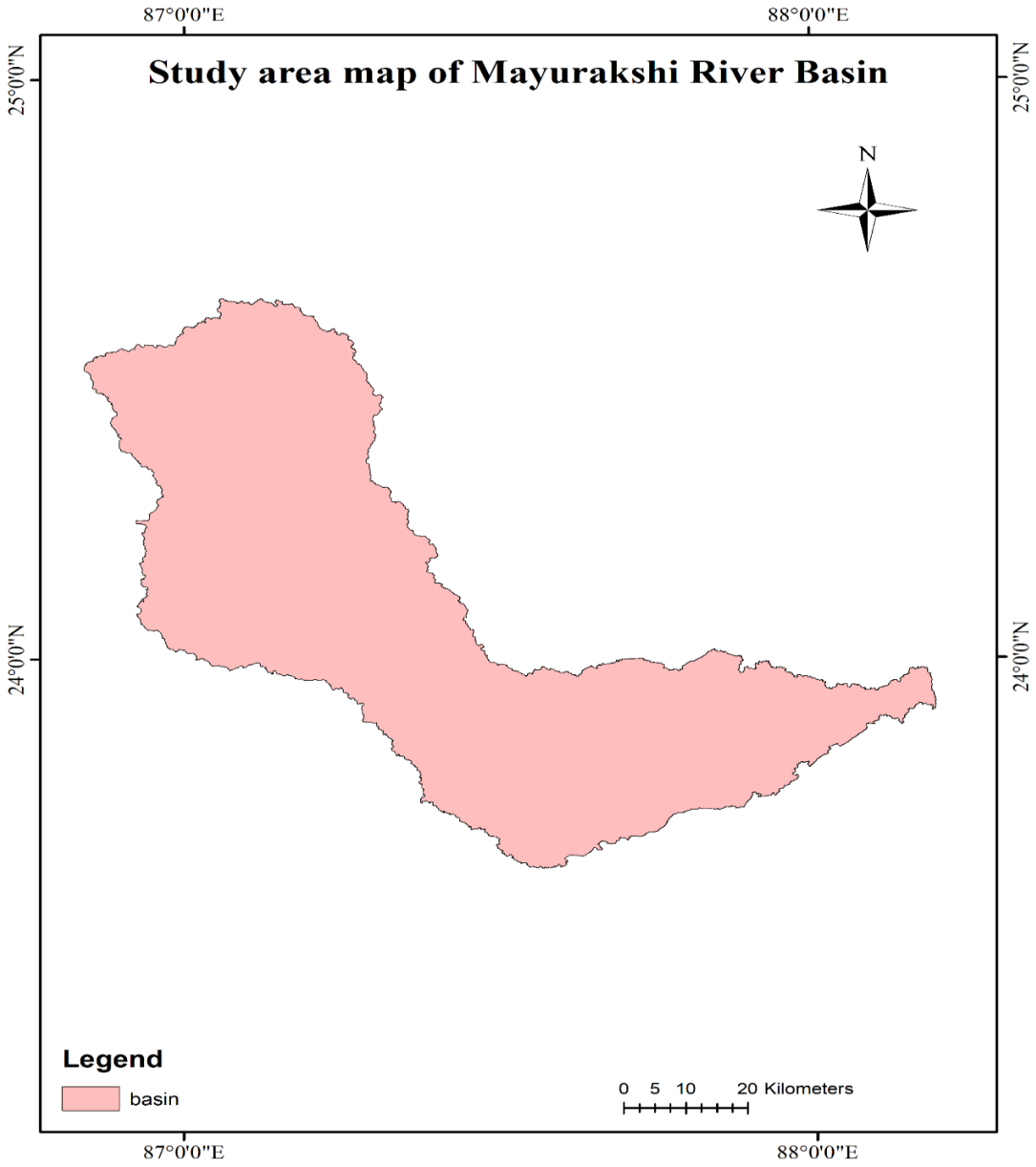

Fig 3.7 Basin Map of the study area

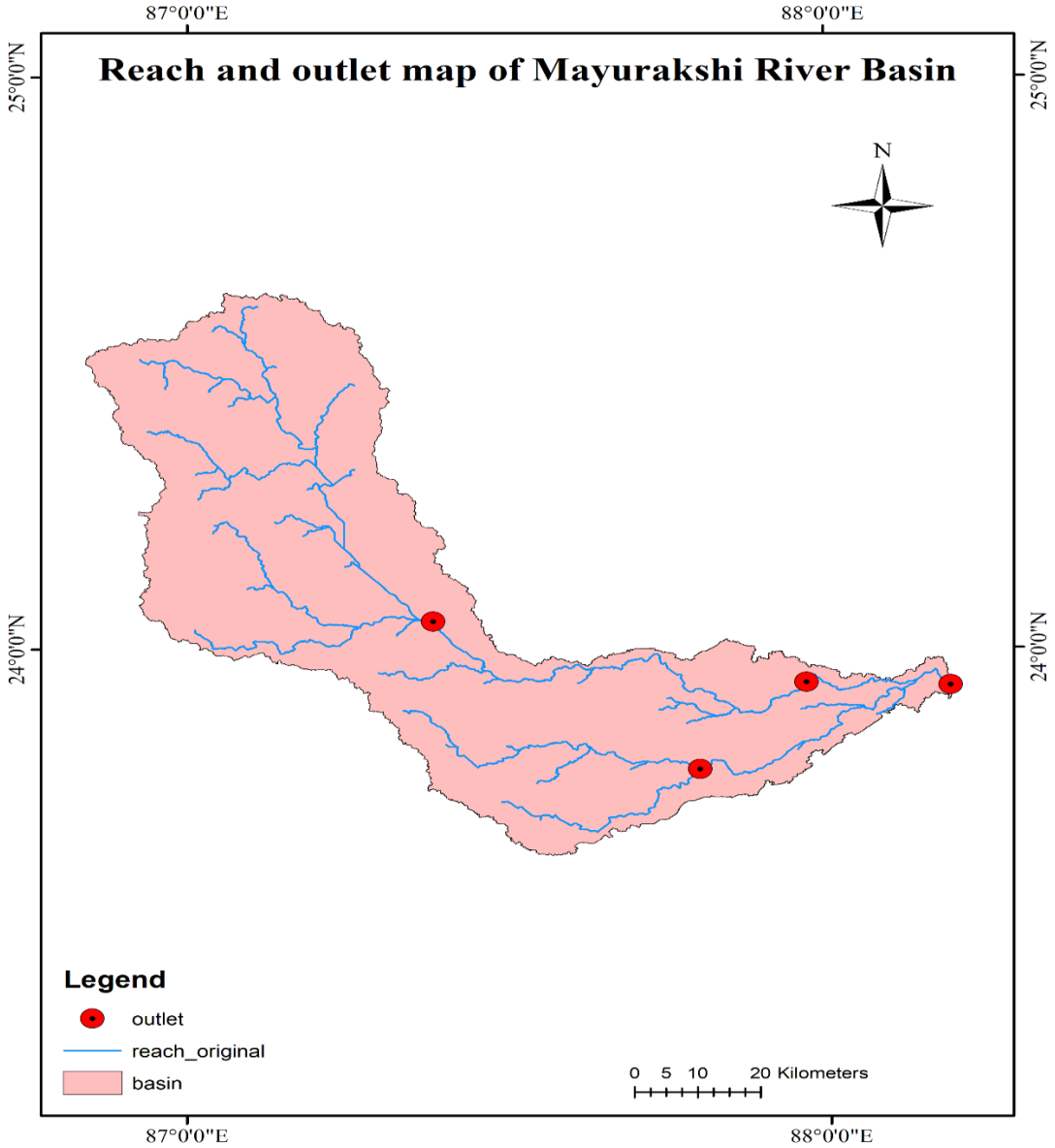

Fig 3.8 Reach & Outlets Map of the study area

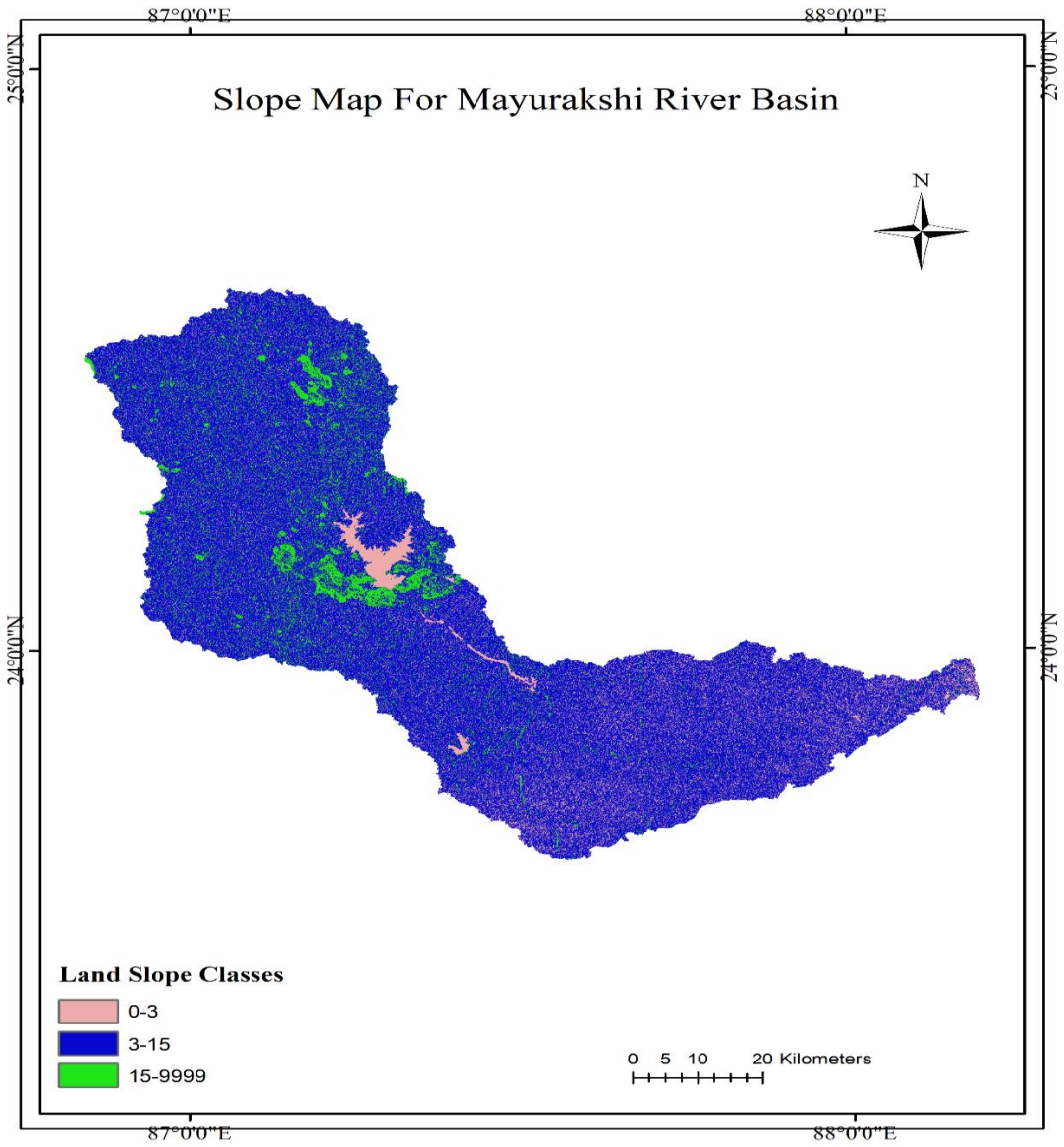

Fig 3.9 Slope Map of the study area

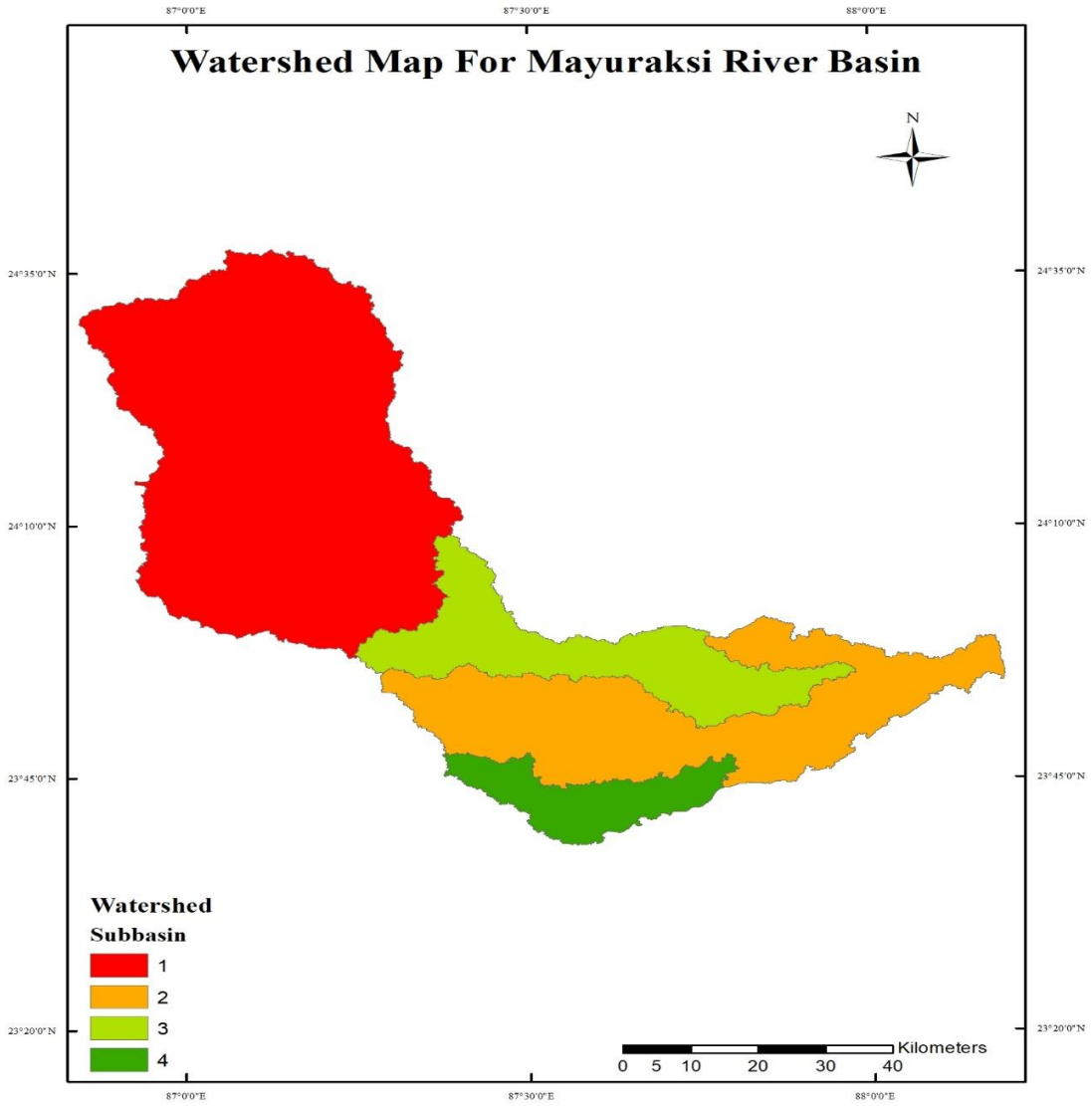

Fig 3.10 Watershed Map of the study area

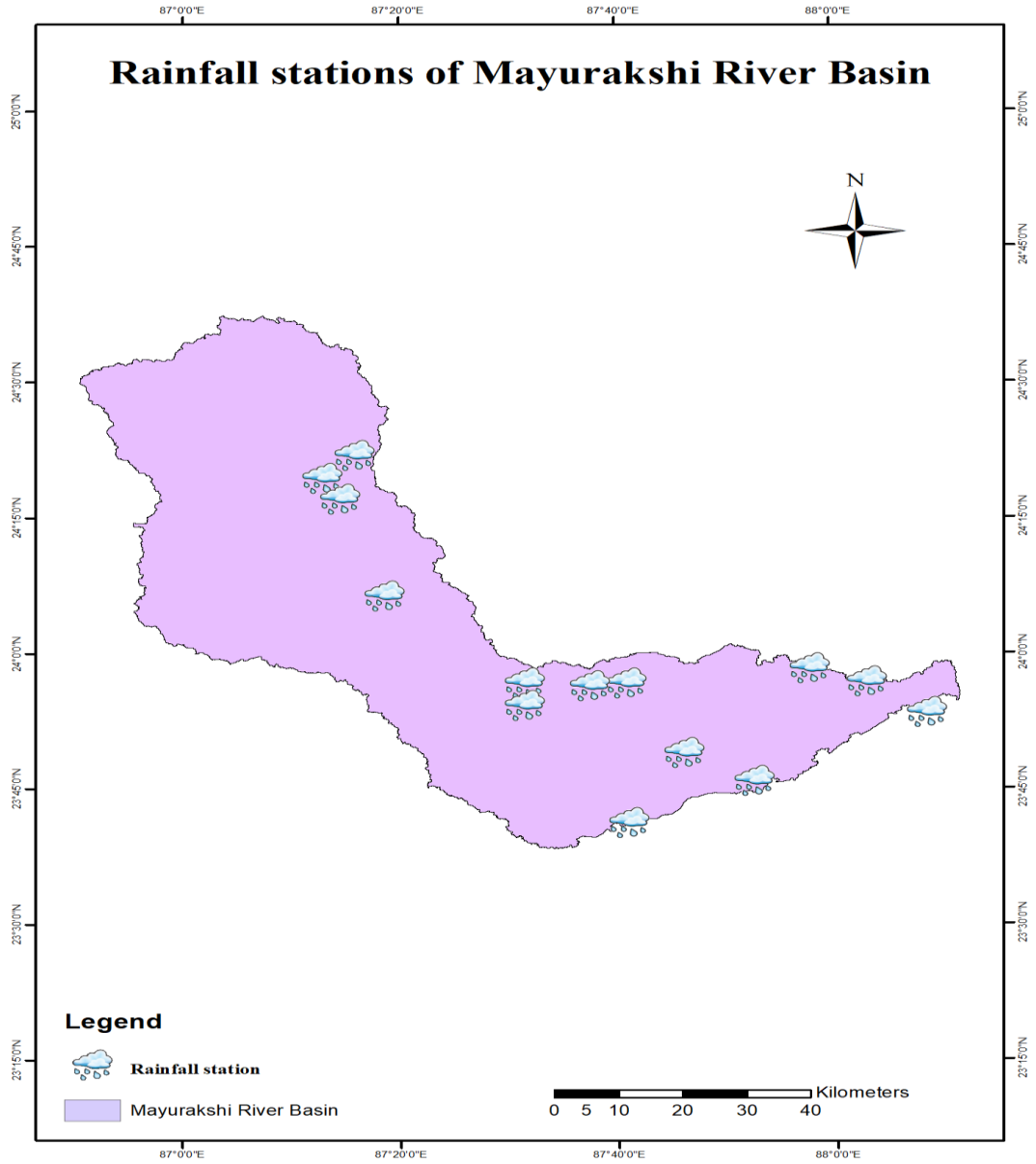

Fig 3.11 Rainfall stations Map of the study area

CHAPTER 4: METHODOLOGY

4.1 Data Collection

4.1.1 Rainfall dataset for spatial-temporal railfall trend and variability assessment

The Copernicus climate data store (https://cds.climate.copernicus.eu/) provided rainfall data for MRB.Monthly rainfall time-series records from 16 stations were collected throughout a 40-year period (i.e., 1982–2021). The rainfall stations were chosen for their long-term dataset, a smaller percentage of missing data, and sub-basin predictive ability. All of the data was subjected to a thorough data quality check. As a result, the data was thoroughly scrutinized for outliers and missing values, which were filled using a combination of cross-checking records from nearby stations and traditional statistical methods.

4.1.2 Dataset for SWAT modelling

Because the SWAT model is based on the Arc GIS environment, it is important to first identify and integrate the software (https://swat.tamu.edu/software/arcswat). The altitude, land slope, river flow direction, and several other hydrological characteristics of the entire region were determined using the ASTER (Advanced Spaceborne Thermal Emission and Reflection Radiometer) DEM (Digital Elevation Model) (1 arc second horizontal resolution) (Fig 3a and b). In addition, a geo-rectified Sentinel-2 Land Use Land Cover (LULC) map was utilized to identify distinct geographical and communicational parameters, which were divided into five groups. In Arc-GIS v 10.4.2 software, these images and base maps were projected using the Universal Transverse Mercator projection with zone 45 north (UTM 45N) and World Geodetic Survey 1984 (WGS 1984).The images were collected from various sources and were not geo-corrected for accuracy.

The present research area's suitable soils and their distribution were collected from an FAO soil map with four distinct classifications (http://www.fao.org/geonetwork/srv/en/metadata) and for the

Table 4.1 Datasets for SWAT modelling

SL NO	SPATIAL DATA	DESCRIPTION	SOURCE
1	Digital elevation mode	ASTER (Advanced Spaceborne Thermal Emission and Reflection Radiometer) DEM (Digital Elevation Model) (1 arc second hori-zontal resolution)	(https://earthexplorer.usgs.gov/)
2	Land use & land cover	geo-rectified Nasa earth data (Sentinel-2)	(https://search.earthdata.nasa.gov/)
3	Soil Data	FAO soil	(http://www.fao.org/geonetwork/srv/en/metadata
4	Weather Data	Precipitation: 0.5 km×0.5 km regridded data Temperature: 1.0 km×1.0 km regridded data	IMD
5	Hydrological data & Discharge Data	maximum and minimum temperature, precipitation, wind speed, solar radiation, and relative humidity,Discharge.	China Meteorological Assimilation Driving Datasets for the SWAT model (CMADS) & Tilpara Irrigation Department.

SWAT model, daily grid-based meteorological data for the whole sub-catchment basin (2008-2016) were used from China Meteorological Assimilation Driving Datasets, including maximum

and lowest temperature, precipitation, wind speed, solar radiation, and relative humidity (CMADS). Observed discharge data was collected from Tilpara Irrigation department.The SWAT model, on the other hand, includes weather (https://swat.tamu.edu/media/99082/cfsr world.zip) and soil data (http://downloads.indiaremotesensing.com/SWAT2012.zip), which it mixes with data from other sources Because all of the work is based on territory of India, the SWAT model uses data from the SWAT website (https://swat.tamu.edu/software/links/india-dataset/) to collect information about India, such as weather, soil, and so on.

4.2. Rainfall Variability & Trend assessment

The data on rainfall patterns and variations throughout time was evaluated using a variety of approaches. The Coefficient of Variation (CV), Precipitation Concentration Index (PCI), and Standardized Anomaly Index (SAI) were used to calculate rainfall variability (Bewket and Conway, 2007). To analyze the existence of trends in the data, the innovative trend analysis (ITA) technique, Mann–Kendall (MK) test, and Sen's slope estimator (SSE) were used with a 5% ,10% significant level. All of the techniques are described in the sub-sections that follow.

4.2.1 Method for rainfall variability assessment

4.2.1.1 Coefficient of Variation (CV)

The CV is used to determine how variable annual and seasonal rainfall data are. A greater CV value indicates that the rainfall time-series data is more variable, and it was calculated using the following formula:

$$CV = \frac{\sigma}{\bar{X}} \times 100 \quad (1)$$

where σ is the standard deviation and $\bar{X}$ is the average rainfall data.

Commonly, CV classification is based on table 4.2.

Table 4.2 CV Classification

CV Range	Classification
(CV < 20 %),	Less
(20 % < CV < 30 %),	Moderate
(CV > 30 %)	High
(CV > 40 %	Very high

4.2.1.2 The Standard Anomaly Index (SAI)

Another method for assessing rainfall variability is the SAI, which is used to assess the nature of trends and determine the dry and wet years in the record (Bekele et al., 2017a,2017b). It was calculated as:

$$SAI = Z = \frac{(x-\mu)}{\delta} \quad (2)$$

where,

x =Annual rainfall; μ = Mean annual rainfall , δ = Standard deviation of annual rainfall .

In Eq. (2), a negative SAI value indicates a drought period when compared to the specified reference period, whereas a positive value suggests a wet scenario.

According to Koudahe et al. (2017), Z value classification is based on table 4.3

.

Table 4.3 SAI classification

Z Range	Classification
(Z > 2)	Extremely wet
(1.9 > Z > 1.5),	Very wet
(1.49 > Z > 1.0),	Moderately wet
(0.99 > Z > -0.99)	Near normal
(-1.0 > Z > -1.49)	Moderately dry
(-1.5 > Z > -1.99),	Severely dry
(Z < - 2)	Extremely dry

4.2.1.3 Precipitation Concentration Index

The PCI analysis was used to obtain the seasonality of rainfall. It is a statistic that shows the distribution of monthly rainfall data and may be used to predict floods and droughts (Gocic and Trajkovic, 2013). Eq. (3) (De Luis et al., 2000) was used to calculate PCI:

$$PCI = \frac{\sum_{i=1}^{12} {p_i}^2}{(\sum_{i=1}^{12} p_i)^2} \times 100 \quad (3)$$

where Pi is the monthly rainfall amount in an ith month.

As described by Oliver (1980),

Table 4.4 PCI classification

PCI Range	Classification
PCI <10	Uniform monthly rainfall distribution
11<PCI <16	Moderate concentration of rainfall
16<PCI<20	Irregular distribution of monthly rainfall
PCI≥20	Very high concentration of rainfall

4.2.2 Method for rainfall trend detection Mann–Kendall test

4.2.2.1 Mann-Kendall test (MK)

The non-parametric rank-based MK test (Mann, 1945; Kendall, 1975) has been widely used to detect patterns in hydro-climatic time-series data (Cailas et al., 1986; Yu et al., 1993; Gan, 1998; Zhang et al., 2001; Tesemma et al., 2010; Birara et al., 2018; Jilo et al., 2019). It may be used to detect non-normally distributed data that isn't influenced by outliers (Hamed, 2008). This test accepts or rejects the null and alternative hypotheses. The null hypothesis (H0) of the test implies that the data are random and evenly distributed with no trend, whereas the alternative hypothesis (H1) suggests that the series is rising or decreasing.The following is the test statistic S:

$$S = \sum_{i=1}^{n-1} \sum_{j=i+j}^{n} sgn(x_j - x_i) \quad (4)$$

where,n is number of observations,x_i and x_j are the ith and jth (j > i) observations in the time-series,

respectively, and sgn(x_j - x_i) is the sign function computed as:

$$sgn\left(x_j - x_i\right) = \begin{cases} +1, if\left(x_j - x_i\right) > 0 \\ 0, if\ \left(x_j - x_i\right) > 0 \\ -1, if\ \left(x_i - x_j\right) > 0 \end{cases} \quad (5)$$

For series with sample size n > 10, the test statistic S is considered to be asymptotically normal, with mean E(S) and variance Var (S) as follows:

E(S) = 0, and

$$Var\ (S) = \frac{n\ (n-1)(2n+5)}{18} \quad (6)$$

When n is more than 10, and there is a chance of a tie in the value of X, the distribution of statistics S tends to normality (Kendall, 1975); therefore, the variance is computed as:

$$Var(S) = \frac{n\ (n-1)(2n+5) - \sum_{k=1}^{m} t_k\ (t_k-1)\ (2t_k+5)}{18} \quad (7)$$

tk is the number of ties of extent k, and m is the number of tied groups. The standard normal test statistic Z, which is used to detect a significant trend, is:

$$Z = \begin{cases} \frac{S-1}{\sqrt{Var(S)}}, if\ S > 0 \\ 0, if\ S = 0 \\ \frac{S+1}{\sqrt{Var(S)}}, if\ S < 0 \end{cases} \quad (8)$$

The null hypothesis of 'no trend' should be accepted at the significance level for - $Z_{1-\alpha/2} \leq Z \leq Z_{1-\alpha/2}$, where $Z_{1-\alpha/2}$ is the standard score (z-score) of the standard normal distribution with the cumulative probability of $1-\alpha/2$ in a two-tailed test. Otherwise, the null hypothesis should be rejected, and at the significance level, a monotonic trend has been observed. As a result, the positive and negative values of Z display an upward and downward trend.

4.2.2.2 Sen's slope estimator test (SSE)

The SSE is a nonparametric method for estimating trend slope in hydro-climatic time series (Yue and Hashino, 2003; Partal and Kahya, 2006; Tabari and Marofi, 2011).

The slope (Ti) for all data pairs is calculated as (Sen, 1968);

$$f(t) = Qt + B \tag{9}$$

In Eq. (9), *Qt* indicates slope, while *B* is a constant. To get the slope estimation (Q) initially, the slopes (value) of the entire time-series data were calculated as shown in Eq. (10)

$$Q_i = \frac{X_j - X_k}{j - k} \tag{10}$$

Xj and Xk denote the data values at times j and k (j > k), respectively. If each period has only one datum, N= n(n-1)/2, where n is the number of periods.N < (n(n-1))/2 if there are numerous observations in one or more periods. The N values of Qi are sorted in ascending order, and the median slope, also known as Sen's slope estimate, is reported as

$$Q_{med} = \begin{cases} Q * \left[\frac{(N+1)}{2}\right], if\ N\ is\ odd \\ \frac{Q*\left[\frac{N}{2}\right]+Q*\left[\frac{(N+2)}{2}\right]}{2}, if\ N\ is\ even \end{cases} \tag{11}$$

Finally, using a non-parametric model Q_{med} was computed to determine the trend and slope magnitude. When Q_i is positive, it indicates an upward trend, however when is negative, it indicates a declining or falling trend in time series analysis.

On the other hand, A zero value indicates that there is no trend in the data. The magnitude of the slope in original units per year or percent per year would be the unit of resulting Q_i (Salmi et al., 2002).

4.2.2.3 Innovative trend analysis method (ITA)

Sen (2012) developed the ITA approach, which may be used to any time-scale data without making any assumptions about hydro-meteorological concepts.Rainfall time-series data must be divided into two equal portions & sorted in ascending order using the ITA technique. As a result, both parts are categorised independently in ascending order and displayed on the horizontal and vertical axes in this study. On the cartesian coordinate system, the first portion of the time-series (X_i: i = 1, 2, 3, …, n/2) is placed on the horizontal X-axis, while the remaining segment (Xj: j = n/2 + 1, n/2 +2, …, n) is placed on the vertical y-axis. On the coordinate system, the rainfall data points are shown on a 1:1 (45 °) line (if the point falls exactly on this line, it indicates that there is no trend in the time-series data). Rainfall data points above the 1:1 line indicate a monotonic increasing trend in time-series data, whereas rain data points below the 1:1 line indicate a monotonic decreasing trend in time-series data (Sen, 2012; Sen, 2014). Similarly, if the rainfall data points in a scatter diagram fall above and below the 1:1 line, a non-monotonic trend can be seen.

The straight-line trend slope (s) is estimated using the following expression (Sen, 2017)

$$s = \frac{2(\bar{x}_2 - \bar{x}_1)}{n} \tag{12}$$

where S is the trend line's slope; $\bar{x}_1, \bar{x}_2$ are the arithmetic mean of the first and second halves of the dependent variable, and n is the total number of data points use.

The stochastic features of S are a function of the first and second half time-series of arithmetic mean rainfall data values, according to the trend slope line in Eq. (12). Because $\bar{x}_1, \bar{x}_2$are both stochastic variables, the slope's expectation E(s) may be determined by:

$$E(s) = \frac{2}{n}[E(\bar{x}_2) - E(\bar{x}_1)] \tag{13}$$

If the values of the $E(\bar{x}_2) = E(\bar{x}_1)$,therefore E(s)=0; and this implies there is no trend.

Otherwise the difference between $E(\bar{x}_2), E(\bar{x}_1)$ gives the variance of the slope:

$$\sigma_s^2 = E(s^2) - E^2(s) = \frac{4}{n^2}[E(\bar{x}_2) - 2E(\bar{x}_2\bar{x}_1)] + E({\bar{x}_1}^2) \quad (14)$$

As, $E({\bar{x}_2}^2) = E({\bar{x}_1}^2)$;

the above equation becomes

$$\sigma_s^2 = \frac{8}{n^2}[E(\bar{x}_2) - E(\bar{x}_2\bar{x}_1)] \quad (15)$$

Therefore, the relationship is obtained as follows

$$If, \bar{x}_2 = \sigma\bar{x}_1 = {\sigma}/{\sqrt{n}}$$

$$\sigma_s^2 = \frac{8}{n^2}\frac{\sigma^2}{n}(1 - \rho\bar{x}_1\bar{x}_2) \quad (16)$$

$$\sigma_s = \frac{2\sqrt{2}}{n\sqrt{n}}\sigma\sqrt{1 - \rho\bar{x}_1\bar{x}_2} \quad (17)$$

Where,

$$\rho\bar{x}_1\bar{x}_2 = \frac{E(\bar{x}_1\bar{x}_2) - E(\bar{x}_1)E(\bar{x}_2)}{\sigma\bar{x}_1\sigma\bar{x}_2} \quad (18)$$

Then, the trend slope confidence limit (CL) was determined as follows:

$$CL_{(1-\alpha)} = 0 \pm S_{cri} * \sigma_s \quad (19)$$

There is no trend in time-series data, according to the null hypothesis (Ho), and there is a trend in time-series data, according to the alternative hypothesis (H1). As a result, the Ho and H1 are examined at α = 5% with Z = ±1.96. If ± s >±CL (1 – α), then Ho is rejected and H1 is accepted. The positive and negative value of *S* indicates a rising and falling trend in the time-series data, respectively (Sen, 2017).

4.2.2.4 Spatial distribution method

The spatial mapping of rainfall variability in annual and seasonal time scale, as well as trend analysis, were analyzed using the inverse distance weighted (IDW) & Thiessen polygon (TP) methods, respectively. The most prevalent deterministic interpolation methods are IDW and TP. Both techniques have been used at various spatial and temporal scales (Cheng et al., 2017). In this study, which involved 16 rainfall gauge stations, the spatial distribution of stations was evaluated using the IDW for variability and the TP approach for trend analysis. The overall, methodological flowchart of the study field is represented in Figure 4.2.

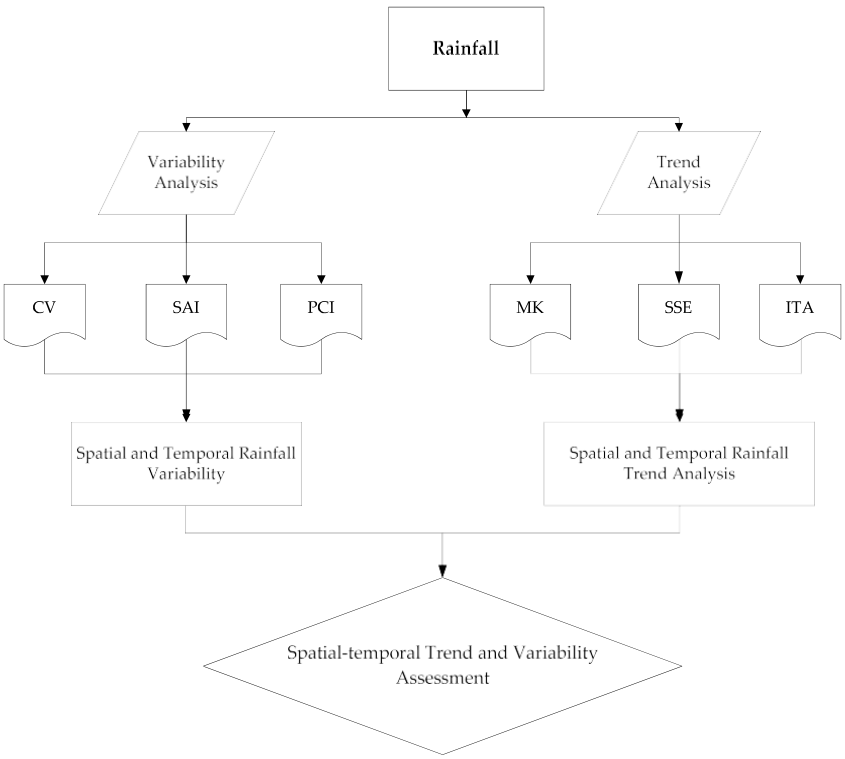

Fig 4.1 Flowchart of the methodology

4.3. Hydrological Modelling

Rainfall–runoff simulation may be performed in a completely analytical framework based on observations of the catchment area's outputs and inputs. The catchment is considered as if it were a black box, with no mention of the internal mechanisms that influence the translation of rainfall into runoff. While the challenge of deterministic prediction of monsoon rainfall on a seasonal scale has yet to be answered, improving the quality of empirical model forecasts through effective predictand, predictor, and technique selection has immediate practical implications. model development, calibration, and data processing have all gotten a lot of attention, but model validation, error propagation, uncertainty, risk, and reliability studies haven't gotten nearly as much attention. The acronym for SWAT is Soil and Water Assessment Tool. It is a scale model for river basins or watersheds created by Dr. Jeff Arnold for the USDA Agricultural Research Service (ARS). SWAT was designed to forecast the influence of land management methods on water, sediment, and agricultural chemical yields over extended periods of time in wide, complex watersheds with varied soils, land use, and management conditions. It takes a long time to analyse the hydrology of major watersheds that drain thousands of square kilometres. Large-scale analyses are required for regional and national-scale water resource management strategies and decision-making for sustainable domestic, agricultural, and industrial water supply, as well as environmental protection against negative consequences of development activities. SWAT, a computer-based environmental simulation model, is a useful tool for such research. As hydrologic systems are heterogeneous, with significant spatial variability in model inputs such as soil and land use, creating input files for large watershed models takes time. SWAT requires specific information regarding weather, soil qualities, topography, vegetation, and land management methods that occur in the watershed, rather than regression equations to characterise the link between input and output variables.

After that, the entire model is run using hydro-meteorological data. Through model– GIS interfaces, GIS plays a key role in producing model inputs from digital geographic datasets. When compared to other existing distributed parameter models, the SWAT model and its GIS interfaces assist water resources professionals perform basin-scale analyses of availability of water and quality of water, and help minimise the time and expense required to undertake such studies several-fold. Valley/ridge scale interactions are underrepresented by global and regional climate models (GCMs/RCMs).

The whole hydrological method of the SWAT model is based on a water balance equation.

$$SW_t = SW_0 + \sum_{i=1}^{t}(R_{day} - Q_{surf} - E_{a-} W_{seep} - Q_{gw}) \quad (20)$$

Where,

t is the time in days.

SW_t is the total water content (mm),

SW_0 is the amount of water content in first soil in day i (mm),

R_{day} is the amount of rainfall in day i (mm),

Q_{surf} is the amount of surface runoff in day i (mm)

E_a is the amount of evapotranspiration in day i (mm),

W_{seep} is the amount of percolated water in vadose zone from surface soil profile in day i (mm)

Q_{gw} is the amount of return flow in day i (mm)

Table 4.5 SWAT components

SWAT COMPONENTS	DESCRIPTION
Hydrology	Runoff, evapotranspiration, soil water movement, and groundwater are the four main processes considered. The water balance equation in the model accounts for all of these processes.
Weather	he fundamental process initiating agent of the hydrological cycle's terrestrial phase is climate. Daily and monthly data of numerous meteorological variables are required by the model.
Erosion/Sedimentation	The Modified Universal Soil Loss Equation is used to compute the sediment yield for each HRU. When estimating soil particle detachment and transport, vegetation cover and agricultural residues are considered.
Land use and Plant growth	Plant growth is simulated using an EPIC simplification and happens only on days when the average daily temperature reaches a plant-specific base temperature.
Nutrients and Pesticides	Within the basin, nitrogen and phosphorus transport and transformation are traced. It's also possible to calculate pesticide loading and bacterial contamination.
Management practices	Crop cultivation, growth, and grazing, as well as irrigation, nutrition, and pesticide applications, are all simulated. Consider the year-round soil protection provided by vegetation, as well as the crop deposition that remains on the soil after harvest
Main channel processes	The channel's flow of water, sediment, nutrients, and pesticides is calculated. The channel dimensions are often considered to be constant, although they can also be thought to be subject to erosion and deposition.
Water bodies	Water may also flow through ponds, wetlands, depressions, and reservoirs, in addition to channels.

4.3.1 SWAT Model

SWAT is chosen as the study's model because it is free, open-source, actively supported by model developers, well-documented, and has been thoroughly tested all around the world. The papers submitted at its biennial conference demonstrate that it has a large and rising number of users in the developing countries. The SWAT interface was created as an ArcGIS plug-in, which appears to be the most dynamic approach to implement a SWAT module. For the research, ArcGIS version 10.4.2 with SWAT 2012 is utilized, much like any other semi-distributed hydrological model. It collects a variety of geographical data in the form of maps, as well as certain temporal data such as weather files.

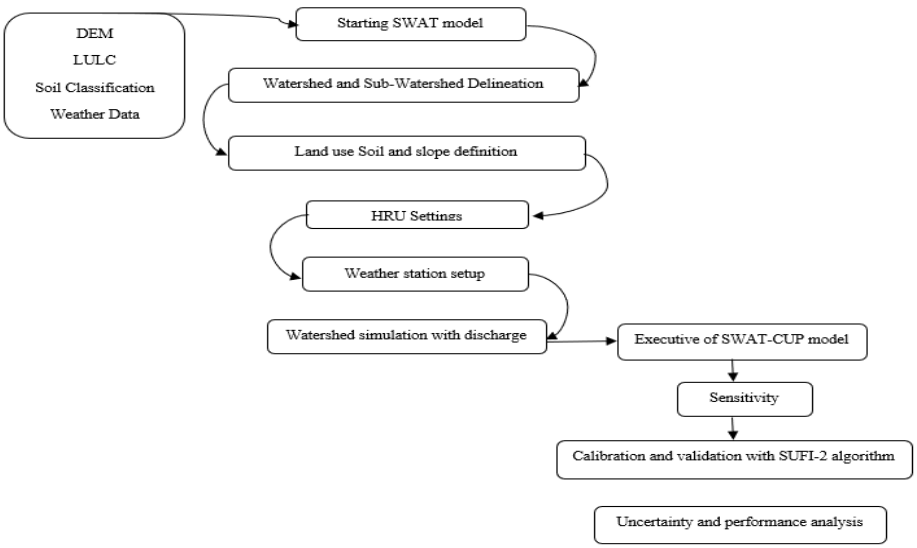

Fig 4.2 Processing and display concept for SWAT mode

The model run takes four steps to obtain the results;

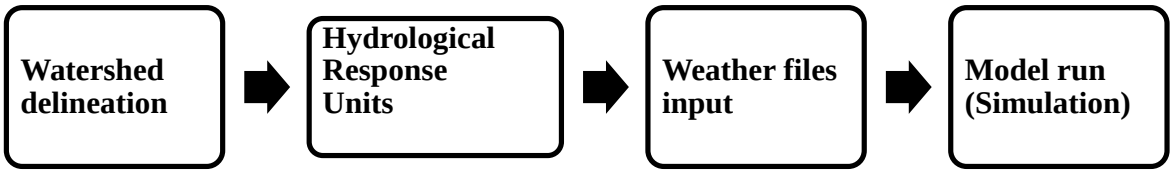

Fig 4.3 Steps for ArcSWAT model run

4.3.1.1 Watershed delineation

After setting up the project file, this is the preliminary step in modelling. To complete this stage, the model acquires a digital elevation model in a certain unit, format, and projection. The following features in the map (DEM) are formed by this section of the modelling:

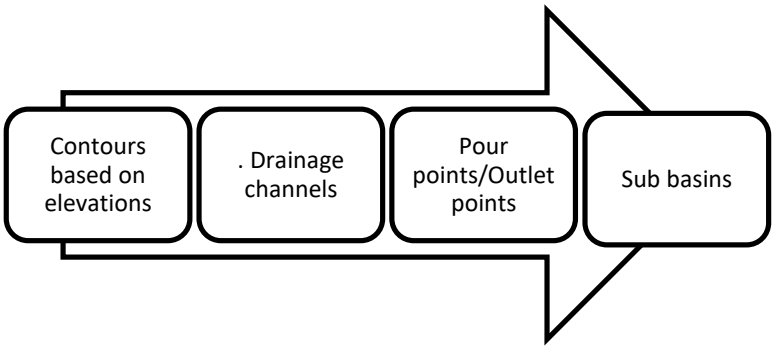

Fig 4.4 Features of Watershed delineation

4.3.1.2 Hydrological Response Units (HRU) formation

This module can be made life only after sub-basins parameters have successfully been calculated in the previous step. Hydrological response unit formation is one of the strongest reasons that SWAT is considered as one of the most promising tools in hydrology. HRUs can be defined as the features developed by the model based on the regression of the number of types of land use, soil cover, and soil map. This can be explained in a simple way as, for a watershed having a single type of 1) Landcover 2) Soil, and 3) Slope, the number of HRUs formed would be one. The model retrieves spatial data in the form of maps, such as land-use maps and soil maps, in the same unit (metre), format (.tiff), and projection as the model (WGS 1984).

This step is classified into two parts as

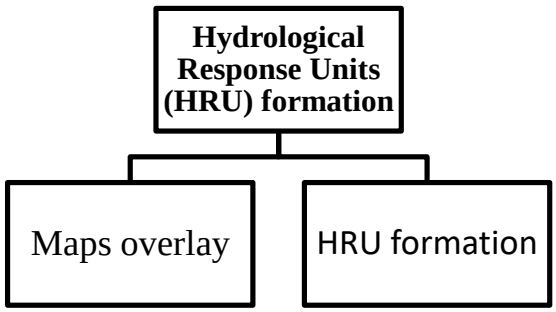

Fig 4.5 Parts of HRU analysis

Where the first part again has three activities as;

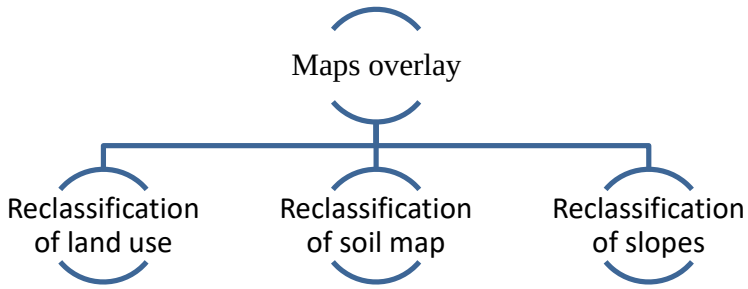

Fig 4.6 Parts of Maps overlay

4.3.1.3 Weather files input

After finishing of generating HRUs in step 2, this module will be enabled. This stage converts all of the model's collateral data into a pre-defined format. In the event that the observed values are unavailable, SWAT offers the option of simulating all collateral data. This simulation is based on meteorological data from the United States, which may have a significant impact on the findings, especially when dealing with hydrological assessment. Observed data has been used in a study, and information of rain gauge stations and climate stations are added into the model. The model can create several output tables such as hru,.rch, and.sub if this phase is completed successfully.

4.3.1.4 Model run (Simulation)

Only after completion of creating HRUs in step 2, this module will be activated. This stage converts all of the model's collateral data into a pre-defined format. In the event that the observed values are unavailable, SWAT offers the option of simulating all collateral data. Observed data was used in this study, and information of rain gauge stations and climate stations were added into the model. The model can create several output tables, such as hru, rch, and sub, if this stage is completed correctly.

4.3.2 Introduction to SWAT Output Viewer

SWAT results can be shown in a variety of ways. The model findings are visualized spatially on a map. It will illustrate how the selected results are spread throughout sub-basins or reaches in a transparent way. The ability to detect areas in the watershed is really valuable. Michael Yu (GIS Programmer and Developer, Hydrologist, Water Resource Engineer, ArcGIS,.NET, C++, Flex, FORTRAN, SWAT) has created a new tool that perfectly presents the outputs. SWAT output viewer has been used to demonstrate the outputs in this analysis.

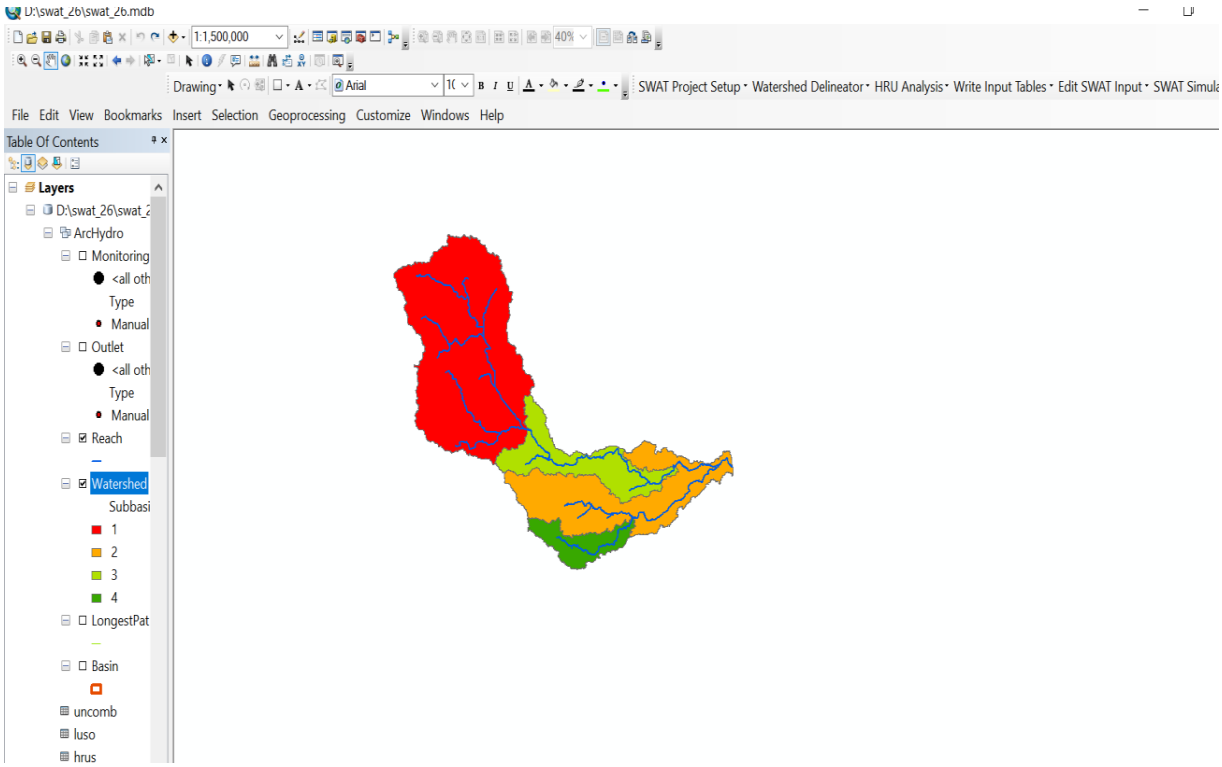

Fig 4.7 Watershed as seen in swat output viewer

4.3.3 Swat Run (Modelling)

The model run is classified in three modules as;

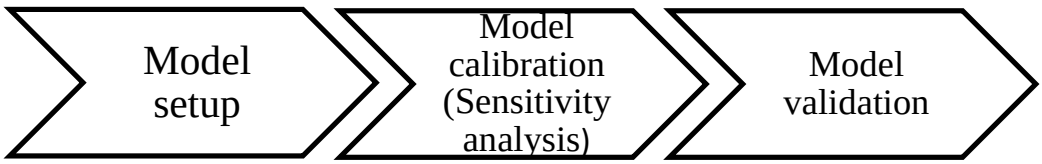

Fig 4.8 Modules of SWAT model

4.3.3.1 Model setup

From 2008 to 2016, the model is set up for simulation and results were collected (8 years). All of the preceding processes have been done successfully, and the results have been obtained. The default database was installed, and the model produces a Nash Sutcliffe efficiency of 0.66 when comparing observed and modelled discharges in millimetres.

4.3.3.2 Model calibration (Sensitivity Analysis)

After running the complete SWAT model, the SUFI-2 technique is used to calculate the uncertainty between the variables, parameters, and measurement data. SUFI-2 is also used to determine sensitivity by calculating the effective and unnecessary parameters in the model's parameters. Uncertainty is calculated using a 95 percent forecast, with a 97.5 percent upper limit and a 2.5 percent lower limit. In addition, the r-factor and p-factor may be used to calculate the model's calibration efficiency and uncertainty. When the p-factor is 1, it suggests a high level of uncertainty and poor output quality. The r-factor, which is closer to 0 and matches the observed data, reveals the calibration quality factor. A balance between the two factors is required; otherwise, the model's

output may be entirely disrupted. The amount of uncertainty of the parameter remains within range when both components achieve an acceptable and balance value.

Table 4.6 List of parameters selected for sensitivity analysis

	PARAMETERS	DESCRIPTION	UNIT
1	CN2	CURVE NUMBER	-
2	ALPHA_BF	BASEFLOW ALPHA FACTOR	Days
3	GW_DELAY	DELAY TIME OF GROUNDWATER SUPPLY FLOW	Days
4	GWQMN	SHALLOW AQUIFER'S THRESHOLD WATER DEPTH TO RETURN FLOW TO OCCUR	mm
5	GW_REVAP	GROUNDWATER REVAP COEFFICIENT	-
6	ESCO	COMPENSATION FACTOR FOR EVAPORATION FROM SOIL	-
7	CH_N2	MANNING COEFFICIENT IN THE MAIN CHANNEL	-
8	CH_K2	HYDRAULIC CONDUCTIVITY IN THE MAIN CHANNEL	mmh^{-1}
9	ALPHA_BNK	BASEFLOW ALPHA FACTOR FOR BANK STORAGE	Days
10	SOL_AWC	AVAILABLE WATER CAPACITY OF SOIL LAYER	$mmmm^{-1}$
11	SOL_K	SATURATED HYDRAULIC CONDUCTIVITY	mmh^{-1}
12	SOL_BD	DENSITY OF SOIL MASS	gcm^{-3}
13	SURLAG	SURFACE RUNOFF LAG COEFFICIENT	-

4.3.3.3 Model validation(Model Performance Indices)

Three statistical measures, Coefficient of Determination (R^2), Nash–Sutcliff efficiency (NSE), and Percent bias, have been used to evaluate the SWAT model's performance in the Mayurakshi river sub-catchment basin (PBIAS).

R^2 is calculated as :

$$R^2 = \left\{\sum_{t=1}^{T}(Q_{m,t} - \overline{Q_m})(Q_{s,t} - \overline{Q_s}) / \left[\sum_{t=1}^{T}(Q_{m,t} - \overline{Q_m})^2\right]^{0.5} \left[\sum_{t=1}^{T}(Q_{s,t} - Q_s)^2\right]^{0.5}\right\}^2 \quad (21)$$

R^2 always has a value between 0 and 1. When the value of R^2 is near to 1, the model performs well, but when the value of R^2 is more than 0.5, it is readily accepted.

NSE can calibrate both observed and simulated data at a 1: 1 ratio. The NSE values always range from infinite to one, with one being the optimum value. While all NSE values between 0 and 1 are regarded good in terms of model performance, model performance below 0 is considered poor.

$$NSE = 1.0 - \frac{\sum_{t=1}^{T}(Q_{m,t} - Q_{s,t})^2}{\left[\sum_{t=1}^{T}(Q_{m,t} - \overline{Q_m})^2\right]} \quad (22)$$

The average tendency of simulated values that are either less or bigger than observed values is measured by PBIAS. The model is underestimated if the PBIAS value is positive, while it is overstated if it is negative.

$$PBIAS = \left(\sum_{t=1}^{T}(Q_{s,t} - Q_{m,t}) \Big/ \sum_{t=1}^{T}(Q_{m,t})\right) \times 100 \quad (23)$$

CHAPTER 5: RESULTS & DISCUSSION

5.1 Assessment of variability and trend analysis

5.1.1 Statistical analysis and spatial distributions of rainfall

Table 5.1 shows the statistical charecteristics of mean rainfall data of annual and seasonal time scale in the Mayurakshi River Basin. The maximum and minimum mean annual rainfall is recorded in Narayanpur (1545.81mm) and Dumka (1323.91 mm).The mean annual rainfall in Mayurakshi River Basin is 1428.98 mm, with CV and standard deviation of 14.65% and 201.89mm, respectively.

The spatial mapping of rainfall in seasonal and annual time scale for the period from 1982– 2021 is shown in Fig.5.1(a–c). During annual time scale,the maximum rainfall were found in the lower part of the Mayurakshi River Basin, while the minimum was observed in the upper part of the Mayurakshi River Basin (Fig.5.1a).

Table 5.1 Annual and seasonal mean rainfall(mm),coefficient of variation and PCI in Mayurakshi River Basin

	Annual			Premonsoon(MAM)			Monsoon(JJAS)			Post Monsoon(OCD)			Winter(JF)		
Stations	Mean	Cv%	PCI	Mean	Cv%	PCI	Mean	Cv%	PCI	Mean	Cv%	PCI	Mean	Cv%	PCI
Tilpara barrage	1425.36	14.29	17.54	205.35	42.51	14.08	1075.60	17.12	8.96	118.60	57.85	18.37	33.46	74.80	12.34
Suri	1420.33	14.46	17.62	199.35	41.50	14.07	1076.66	16.91	8.96	118.80	57.06	18.35	33.51	74.56	12.44
Shyambati	1440.25	14.55	17.68	220.79	37.92	14.50	1078.89	17.23	9.04	118.55	60.08	18.38	31.21	82.70	12.27
Shekhampur	1438.46	14.56	17.71	220.77	39.21	14.48	1077.90	17.32	9.05	117.42	61.10	18.36	31.19	82.78	12.26
Sainthia	1442.75	14.36	17.54	215.63	39.92	14.15	1083.91	17.12	8.99	119.49	57.15	18.49	31.08	77.72	12.50
Narayanpur	1545.82	15.48	16.97	271.06	40.62	14.01	1121.50	18.37	8.97	132.10	50.27	18.17	30.46	81.95	12.38
Massanjore	1394.75	14.56	17.76	181.46	39.90	14.03	1073.11	17.70	8.93	115.06	54.78	18.22	34.17	70.34	12.28
Maharo	1328.86	13.79	17.95	167.05	38.63	13.89	1030.05	15.86	8.95	107.45	57.37	18.40	31.84	74.24	11.87
Kundahit	1398.06	14.74	17.79	181.30	38.73	14.01	1077.46	17.39	8.92	113.88	55.91	18.24	33.24	73.45	11.90
Kultore	1420.35	14.52	17.76	197.28	42.10	14.02	1080.58	16.86	8.98	116.82	58.32	18.40	33.34	75.44	12.35
Kirnahar	1494.38	14.97	17.49	246.55	40.13	14.32	1101.50	17.20	9.08	125.50	58.95	18.27	30.12	84.56	12.45
Kandi	1487.99	14.67	17.40	234.87	38.74	14.20	1108.27	17.22	8.99	123.36	54.54	18.49	29.31	81.18	12.43
Jama	1329.82	15.32	17.93	166.68	38.59	13.87	1030.18	15.79	8.94	108.67	57.78	18.32	31.96	73.51	11.97
Dumka	1323.91	15.39	17.96	164.82	37.97	13.88	1027.07	16.03	8.94	107.58	57.36	18.38	31.96	73.50	11.88
Bharatpur	1487.37	13.69	17.39	235.93	38.65	14.21	1105.93	17.52	9.00	123.76	54.55	18.46	29.41	80.49	12.43
Kuli	1485.18	15.00	17.39	233.66	39.17	14.17	1105.87	17.52	8.99	123.78	54.55	18.40	29.52	79.81	12.43

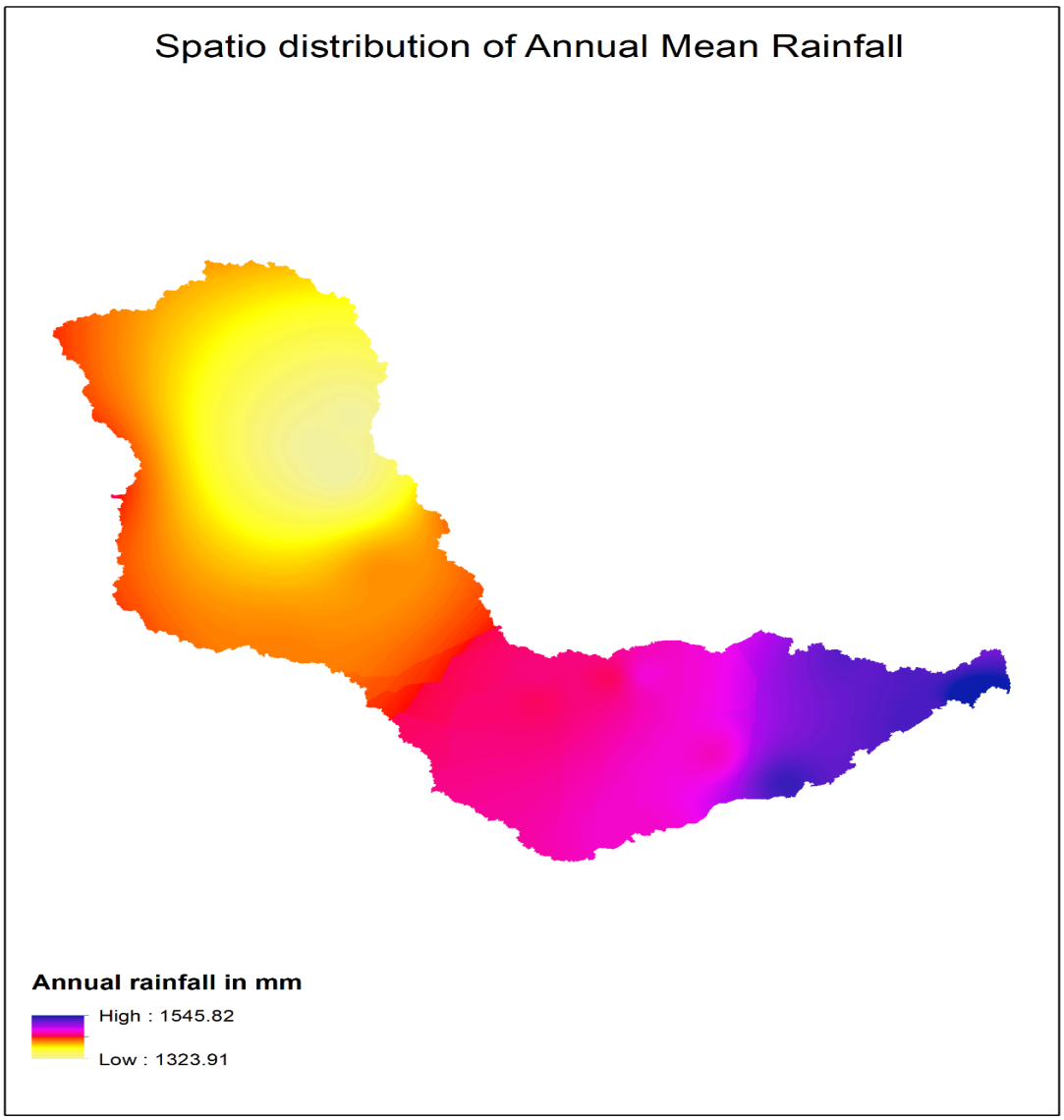

Fig 5.1 (a)Spatial Distribution of mean Annual rainfall

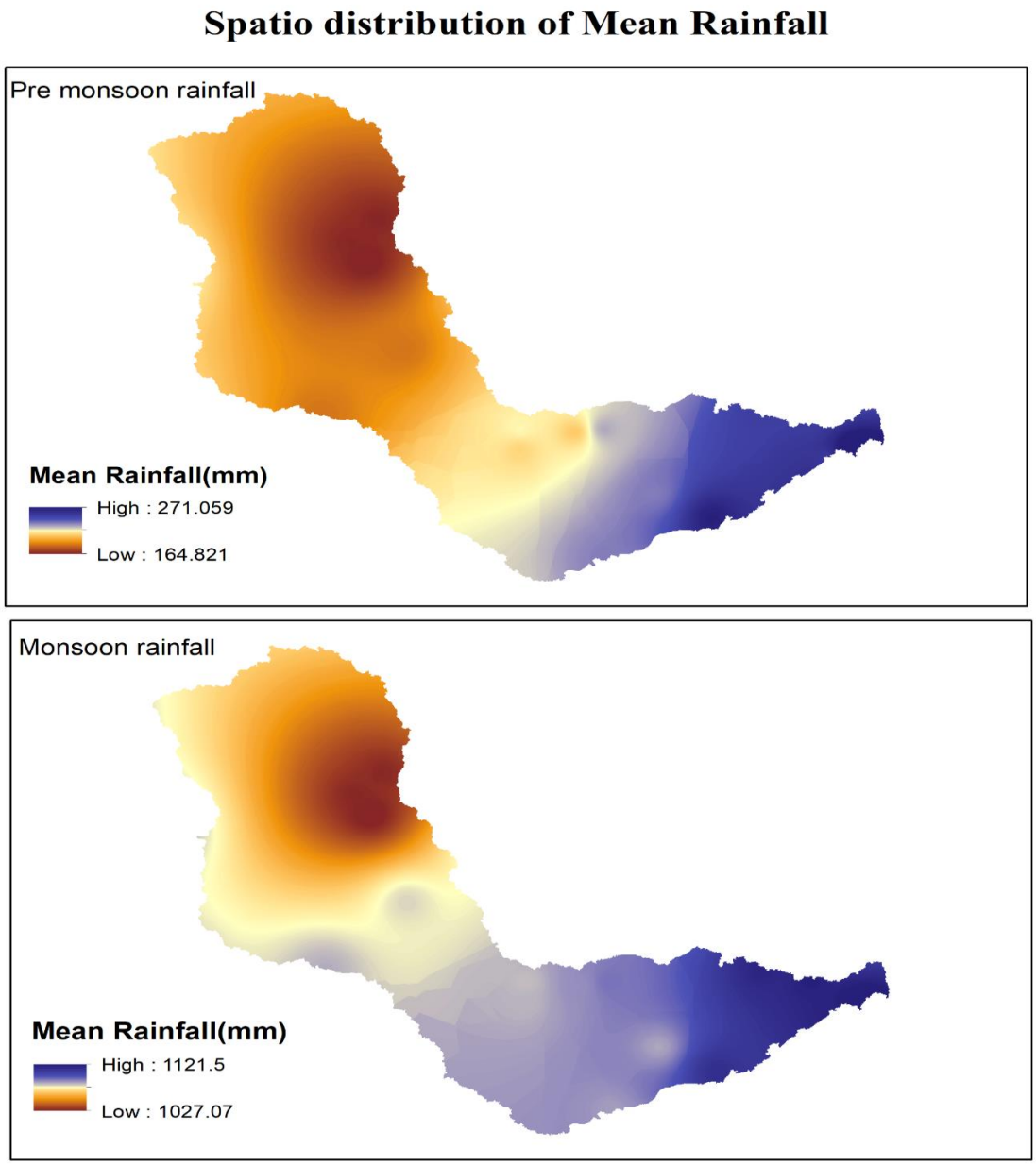

Fig 5.1 (b)Spatial Distribution of mean Pre-monsoon and Monsoon rainfall

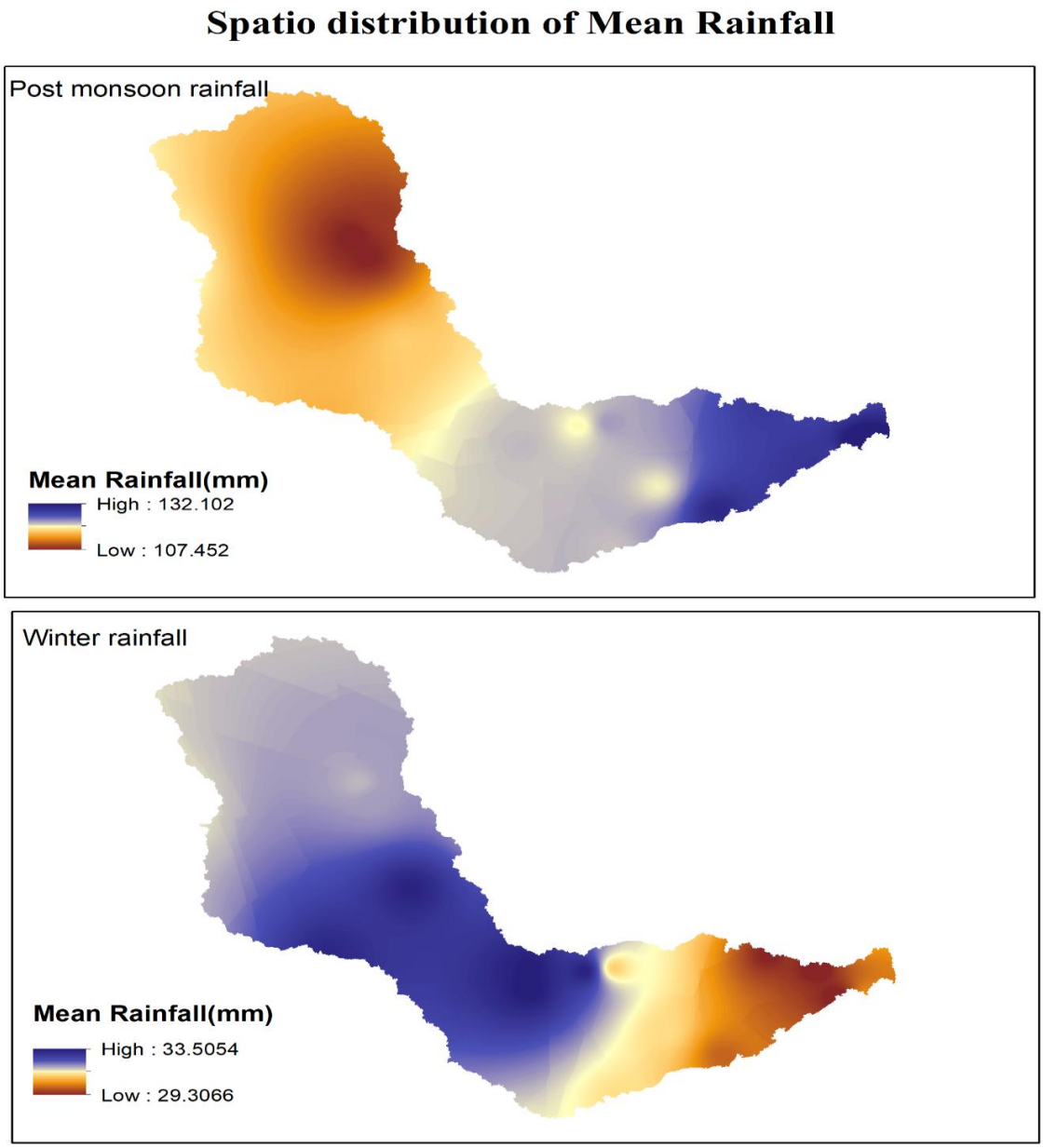

Fig 5.1 (c)Spatial Distribution of mean Post monsoon and Winter rainfall

For all seasons, the maximum and minimum amounts of rainfall were found in the lower and upper portions of MRB. (Fig. 5.1b-c).

For the Winter, Pre-monsoon, Monsoon, and Post-Monsoon seasons the mean annual rainfall was 31.62 mm (2.21%),208.91mm (14.62%),1078.41 mm (75.47%),118.18 mm (8.27%) respectively. As shown in Table 5.1, the CV % of rainfall in the stations in annual and monsoon time searies are less than 20 %, For the Pre-monsoon, Post-Monsoon, and Winter seasons all the stations show high and very high rainfall variables.Threfore, rainfall variability was higher in the seasonal period than in the annual timeframe.Most areas show low variance in annual and monsoon periods, but high and extremely high variability in seasonal time scale, as depicted in Fig. 5.2 (a–c).For the Post monsoon and winter , the CV value is more than 40 % in the Mayurakshi River basin (Fig. 5.2c), which indicates very high rainfall variability. In addition, Winter and Monsoon seasons showed the highest and lowest CVs, respectively.

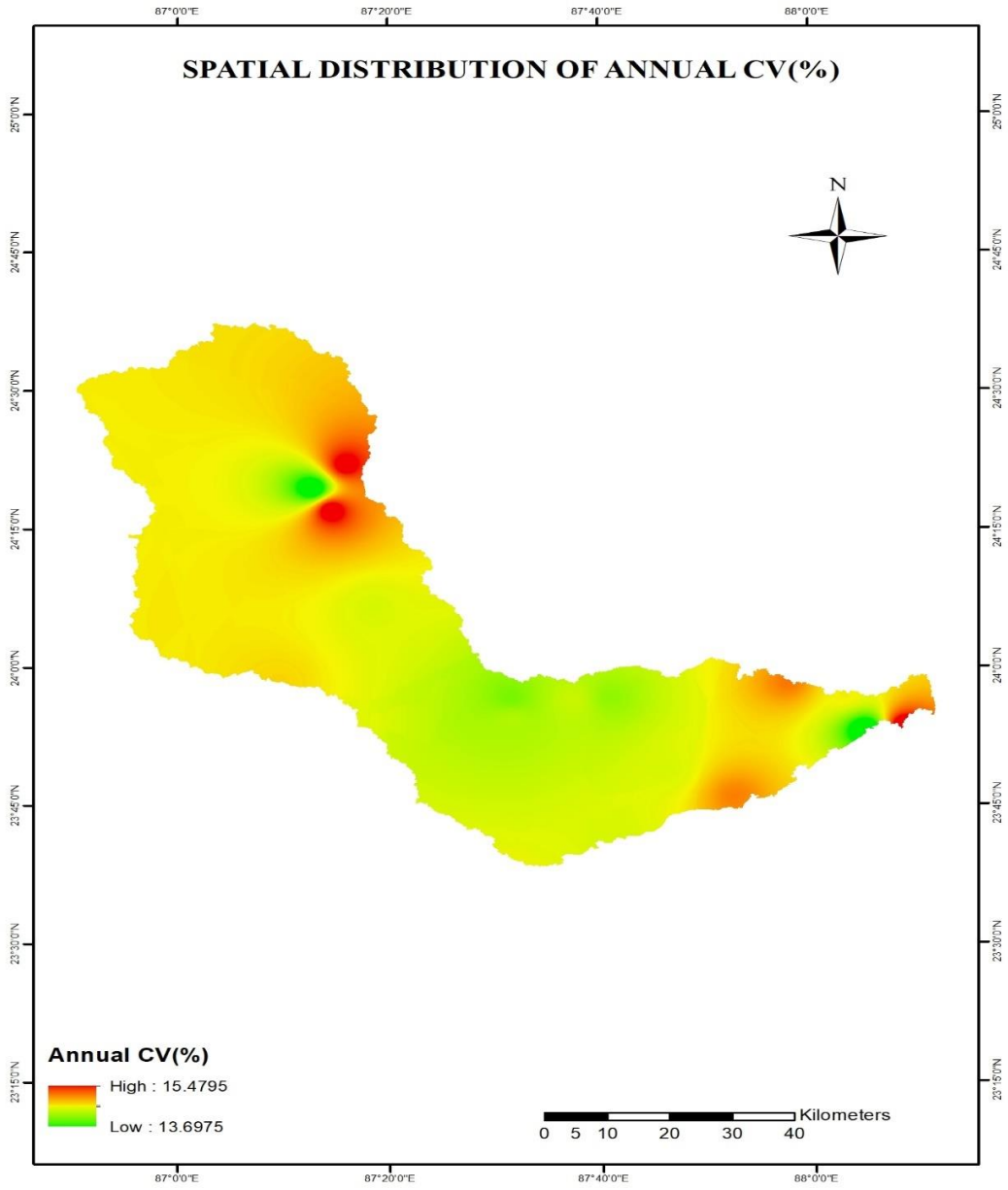

Fig 5.2(a) Spatial Distribution of Annual CV%

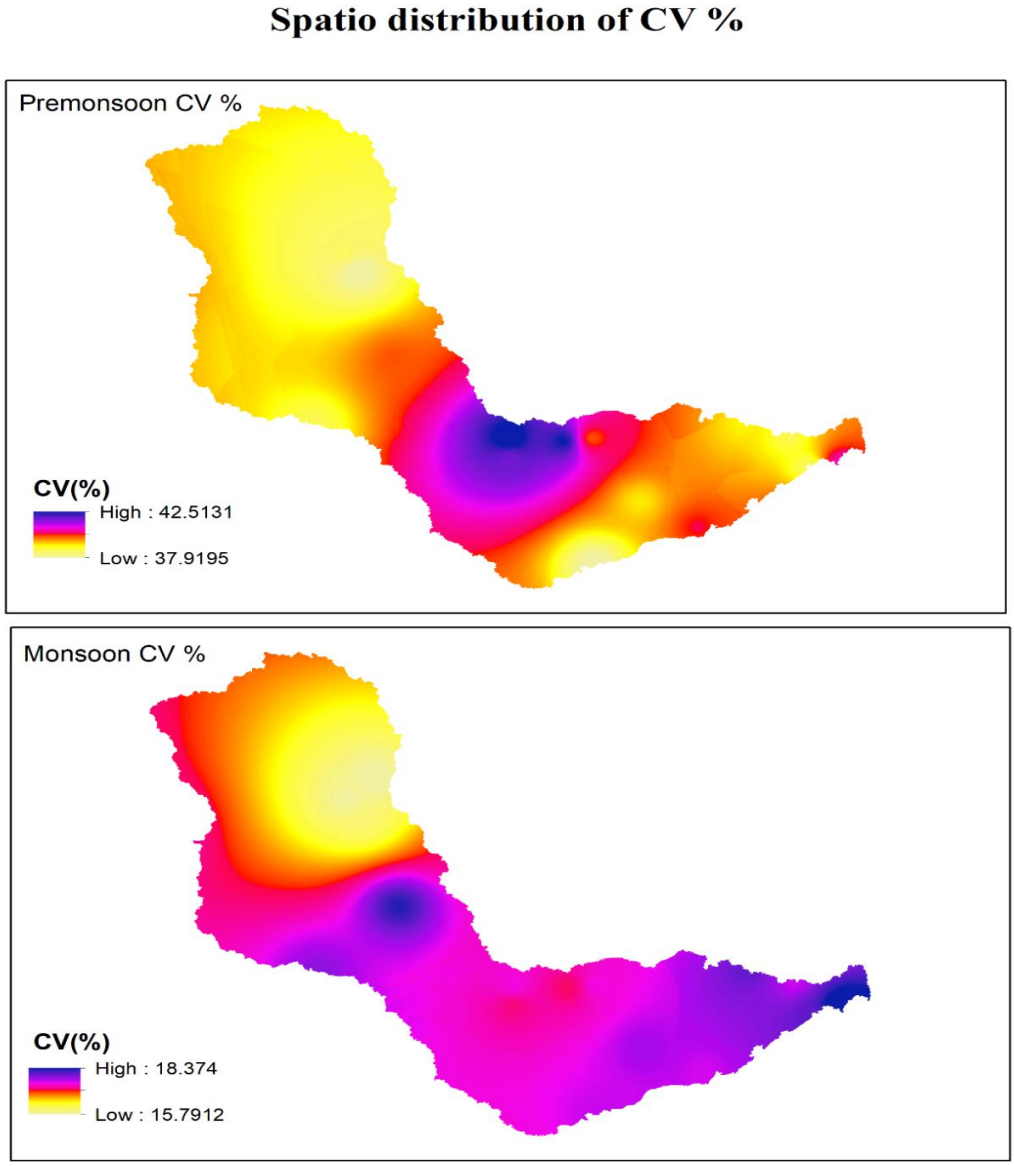

Fig 5.2(b) Spatial Distribution of Pre-monsoon and Monsoon CV%

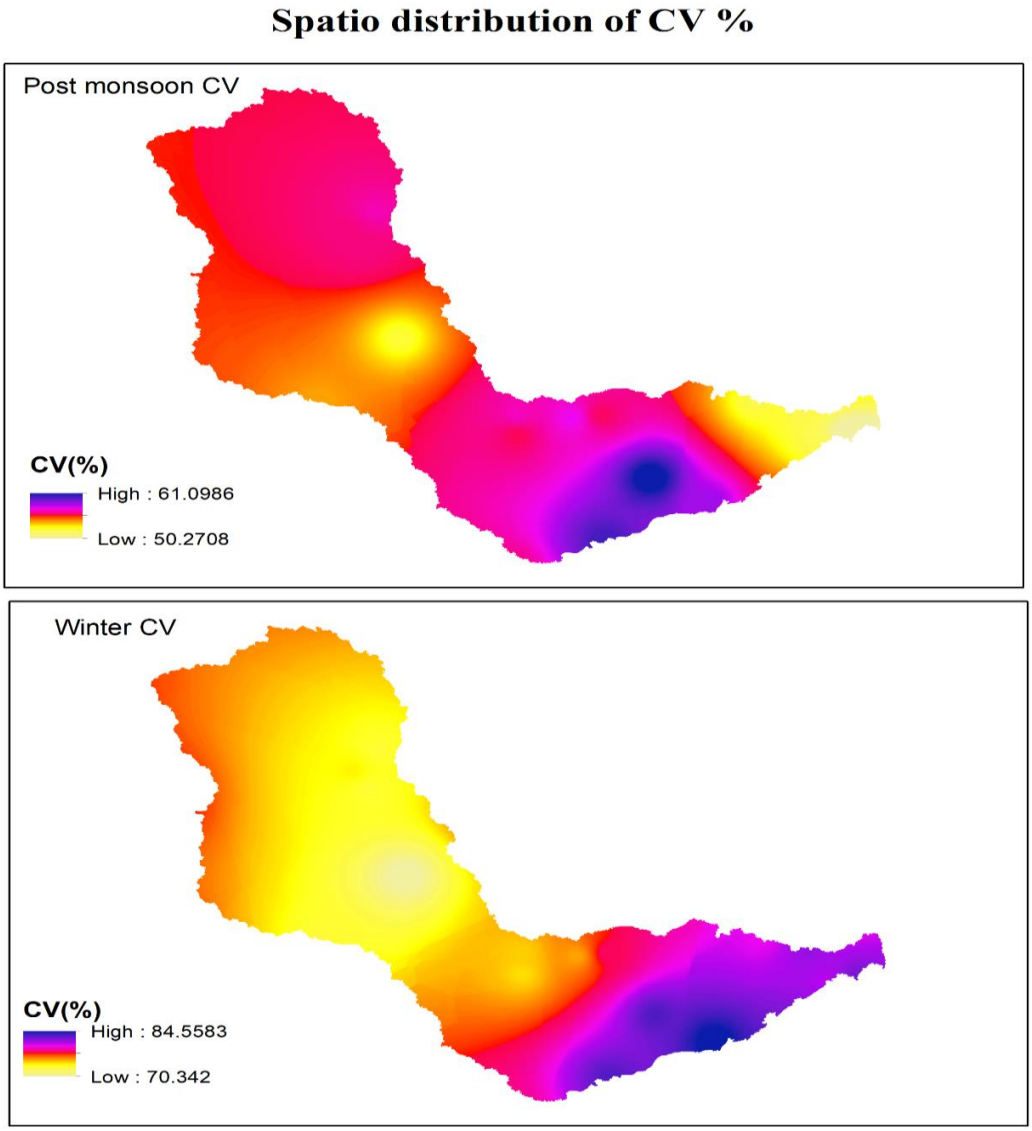

Fig 5.2(c) Spatial Distribution of Post Monsoon and Winter CV%

The PCI spatial distributions for annual and seasonal timescale are presented in Fig.5.3 (a–c). In the annual PCI ranged from 17.38 to 17.96. As shown in Table 5.1 and Fig. 5.3(a), In the annual time series, the findings of PCI indicate an uneven distribution of monthly rainfall in all stations. Moreover, in Fig.5.3(b), the values of Pre-monsoon and Winter PCI are in the moderate range, which indicates a moderate concentration of monthly rainfall distribution. In the monsoon period, PCI are less than 10, which means a uniform concentration of rainfall. Moreover, during post-monsoon, there was an irregular distribution of monthly rainfall in all stations. during the post-monsoon, the PCI values were higher than that of all other seasons.

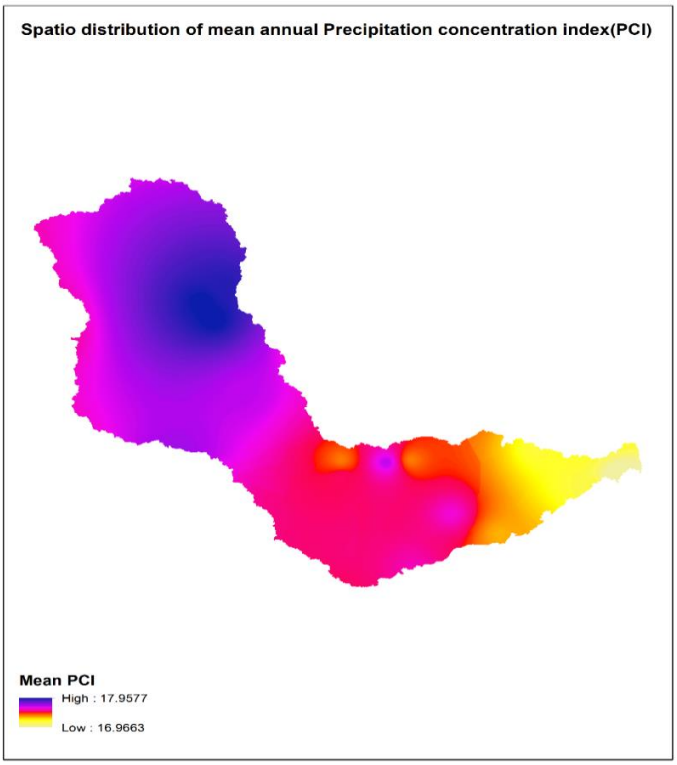

Fig 5.3(a) Spatial distribution of mean Annual precipitation concentration index (PCI)

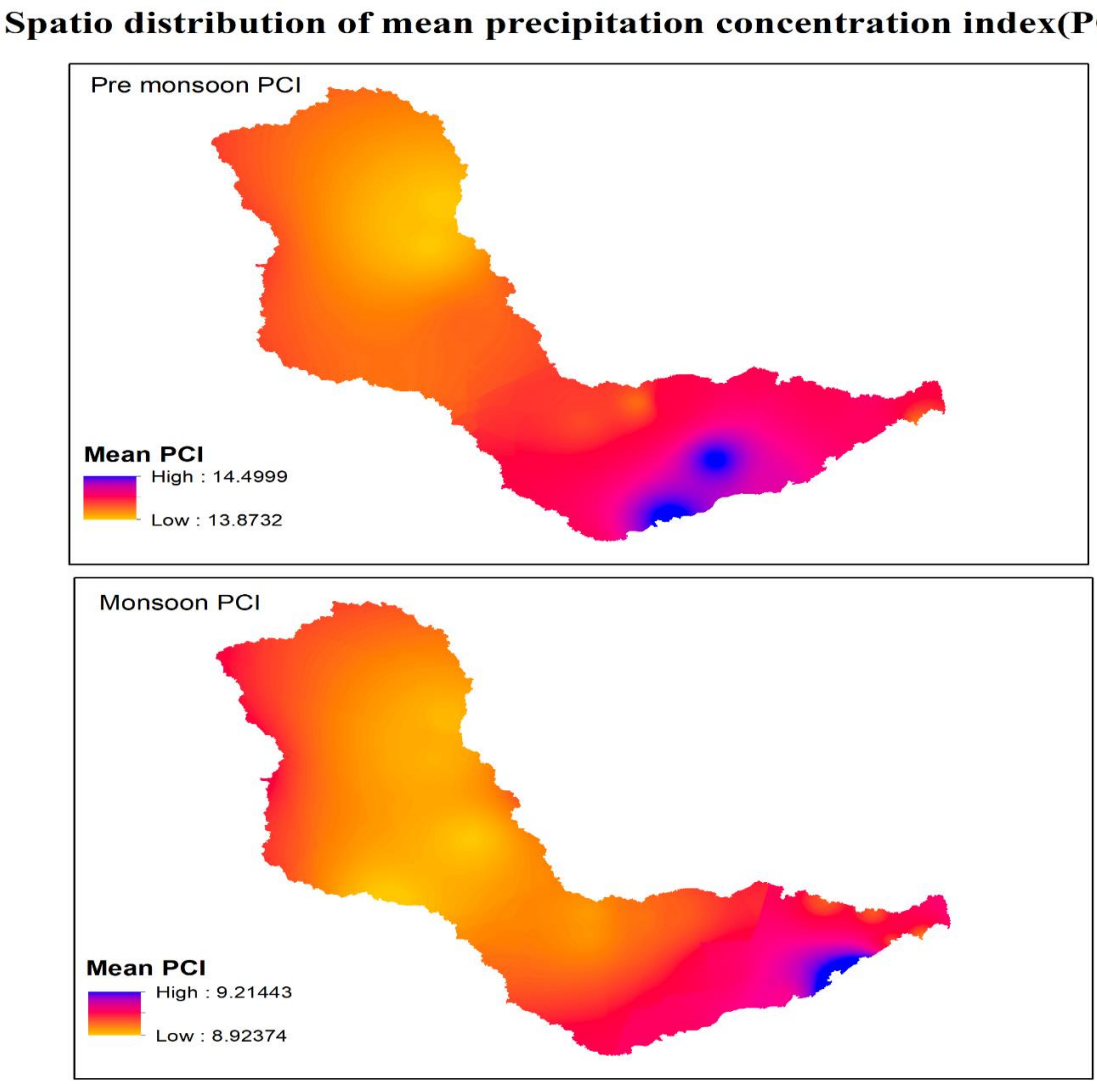

Fig 5.3(b) Spatial distribution of mean Pre-monsoon, Monsoon precipitation concentration index (PCI)

Spatio distribution of mean precipitation concentration index(PCI)

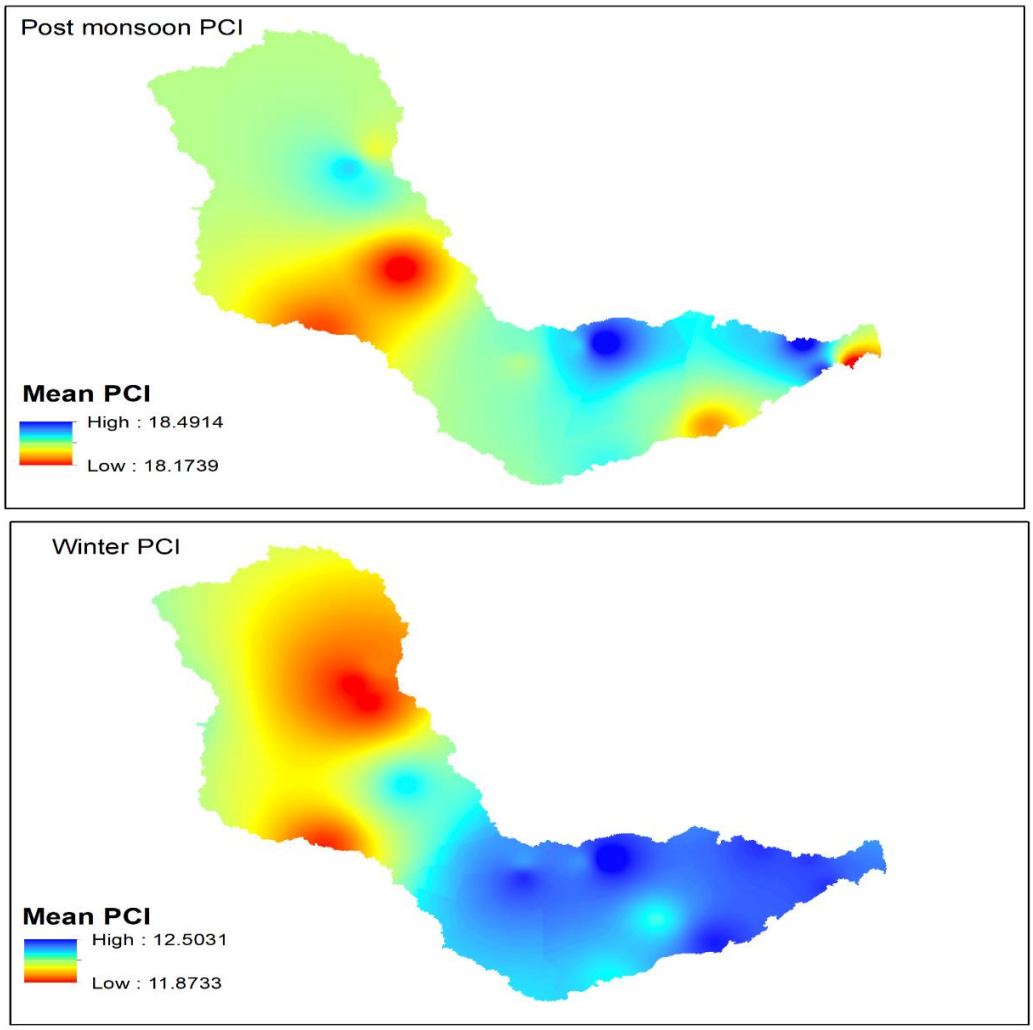

Fig 5.3(c) Spatial distribution of mean Post monsoon and Winter precipitation concentration index (PCI)

Fig. 5.4(a–c) shown the SAI spatial distribution for annual and seasonal time scale in the Mayurakshi River Basin. As shown in Fig. 5.4 (a) negative anomalies of 43.75% were found in annual scale.

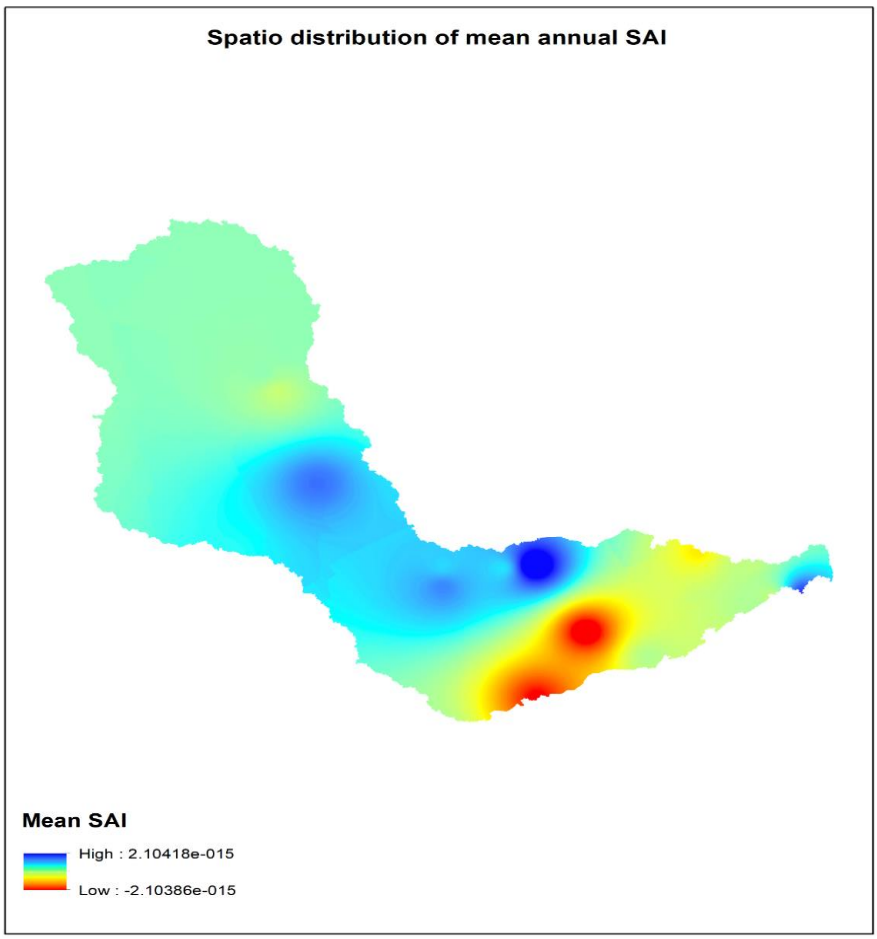

Fig 5.4(a) Spatial distribution of mean Annual SAI

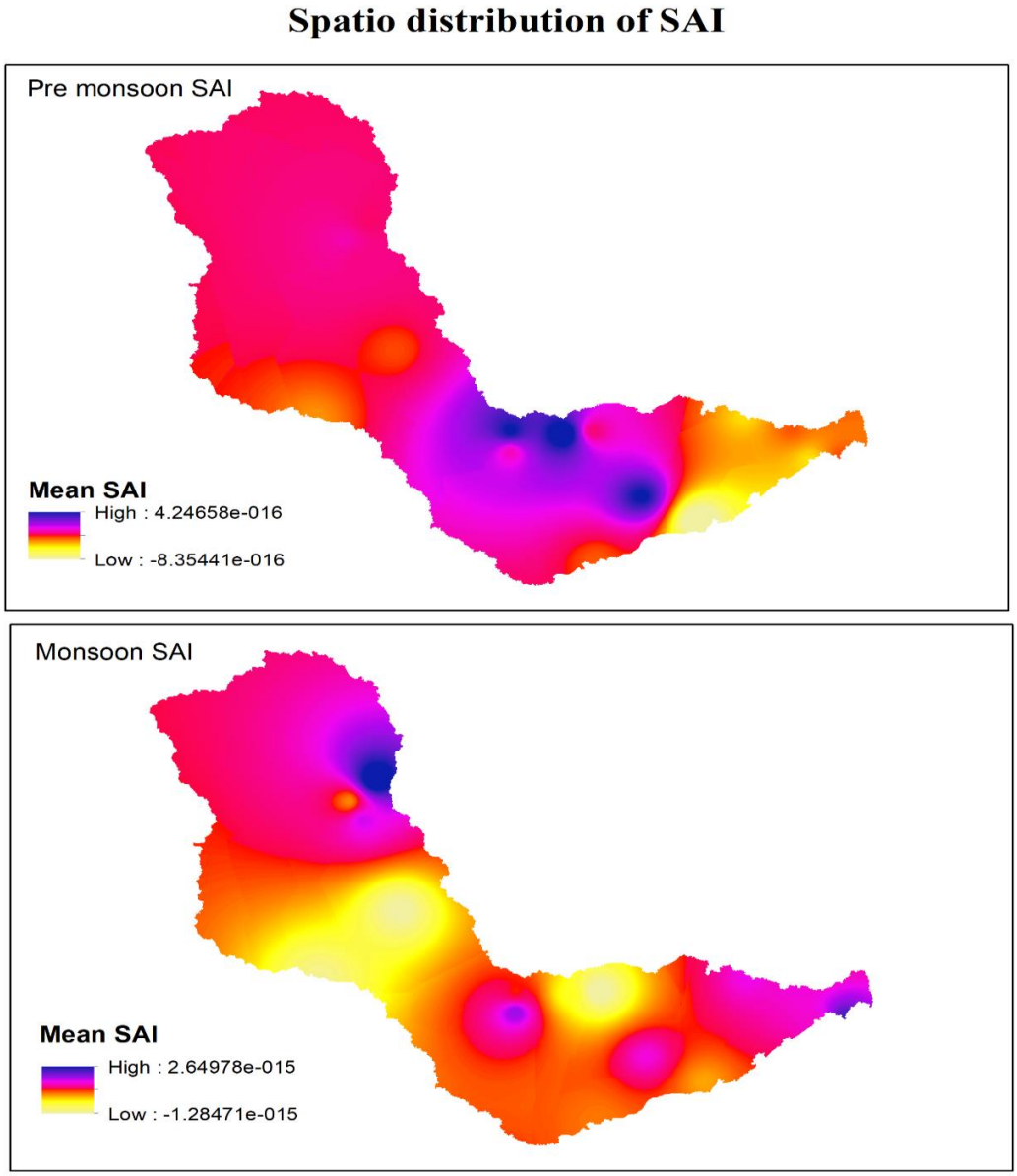

Fig 5.4(b) Spatial distribution of mean Pre-monsoon and Monsoon SAI

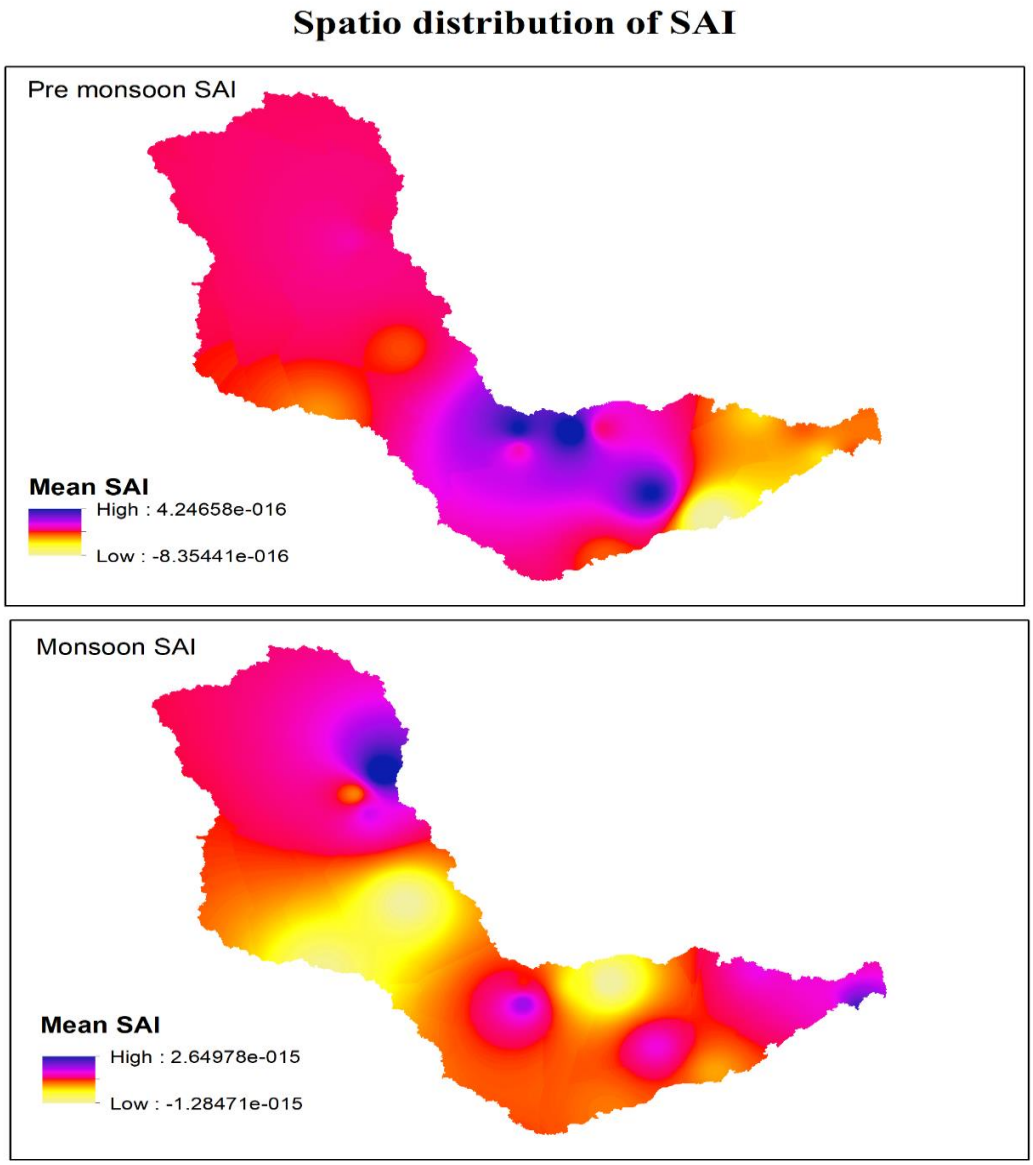

Fig 5.4(c) Spatial distribution of mean Post-monsoon and Winter SAI

The negative SAI values of pre-monsoon, monsoon, post-monsoon, and winter seasons were 81.25%, 25%, 37.5%, and 37.5% respectively. The dryness probability for the pre-monsoon is substantially higher than in other seasons. The SAI value indicates the severity and frequency of drought at various times of the year.Dry and wet periods can be identified quickly by looking at the spatial distribution of annual and seasonal rainfall patterns.

Altogether, CV, PCI, and SAI approaches were used to estimate seasonal and annual rainfall variability, and they had diverse characteristics. The CV value indicated the variability of rainfall; areas with low CV values are prone to floods, whereas those with high CV values are prone to drought. When the PCI is less than 10, it indicates a regular monthly rainfall distribution, which is usual throughout the rainy season. However,during dry seasons the highest value of PCI showed a very high irregular distribution of rainfall patterns. The PCI and SAI can be utilised as flood and drought indicators. Rainfall variability has the largest impact on water resource planning and management, agriculture production, soil fertility, and nutrition security. Furthermore, in rain-fed agricultural systems, seasonal variability in rainfall has a significant impact on crop productivity.

5.1.2. Temporal trend analysis by MK & ITA

5.1.2.1 Annual trend analysis

Table 5.2 shows the detected rainfall trend summaries in annual as well as seasonal time scale. The only significant increasing trend is detected Maharo at the level of 10% significance. In annual time series, 15 of the 16 rainfall stations exhibited statistically non-significant rising or declining patterns. In Table 5.2, Sen's slope estimators for annual rainfall are shown.

Table 5.2 MK and Sen's slope estimator in annual and seasonal rainfall trend analysis

Stations	Annual		Premonsoon		Monsoon		Post Monsoon		Winter	
	MK	Sen's slope	MK	Sen's slope	MK	Sen's slope	MK	Sen's slope	MK	Sen's slope
Tilpara barrage	0.15	3.96	0.18**	1.61	0.05	1.37	-0.01	-0.11	0.04	0.13
Suri	0.08	2.27	0.19**	1.68	0.06	0.15	0.02	0.15	0.04	0.12
Shyambati	0.17	4.70	0.11	1.05	0.06	1.41	0.09	0.87	0.03	0.07
Shekhampur	0.17	4.60	0.14	1.39	0.06	1.40	0.07	0.75	0.04	0.08
Sainthia	0.11	3.56	0.18	1.95	0.06	1.57	0.02	1.95	0.04	0.09
Narayanpur	0.10	2.73	0.10	1.69	0.07	1.81	0.09	0.60	-0.03	-0.10
Massanjore	0.15	4.40	0.22*	1.65	0.07	1.34	0.22	0.09	-0.01	-0.01
Maharo	0.14**	3.67	0.25	1.96	0.11	2.42	-0.01	-0.09	0.01	0.04
Kundahit	0.18	4.72	0.17	1.23	0.06	0.99	-0.04	-0.18	0.03	0.12
Kultore	0.16	4.22	0.19**	1.65	0.05	1.37	0.01	0.08	0.04	0.13
Kirnahar	0.10	3.07	0.11	0.90	0.08	2.51	0.08	0.70	0.01	0.03
Kandi	0.14	3.87	0.09**	1.10	0.03	1.23	0.07	0.42	0.02	0.03
Jama	0.13	4.07	0.21	1.77	0.12	2.66	-0.02	-0.19	0.01	0.03
Dumka	0.17	5.08	0.23*	1.77	0.11	2.52	-0.01	-0.08	0.10	0.05
Bharatpur	0.12	2.89	0.07	0.80	0.06	1.12	0.06	0.34	0.02	0.04
Kuli	0.13	3.37	0.10	1.10	0.02	1.12	0.06	0.34	0.01	0.03

*Significant at 5% confidence level, ** Significant at 10% confidence level

Sen's slope estimator magnitudes are recorded at all rainfall stations. In Dumka,the maximum magnitude of Sen's slope estimator of annual rainfall and in Suri the minimum magnitudes of Sen's slope estimators of annual rainfall were obtained. The ITA method's findings are shown in Fig. 5.5. (a, b). The majority of rainfall datasets are above the 1:1 (45°) line. The trend at all rainfall stations were non-monotonic. The findings of the ITA approach in the MRB are significant because it provide adequate knowledge about water resource management and flood and drought mitigation.

Table-5.3 Thes results of innovative trend analysis of annual rainfall at α=5%(1982-2021)

Station	Trend Slope	Slope Standard deviation	Lower CL	Upper CL
Tilpara	1.50	0.23	-0.45	0.45
Bharatpur	0.60	0.49	-0.95	0.95
Dumka	2.88	0.32	-0.63	0.63
Jama	2.78	0.24	-0.48	0.48
Kandi	1.03	0.54	-1.06	1.06
Kirnahar	1.76	0.76	-1.49	1.49
Kuli	0.82	0.47	-0.92	0.92
Kultore	1.42	0.28	-0.56	0.56
Kundahit	1.73	0.32	-0.62	0.62
Maharo	3.07	0.26	-0.51	0.51
Massanjore	2.25	0.36	-0.71	0.71
Narayanpur	1.64	0.50	-0.98	0.98
Saithia	1.15	0.35	-0.69	0.69
Suri	1.64	0.29	-0.57	0.57
Shyambati	1.25	0.58	-1.14	1.14
Sekhampur	1.51	0.55	-1.08	1.08

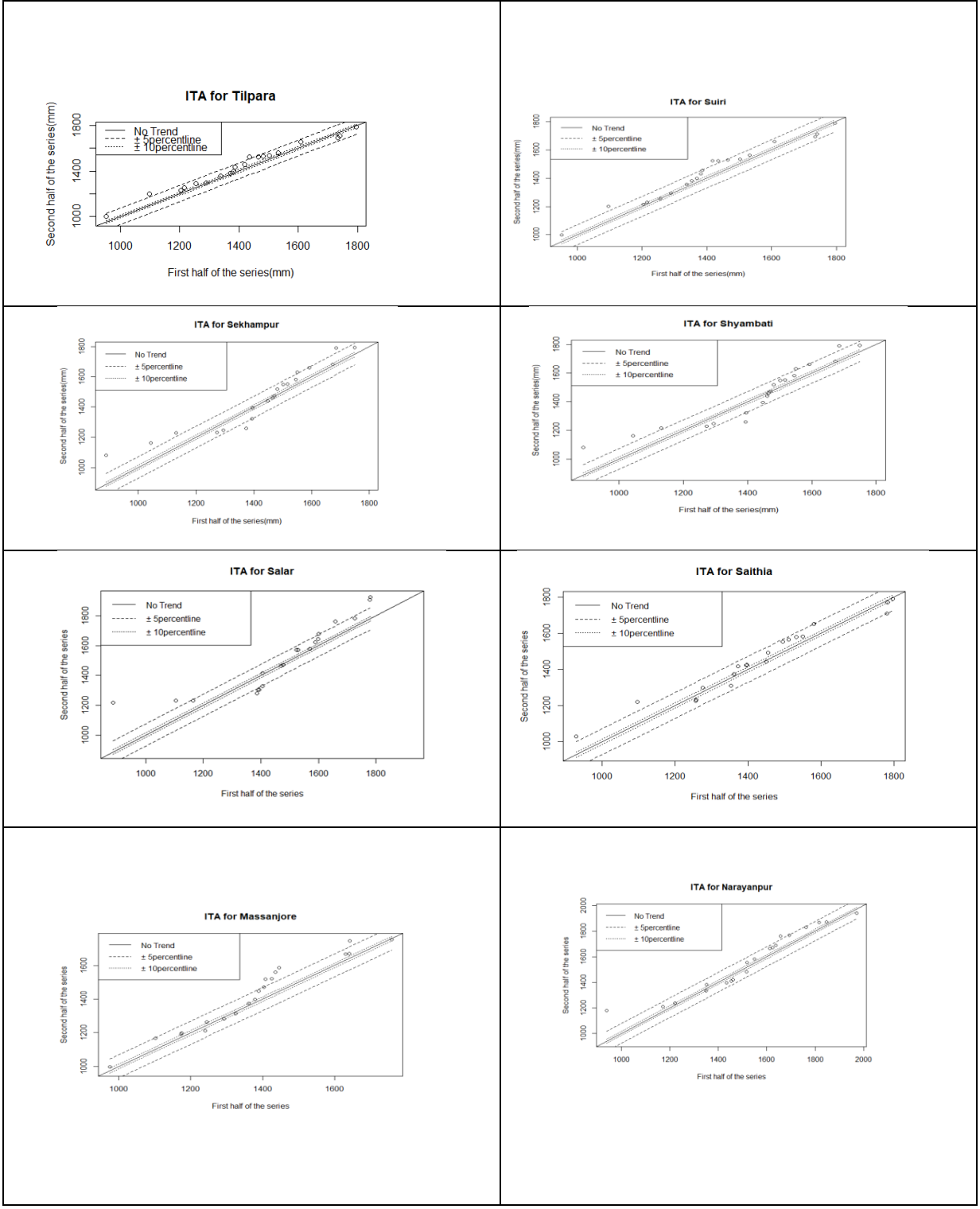

Fig 5.5(a) The Results of ITA method for annual rainfall in the study area

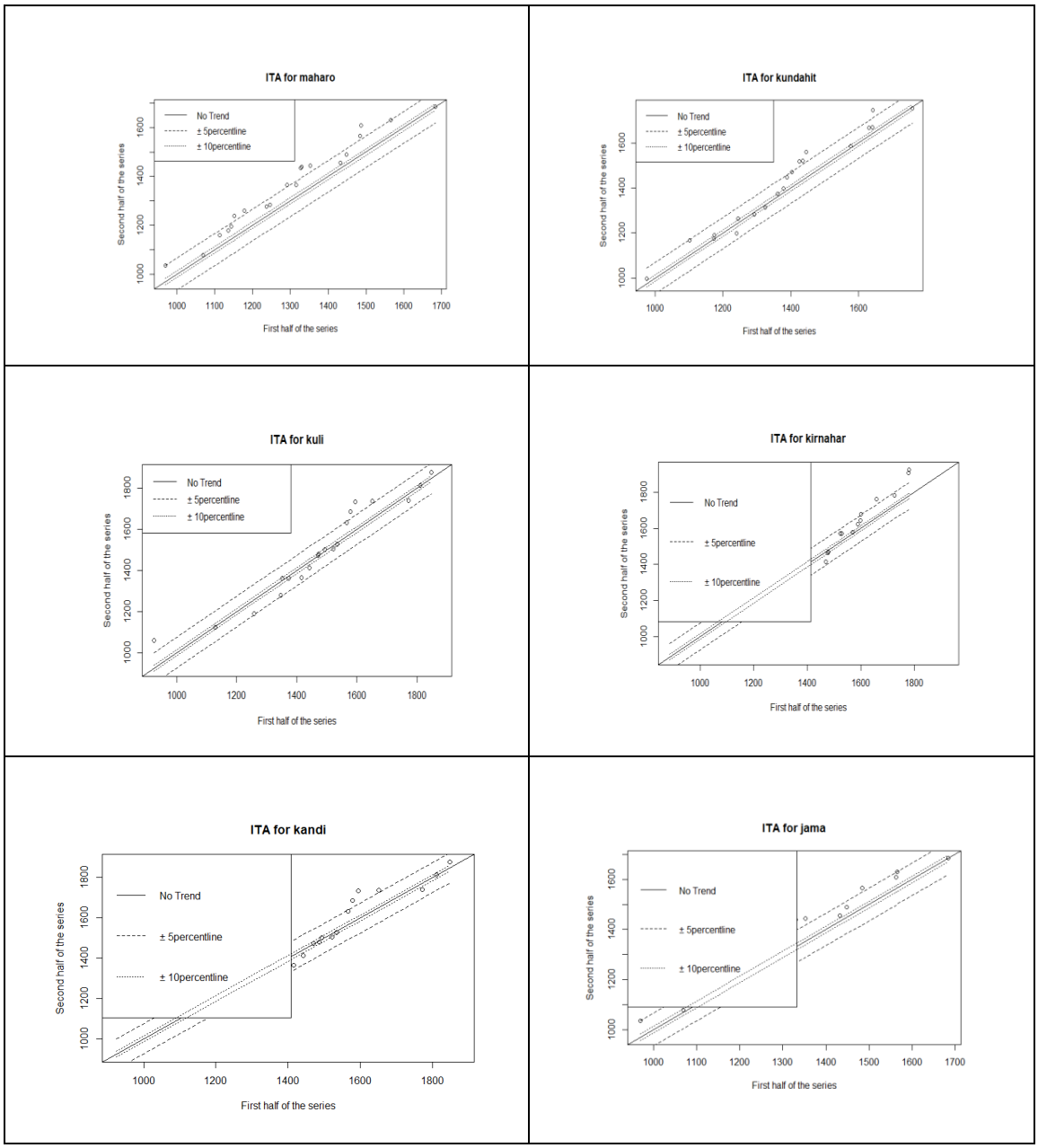

Fig 5.5(b) The Results of ITA method for annual rainfall in the study area

5.1.2.2 Seasonal rainfall

Table 5.2 shows the statistical findings of the MK trend test and Sen's slope estimators for seasonal rainfall. From these findings, it is clear that all rainfall stations show an increasing pattern throughout the pre-monsoon season. Six rainfall stations showed statistically significant trends during this season. There was a significant positive trend at a 5% significance level in Dumka and Massanjore, and a significant positive trend at a 10% significance level in Jama, Tilpara, Kultore, and Suri. In the winter, monsoon, and post-season, no significant trend was identified, as shown in Table 5.2. MK and SSE's results indicate that rainfall patterns and trends in the annual and monsoon season are comparable. This commonality also implies that monsoon rainfall contributes significantly to annual rainfall throughout all Mayurakshi river basin stations. The correlation coefficient between mean annual rainfall and Monsoon rainfall is 0.86, which is considered as strong correlation. In general, these studies revealed that the monsoon season is the primary contributor of annual rainfall. In addition, there was a rising and declining trend in the Mayurakhi river basin, although the patterns were non- significant. The ITA approach differed depending on the season. All rainfall stations were found to have higher tendency throughout the Monsoon season. (See Figure 5.6(a,b))

Table 5.4. The results of innovative trend analysis(slope s) seasonal rainfall at α=5%(1982-2021)

Station	Premonsoon	Monsoon	Post Monsoon	Winter
Tilpara barrage	0.41	0.30	0.96	-0.16
Suri	0.24	0.51	1.11	-0.17
Shyambati	-0.67	0.61	1.50	-0.03
Shekhampur	-0.31	0.57	1.40	-0.03
Sainthia	-0.18	0.43	1.11	-0.17
Narayanpur	-1.32	1.87	1.49	-0.21
Massanjore	1.01	0.47	0.99	-0.15
Maharo	0.97	1.28	0.89	-0.10
Kundahit	0.47	0.58	0.85	-0.14
Kultore	0.15	0.35	1.09	-0.15
Kirnahar	-1.11	1.63	1.45	-0.06
Kandi	-1.08	1.12	1.24	-0.17
Jama	0.71	1.39	0.78	-0.10
Dumka	0.85	1.22	0.88	-0.09
Bharatpur	-1.23	0.87	1.19	-0.16
Kuli	-1.00	0.88	1.19	-0.17

For the Premonsoon there was some decreasing trends were found. However , during the post-monsoon all stations revealed an increasing trend analysis .The temporal variations of rainfall are more consistent for pre-monsoon season. Winter season shows the most decreasing trend analysis of rainfall. Most rainfall stations exhibited a non-monotonic trend throughout all timescales. Each season has a different level of rainfall variability. If this trend continues in the future period, it will highly influence the water resources potential of the region and, hence, the agriculture, too. The increasing trend during the Monsoon season might predict flood occurrences. The Monsoon is the

best season for agricultural activity due to heavy rain. This finding is significant because it has importance for water resource planning and management strategies.

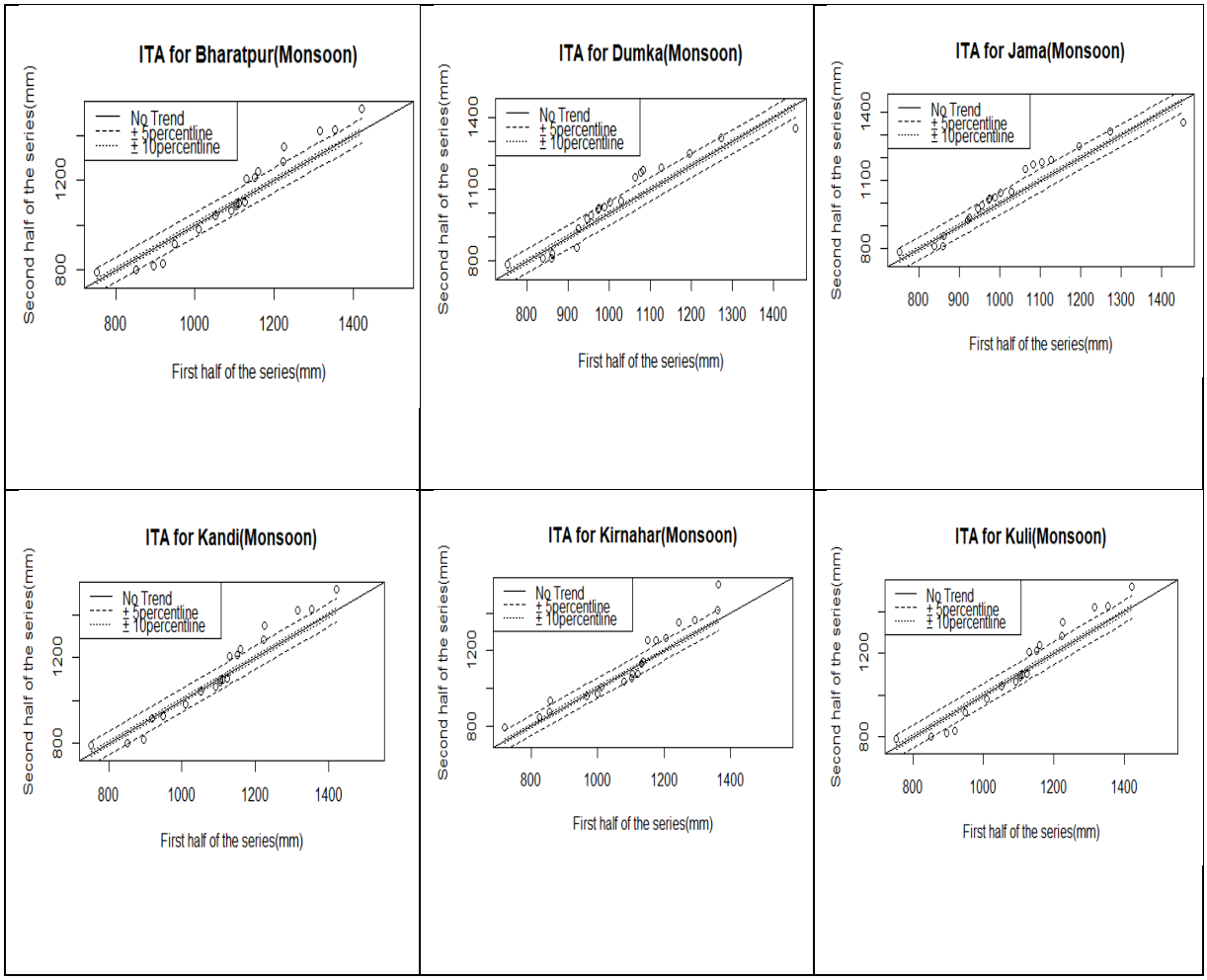

Fig 5.6(a) The Results of ITA method for monsoon rainfall in the study area

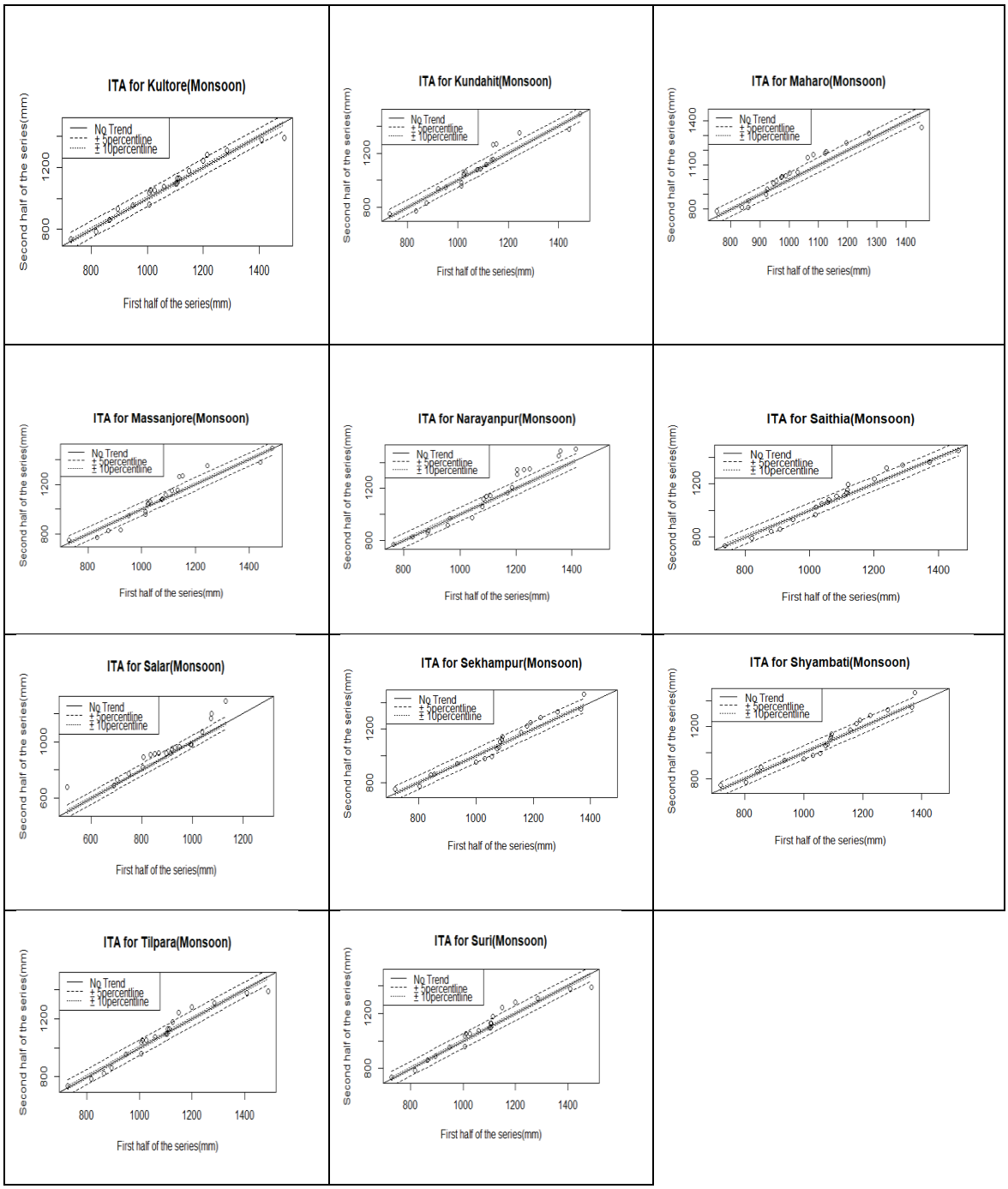

Fig 5.6(b) The Results of ITA method for monsoon rainfall in the study area

The temporal evaluation of SAI in annual and seasonal rainfall is given in Fig. 5.8(a,b), which is comparable to the findings of the MK and ITA methodologies. During the annual time period, nine and seven rainfall stations, respectively, had positive and negative SAI values. Despite the MK trend test findings, all rainfall stations exhibited increasing trends (Table 5.2).

Fig 5.7(a) Temporal evaluation of SAI

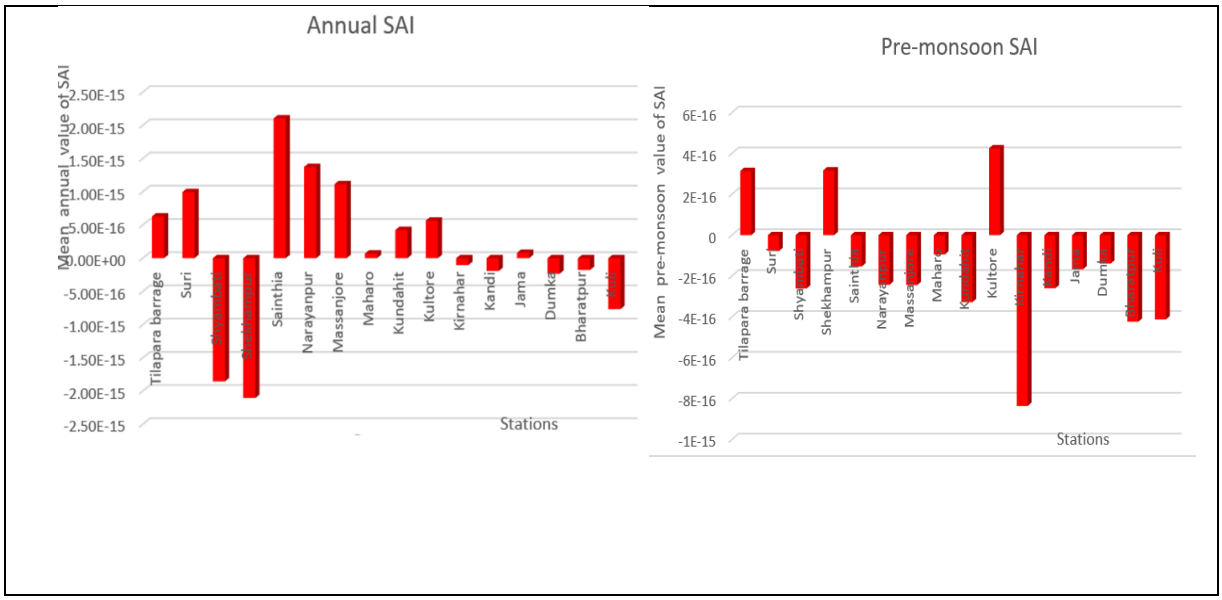

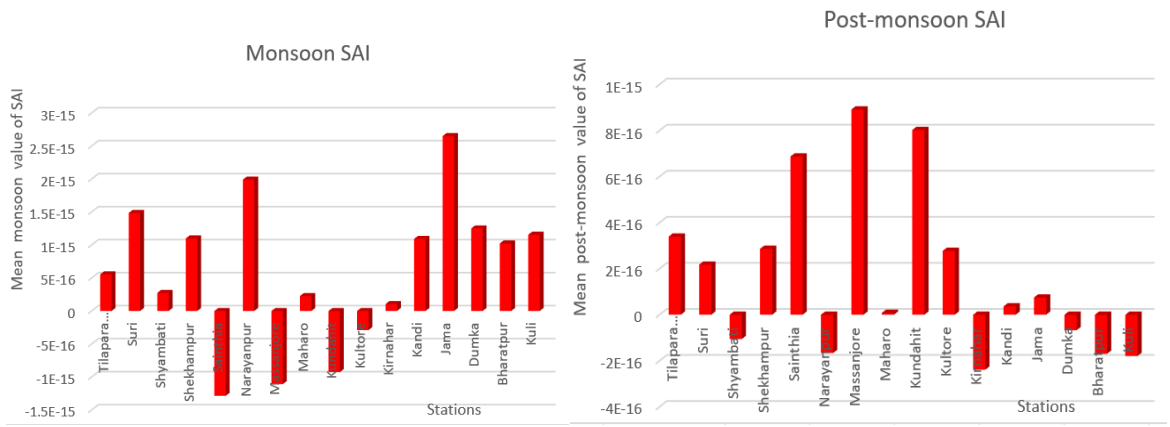

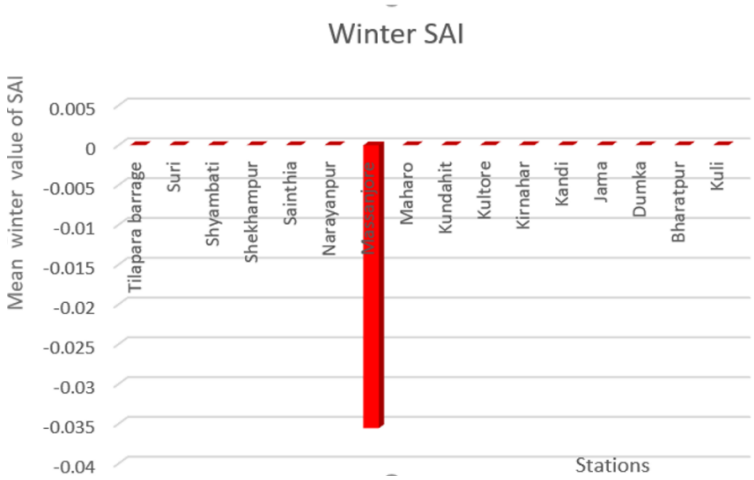

Fig 5.7(b) Temporal evaluation of SAI

Similarly, in the ITA approach, all of the stations exhibit an annual trend analysis that is increasing. During the pre-monsoon and post-monsoon periods, a large portion of the rainfall stations showed positive and negative SAI values. The MK and ITA methods produced similar findings. These findings suggest that SAI has a positive relationship with the MK and ITA procedures in the MRB. Furthermore, in most rainfall stations, the relationship between SAI, MK, and ITA is shown to be consistent. Furthermore, the analysis of this relation may aid in better understanding the temporal variability of rainfall, which may have an impact on the studied area's wet and dry seasons.

5.1.2.3 Spatial mapping of annual and seasonal rainfall trends by MK and ITA method

The MK and ITA techniques were used to determine the spatial distribution of annual and seasonal rainfall trends (Figs. 5.8(a, b) and 5.9(a, b))

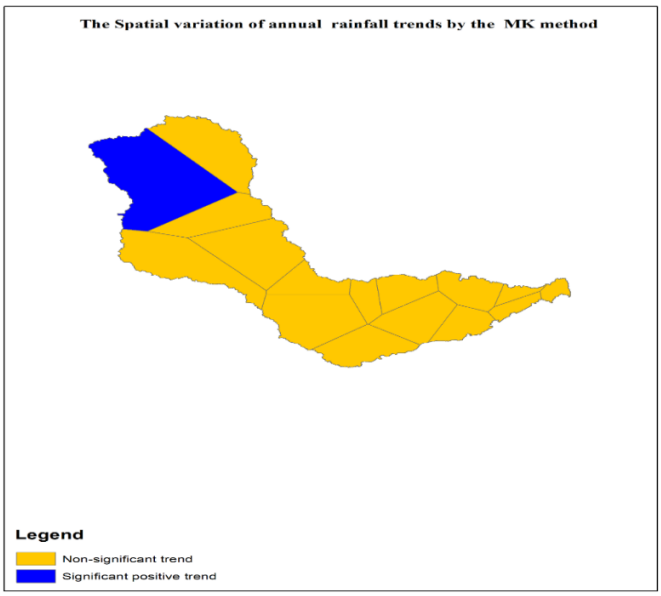

Fig 5.8(a) Spatial distribution of annual rainfall by MK test at 10% significance level

Fig 5.8(b) Spatial distribution of Pre-monsoon, Monsoon, Post-monsoon and Winter rainfall trend identified by MK test at 5%,10% significance level.

The blue colour denotes a significant positive trend, the ginger pink colour denotes a significant negative trend, and the electron gold colour denotes a non-significant trend in the figures. As shown in Fig. 5.8(a, b) and Table 5.8, a considerable percentage of the stations' polygon showed non-significant trend in annual, monsoon, post-monsoon, and winter periods in the MK trend test (5.2).

Fig 5.9(a) Spatial distribution annual rainfall trend identified by ITA method at 5% level.

Fig 5.9(b) Spatial distribution of Pre-monsoon, Monsoon, Post-monsoon and Winter rainfall trend identified by ITA method at 5%significance level.

A few regions of TPs showed a significant trend at a 5% significance level during the pre-monsoon season (Fig. 5.8(b)). However, as shown in Fig. 5.9(a, b) and Tables 5.3 and 5.4, all areas of the stations' polygon showed a significant positive trend in annual, monsoon, and post-monsoon periods in the ITA method's spatial map. In addition, eight station polygons displayed a significant positive and negative trend in the pre-monsoon season. The spatial map of annual and seasonal rainfall indicated heterogeneous trend behaviour in the area using both MK and ITA approaches. Malik et al. (2019) stated that the spatial variability of rainfall trend is critical for flood, drought, and severe event impact assessment and adaptation planning.

Table 5.5 Comparison of results of MK and ITA methods at study area

	Annual		Post-Monsoon		Pre-Monsoon		Mosoon		Winter	
Stations	MK	ITAM	MK	ITAM	MK	ITAM	MK	ITAM	MK	ITAM
Tilapara barrage	No	Yes(+)	No	Yes(+)	Yes(++)	Yes(+)	No	Yes(+)	No	Yes(-)
Suri	No	Yes(+)	No	Yes(+)	Yes(++)	Yes(+)	No	Yes(+)	No	Yes(-)
Shyambati	No	Yes(+)	No	Yes(+)	No	Yes(-)	No	Yes(+)	No	Yes(-)
Shekhampur	No	Yes(+)	No	Yes(+)	No	Yes(-)	No	Yes(+)	No	Yes(-)
Salar	No	Yes(+)	No	Yes(+)	No	Yes(-)	No	Yes(+)	No	Yes(-)
Sainthia	No	Yes(+)	No	Yes(+)	No	Yes(-)	No	Yes(+)	No	Yes(-)
Narayanpur	No	Yes(+)	No	Yes(+)	No	Yes(-)	No	Yes(+)	No	Yes(-)
Massanjore	No	Yes(+)	No	Yes(+)	Yes(+)	Yes(+)	No	Yes(+)	No	Yes(-)
Maharo	Yes(++)	Yes(+)	No	Yes(+)	No	Yes(+)	No	Yes(+)	No	Yes(-)
Kundahit	No	Yes(+)	No	Yes(+)	No	Yes(+)	No	Yes(+)	No	Yes(-)
Kultore	No	Yes(+)	No	Yes(+)	Yes(++)	Yes(+)	No	Yes(+)	No	Yes(-)
Kirnahar	No	Yes(+)	No	Yes(+)	No	Yes(-)	No	Yes(+)	No	Yes(-)
Kandi	No	Yes(+)	No	Yes(+)	Yes(++)	Yes(-)	No	Yes(+)	No	Yes(-)
Jama	No	Yes(+)	No	Yes(+)	No	Yes(+)	No	Yes(+)	No	Yes(-)
Dumka	No	Yes(+)	No	Yes(+)	Yes(+)	Yes(+)	No	Yes(+)	No	Yes(-)
Bharatpur	No	Yes(+)	No	Yes(+)	No	Yes(-)	No	Yes(+)	No	Yes(-)
Kuli	No	Yes(+)	No	Yes(+)	No	Yes(-)	No	Yes(+)	No	Yes(-)

*Yes (±) indicate significant increasing or decreasing trends at 5% significant level,Yes(++/--) indicate significant increasing or decreasing trends at 10% significant level,No indicate non-significant trends at 5% or 10% significant level

5.1.2.4 Comparison

Table 5.5 summarises the results of the MK trend test and the ITA approach for annual and seasonal rainfall. The ITA approach detected all of the important patterns revealed by the MK test. However, the ITA approach identified 15 rainfall sites that were not recognised by the MK trend test during the yearly season. As a result, the ITA approach is probably more suited to detect many hidden significant rainfall patterns Furthermore, the ITA approach is considered to be more resilient for trend analysis in time-scales data because it can be represented graphically using a cartesian coordinate system, providing a clear visual representation for additional understanding. It's a graphical approach that allows a user to view trends in different groups. Sen agreed with this viewpoint (2017).

5.2. Hydrological Modelling

5.2.1 Evaluation of hydro-meteorological dataset

The comparisons of rainfall, ET,and streamflow time series show a Seasonal constancy is significant, and having a strong seasonal cycle that peaks between May and September.During the month of June,July there is often a significant rainfall and high streamflow. The maximum rainfall intensities occurred during the May-July periods, which are associated with several storms. The months of November through February are slightly drier than the rest of the year, as seen by low rainfall.Due to little rainfall in the months of November and February, the discharge is low(Fig.5.10)

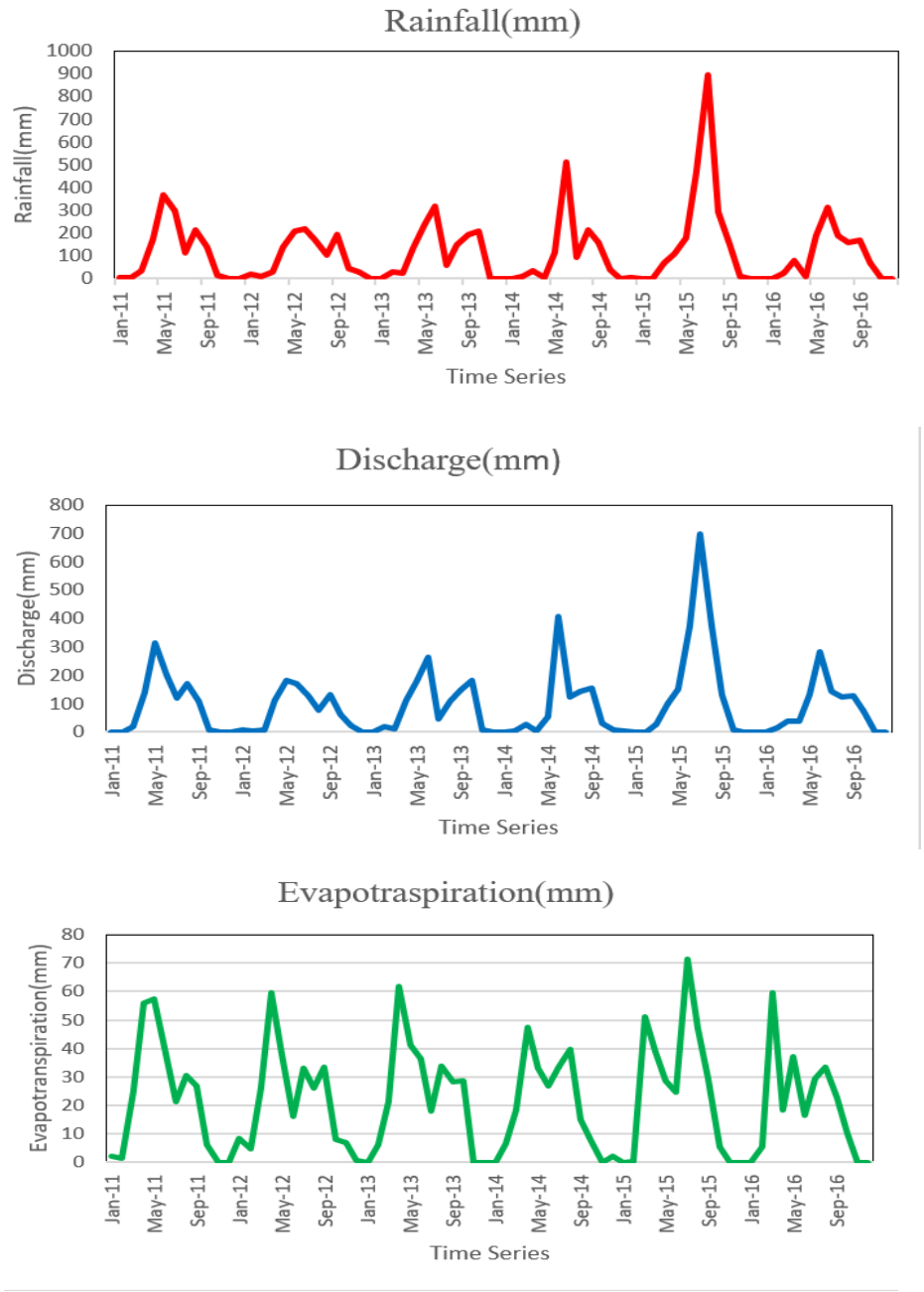

Fig 5.10 Time series plot for (a) Rainfall, (b) Discharge, (c) Evapotranspiration

The trend of ET shows that throughout the post-monsoon and winter seasons, much lower values are recorded; nevertheless, towards the middle of April, the graph shows a progressive increase. High solar radiation and temperature over the summer are responsible for increasing ET, which led to a high soil moisture deficit.

The results indicate that rainfall and discharge in this watershed are highly sensitive to one another, with a consistent pattern throughout the research period. Higher ET values are also obtained from March to September, which may be attributed to the considerable effect of net radiation and temperature.

5.2.2 Model Initialization

Minor land use/land cover, slope, and soil types were ignored while identifying HRUs, with a 10% threshold applied to avoid an excess of HRUs in the analysis. The system was run for eight years, from 2008 to 2016, with the first three years serving as a warm-up period.The calibration period was 2011-2013 (see Fig. 5.11a), while the model was validated using the remaining two years of the dataset, 2014-2016. (see Fig. 5.1b). For model sensitivity, calibration, and uncertainty analysis, the SWAT- CUP (calibration and uncertainty programs) was used.

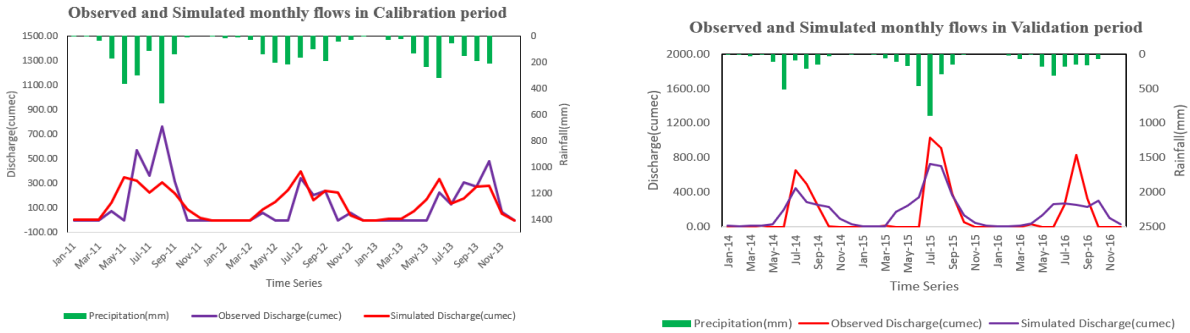

Fig-5.11(a) observed & simulated streamflow during calibration (b)observed & simulated streamflow during validation

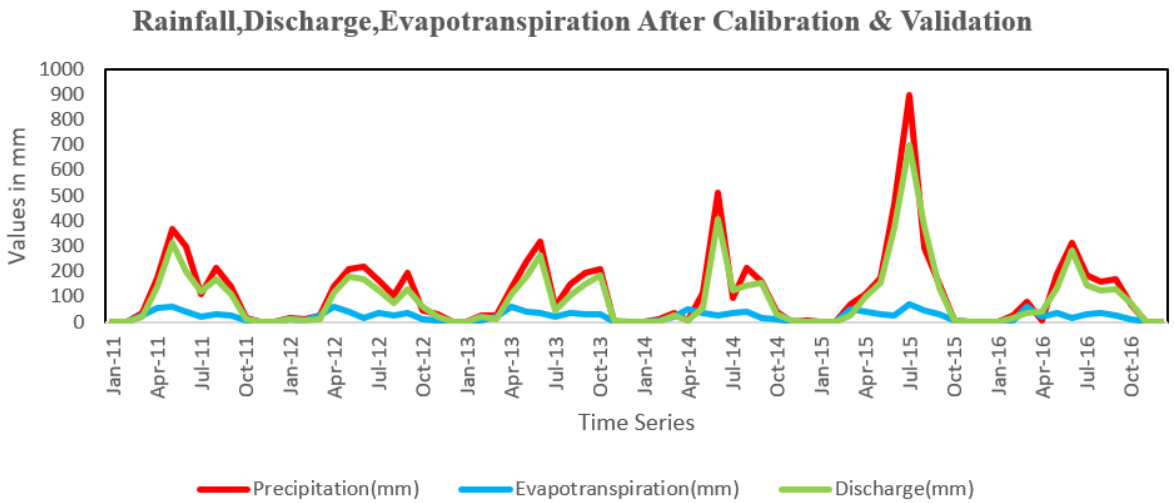

Fig:5.12 Precipitation, Evapotranspiration, and Surface Runoff after calibration and validation

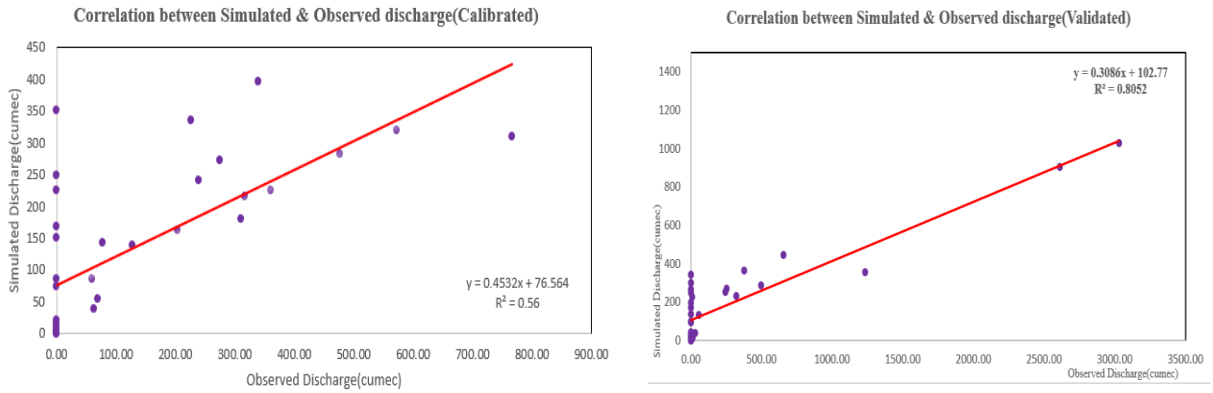

Fig 5.13Correlation between observed and simulated results during (a) calibration (b)validation

Here the SWAT-CUP documentation had been followed and a comprehensive calibration based on sensitivity analysis of model parameters was completed. Based on previous research and SWAT documentation, For streamflow prediction, a total of 14 SWAT parameters were used for model calibration and uncertainty analysis.

Table-5.6 Sensitivity analysis of SWAT model before the calibration & validation

Parameter Name	t-Stat	P-Value
CN2	-0.48	0.64
ALPHA_BF	1.46	0.15
GW_DELAY	0.56	0.58
GWQMN	1.55	0.13
GW_REVAP	-0.21	0.83
ESCO	-0.63	0.53
CH_N2	-0.06	0.96
CH_K2	0.31	0.76
ALPHA_BNK	-2.81	0.01
SOL_AWC	0.61	0.54
SOL_K	-0.20	0.84
SOL_BD	-0.11	0.91
SFTMP	-0.71	0.48
SURLAG	1.28	0.21

5.2.3 Model calibration and Sensitivity analysis

The sensitivity of the model parameters used for SWAT calibration was depicted using dotty plots (Fig 5.14). The results of a calibration run with NS as the goal function are shown hereunder. The dotty plot was conditioned in SUFI-2 with an NS threshold of 0.61, and all of the sampled parameters were gathered as behavioural samples. When a parameter has a clear and unmistakable peak, it is likely to be the parameter with the highest probability. In the Mayurakshi River Basin, insensitive parameters were detected using diffusing peaks represented by cumulative distribution, suggesting that the parameter was less capable of predicting flow. The Sensitivity Analysis of model parameters were within acceptable limits.As a conclusion, this calibrated model may be used for a variety of purposes, including assessing the

influence of climate change on streamflow in the MRB, water resource planning and management, and LULC changes.

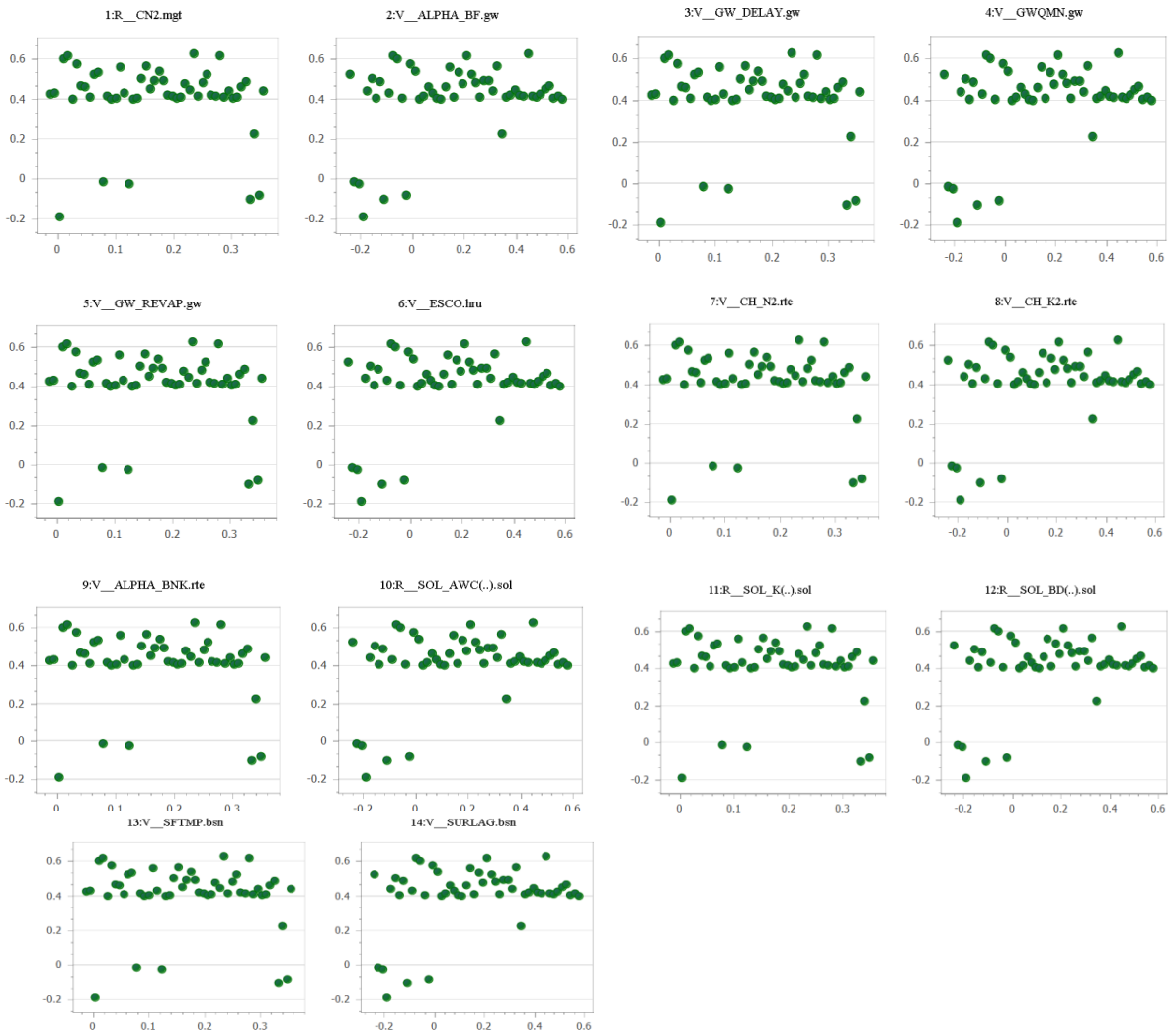

Fig-5.14 Results of Dotty plots for sensitivity analysis

Table It summarizes the results and analysis of the parameters used in the sensitivity analysis. All 14 sensitive factors are found to be applicable for surface flow, groundwater, channel routing, and soil properties, according to the results of the sensitivity analysis. A range of SWAT model parameters were used in model calibration, indicating that some poor findings might be related to model component structural problems.The findings show that the 95PPU covers the majority of the observations with varied parameters, indicating that SUFI-2 may capture model behavior. The results of the SWAT simulations appear to be sufficient for discharge prediction, The final parameter ranges were determined to be the best solution for the Mayurakshi River basin.The majority of observed values during calibration and validation were within the 95PPU boundaries, indicating that SWAT model uncertainties were Include CN2, ALPHA_BF, GWQMN, SOL_K,SOL_BD, GW_REVAP,GW_DELAY, SFTMP,ALPHA_BNK & SURLAG.

Table 5.7 Sensitivity analysis of swat model parameters after calibration & validation

S. NO	Parameters	Fitted Value	Minimum Value	Maximum Value	P	T
1	CN2	0.24	-0.02	0.36	0.34	-0.97
2	ALPHA_BF	0.45	-0.25	0.59	0.01	2.59
3	GW_DELAY	66.95	64.36	323.24	0.32	-1.01
4	GWQMN	0.41	0.40	1.48	0.78	0.28
5	GW_REVAP	0.08	0.08	0.24	0.85	0.19
6	ESCO	0.92	0.86	0.99	0.97	-0.04
7	CH_N2	0.18	0.08	0.23	0.46	0.75
8	CH_K2	58.41	11.45	91.05	0.11	1.65
9	ALPHA_BNK	0.07	-0.28	0.58	0.04	2.13
10	SOL_AWC	-0.06	-0.19	0.21	0.95	0.07
11	SOL_K	-0.30	-0.91	0.24	0.25	1.16
12	SOL_BD	-0.04	-0.18	0.48	0.41	-0.83
13	SURLAG	-1.75	-2.98	2.38	0.44	-0.79
14	SFTMP	14.99	7.52	22.76	0.36	0.93

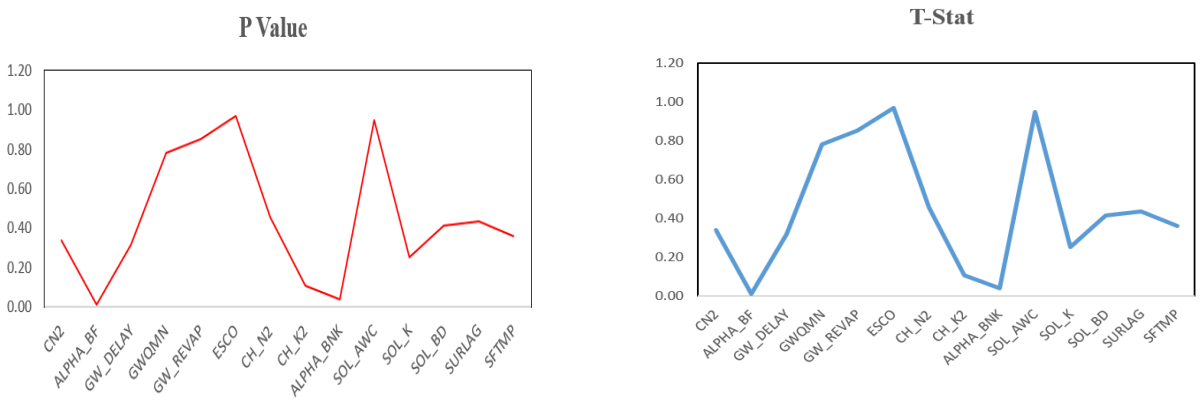

Fig-5.15 The t-stat value and P value for each of parameter

5.2.4 Uncertainty of streamflow

In the current work, The SUFI2 (Sequential Uncertainty Fitting) algorithm was used, which was developed by Abbaspour et al(2004, 2007). "The Uncertainty is an interface for SWAT model calibration, validation, uncertainty, and sensitivity analysis, and it converges with a relatively smaller number of iterations and provides the possibility of restarting an unfinished iteration and splitting iteration into several runs," according to the recommendation. Due to a lack of gauge network, the meteorological data of the stations closest to the sub-centroid basin's is frequently used to depict the conditions. Direct accounting of climatic inputs such as rainfall, humidity levels, wind, solar radiation, or temperature error distribution is challenging since data from multiple stations is often unavailable.

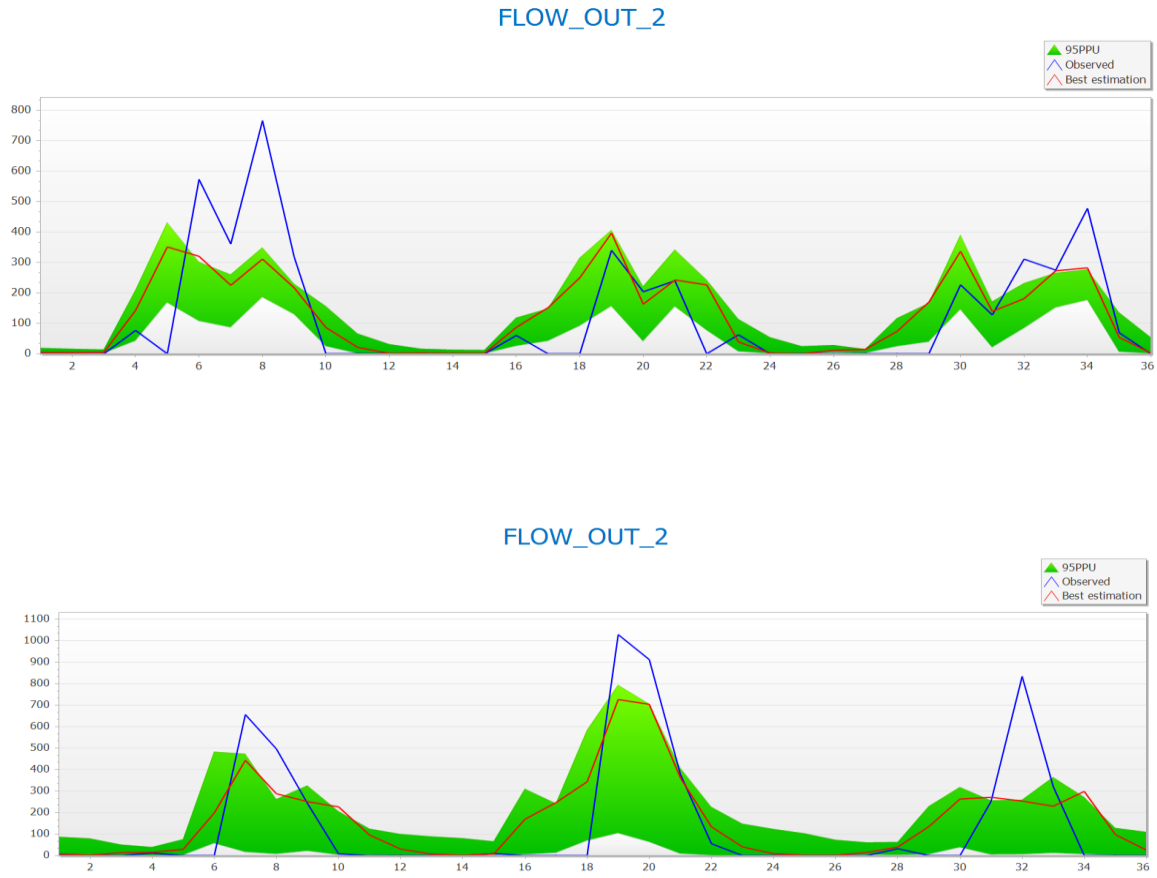

Fig-5.16(a) 95% probability uncertainty plot and observed streamflow during a calibration(2011-2013) and (b) validation(2014-2016) (From SWAT-CUP Output)

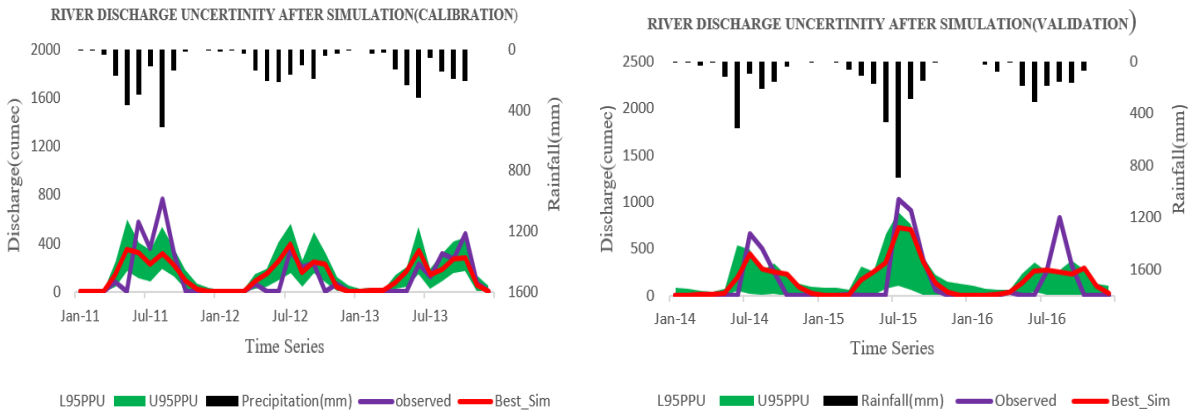

Fig 5.17 (a) River discharge uncertainty after calibratio (b) River discharge uncertainty after validation

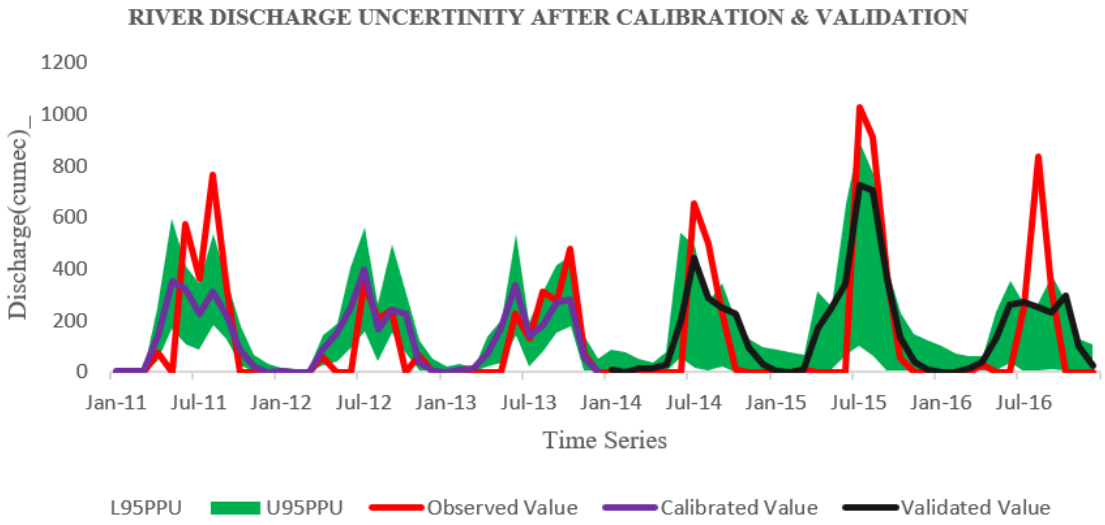

Fig-5.18 Discharge uncertainty after calibration & validation

5.2.5 Model performance Analysis

Performance analysis of the model was done with the help of several statistical parameters. The performance analysis of the model is based on the period of calibration and validation based on the observed and simulated data. All the statistical parameters indicate the good performance of the whole model. Comparison between the observed and simulated values of river discharge during the calibration and validation period with the scatter plot yields good results (0.56 and 0.80 respectively). Similarly, after performing statistical performance analysis separately on the calibration and validation period of monthly observed and simulated data, quite good results are seen according to R^2, NSE, and PBIAS. In the case of monthly calibration, the values of R^2, NSE, and PBIAS on river discharge are 0.56,0.61 and -7.9 respectively and in the case of validation, the values are 0.63,0.66, and -14.2 respectively.

Table-5.8 Performance analysis of swat model

	P FACTOR	R FACTOR	PBIAS	NSE	RSR	R^2
CALIBRATION (2011-2013)	0.24	0.5	-7.9	0.61	0.67	0.56
VALIDATION (2014-2016)	0.25	0.77	-14.2	0.63	0.61	0.66

CHAPTER 6: CONCLUSION

This study focused on assessing the nature of hydrological stress on rainfall variability of Mayurakshi river basin under changed climate scenario. At first, the spatial distribution and temporal rainfall variability and trend analysis was conducted in the Mayurakshi river basin. It was assume that it is important to understand the effects of climate change as it reflects different phenomenon of floods and droughts.For the rainfall variability and trend analysis of Mayurakshi River Basin data of time period 1982-2021 was collected and analyzed. During this study for the mean annual rainfall was 1428.98mm, with a CV of 14.65 % and an SD of 201.89 mm. The Coeffient of Variation of rainfall showed less variability in annual time scale as well as Monsoon time scale.But during post monsoon and winter very high variability of rainfall was observed. It showed a good corelation between distributions of rainfall in the Mayurakshi River Basin.Evenly distributed PCI was observed in annual as well as in seasonal time scale.The spatial distribution of SAI in Mayrakshi river basin was noticed to have experienced variability through out the study period.

In the Mann-kendall trend analysis more non-significant trends were detected in mean annual rainfall except in Maharo station which had significant trend at 10% significance level. At Dumka station the highest magnitude of SSE of mean annual rainfall was observed and lowest was found at Suri station.The MK trend analysis and SSE indicated increasing and decreasing trends in most rainfall stations throughout the monsoon and winter timescales,respectively. No significant trend was detected at Monsoon season. There was significant trend detected in pre-monsoon season at six stations. However, in the post monsoon season, increasing and decreasing trends were detected in all of the rainfall stations but the trends were statistically non-significant. In addition, the results of the ITA method all stations fall above and below the 1:1 (45°) line, and all rainfall stations were significant at the 5% level.For annual time scale non-monotonic trends were observed in most rainfall stations .In monsoon time period increasing trends were found in most rainfall

stations,however low rainfall ocuured in winter time scale mostly exhibited a decreasing trend.All this findings indicate that the Mayurakshi river basin is more likely to experience significant flood risk during monsoon.In addition, the spatial map of the ITA method,all portions of theissen polygon showed significantly positive trends at the 5% level in annual,monsoon and postmonsoon.For the pre-monsoon time scale half rainfall stations have significant negative trend and half stations have significant positive trend. In winter all rainfall stations have significant negative trends at the 5% significance level. In this study, the MK test and ITA approach yielded findings that were completely consistent with trend analysis in both annual and seasonal time scales. All the significant trends which were detected by the MK trend analysis were also observed by using the ITA method at a 5% significance level.Moreover during annual,winter, monsoon, and post monsoon season, the MK trend test could not detect the significant trend,but it could be identified by the ITA method This demonstrated that the ITA approach is more accurate in recognizing several hidden significant rainfall trends . In addition by the MK trend test monotonic trend analysis could be done with time-series data. The ITA approach, on the other hand, gave both monotonic and non-monotonic trend analysis. As a result, the findings of this study may be used to plan and manage water resources, as well as analyse and manage the effects of climatic risks such as floods & droughts. Further research might highlight the study's usefulness and implications in various Indian river basins.

Hydrological modelling is the second objective of the present study For efficient hydrological prediction, such as discharge, thorough model calibration is required. The uncertainty in the model prediction along with the outcomes for good modelling technique is essential. The SWAT model was used to simulate streamflow in the Mayurakshi river basin from 2008 to 2016, after a calibration (2011-2013)and validation(2014-2016) examination using the SUFI-2 approach. SUFI-2 is a prominent algorithm for estimating a hydrological model's sensitivity and uncertainty. The SWAT model's most significant benefit is that it includes a sensitivity analysis of the model's parameters.As a result, it is useful for presenting relatively appropriate results to end-users and

generating appealing model predictions. The model is adequate to predict the stremflow in the Mayurakshi river basin, as per the outcomes of the sensitivity and uncertainty analysis using SWAT and SUFI-2. The SWAT-CUP is beneficial to predict strem flow and to estimate uncertainties in the aspects of water resources, according to the findings of this study . In the case of monthly calibration, the values of R^2, NSE, and PBIAS on river discharge are 0.56,0.61 and -7.9 respectively and in the case of validation, the values are 0.63,0.66, and -14.2 respectively. Based on the calibration and validation findings, the model satisfactorly simulated the streamflow which was observed in the Mayurakshi River Basin.The calibrated model might be used to assess the impact of climate change as well as LULC on water resources in the upcoming days. In future studies, it is suggested to use more uncertainty techniques for hydrological modelling.

REFERENCE

1. "Spatial-temporal rainfall trend and variability assessment in the Upper Wabe Shebelle River Basin, Ethiopia: Application of innovative trend analysis method" by Arus Edo Harkaa, Nura Boru Jiloa, Fiseha Behulub (2021). https://doi.org/10.1016/j.ejrh.2021.100915
2. Alemayehu, T., Furi, W., Legesse, D., 2007. "Impact of water overexploitation on highland lakes of eastern Ethiopia." Environ. Geol. 52, 147–154.
3. Alemu, M.M., Bawoke, G.T., 2019. "Analysis of spatial variability and temporal trends of rainfall in the Amhara region. Ethiopia J. Water Clim." Chang. 11 (4) https:// doi.org/10.2166/wcc.2019.084.
4. Ali, R., Kuriqi, A., Abubaker, S., Kisi, O., 2019. "Long-term trends and seasonality detection of the observed flow in Yangtze River Using Mann-Kendall and sen's innovative trend method." Water 11, 1855. https://doi.org/10.3390/w11091855.
5. Malik, A., Kumar, A., Guhathakurta, P., Kisi, O., 2019. "Spatial-temporal trend analysis of seasonal and annual rainfall (1966–2015) using innovative trend analysis method with significance test." Arab. J. Geosci. 12 (328), 1–23. https://doi.org/10.1007/s12517-019-4454-5.
6. Dave H.K. et al., "Study of Rainfall Variation Pattern in Hathmati Basin (2012)" ISSN 2250-1991, v1 pp 70-71.
7. Koudahe, K., Kayode, A.J., Samson, A.O., Adebola, A.A., Djaman, K., 2017. "Trend analysis in standardized precipitation index and standardized anomaly index in the context of climate change in southern togo." Atmos. Clim. Sci. 7, 401–423. https://doi.org/10.4236/acs.2017.74030.

8. Wang, Y., Xub, Y., Tabaric, H., Wang, J., Wang, Q., Song, S., Hu, Z., 2020. Innovative trend analysis of annual and seasonal rainfall in the Yangtze River Delta, eastern China. Atmos. Res. 231, 104673 https://doi.org/10.1016/j.atmosres.2019.104673.
9. Piras, M., Mascaro, G., Deidda, R., Vivoni, E.R., 2016. Science of the Total Environment Impacts of climate change on precipitation and discharge extremesthrough the use of statistical downscaling approaches in a Mediterranean basin. Sci. Total Environ. 543, 952–964,http://dx.doi.org/10.1016/j.scitotenv.2015.06.088.
10. Conway, D., Mould, C., Bewket, W., 2004. Over one century of rainfall and temperature observations in Addis Ababa. Ethiopia. Int J Climatol. 24, 77–91. https://doi. org/10.1002/joc.989.
11. Daniel, M., Woldeamlak, B., Lal, R., 2014. Recent spatiotemporal temperature and rainfall variability and trends over the upper Blue Nile River basin. Ethiopia. Int. J. Climatol. 34, 2278–2292. https://doi.org/10.1002/joc.3837.
12. De Luis, M., Raventos, J., Gonzalez-Hidalgo, C., Sanchez, J.R., Cortina, J., 2000. Spatial analysis of rainfall trends in the region of Valencia (east Spain). Int. J. Climatol. 20, 1451–1469. https://doi.org/10.1002/1097-0088(200010)20:123.0.CO;2-0.
13. Gummadi, S., Rao, K.P.C., Seid, J., Legesse, G., Kadiyala, M.D.M., Takele, R., Amede, T., Whitbread, A., 2017. Spatio-temporal variability and trends of precipitation and extreme rainfall events in Ethiopia in 1980–2010. Theor. Appl. Climatol. 2–15. https://doi.org/10.1007/s00704-017-2340-1.
14. Harka, A.E., Roba, N.T., Kassa, A.K., 2020. Modelling rainfall runoff for identification of suitable water harvesting sites in Dawe River watershed, Wabe Shebelle River basin, Ethiopia. J. Water Land Dev. (47), 186–195. https://doi.org/10.24425/jwld.2020.135313 (X–XII).
15. Sen, P.K., 1968. Estimates of the regression coefficient based on Kendall's tau. J. Comput. Graph. Stat. 63, 1379–1389. https://doi.org/10.1080/ 01621459.1968.10480934.

16. “SWAT Model Calibration and Uncertainty Analysis for Streamflow Prediction in the Kunwari River Basin, India, Using Sequential Uncertainty Fitting” by Boini Narsimlu & Ashvin K. Gosain & Baghu R. Chahar & Sudhir Kumar Singh & Prashant K. Srivastava. Environ. Process. (2015) 2:79–95. DOI 10.1007/s40710-015-0064-8
17. “Assessing impacts of different land use scenarios on water budget of Fuhe River, China using SWAT model” by Tao Can, Chen Xiaoling, Lu Jianzhong, Philip W. Gassman, Sauvage Sabine, Sanchez Pérez José-Miguel. Article in International Journal of Agricultural and Biological Engineering · July 2015. DOI: 10.3965/j.ijabe.20150803.1132.
18. “Assessing the Impact of Land-Use Land-Cover Change on Stream Water and Sediment Yields at a Watershed Level Using SWAT” by Wubishet Tadesse, Stephanie Whitaker, William Crosson, Constance Wilson. Open journal of Modern Hydrology, 2015. http://www.scirp.org/journal/ojmh.
19. “Use of the SWAT model for estimating reservoir volume in the Upper Navet watershed in Trinidad” by Sharlene L. Beharry, Donald Gabriels, Deyanira Lobo, Deanesh Ramsewak, Ricardo M. Clarke (2021).
20. Suman Bera and Ramkrishna Maiti (2021). “Assessment of Water Availability with SWAT Model: A Study on Ganga River.” DOI: 10.1007/s12594-021-1760-9
21. Biswajit Das, Sanjay Jain, Surjeet Singh, Praveen Thakur (2019). Evaluation of multisite performance of SWAT model in the Gomti River Basin, India. Applied Water Science (2019) 9:134. http://doi.org/10.1007/s13201-019-1013-x.
22. Nyemo A. Chilagane, Japhet J. Kashaigili, Edmund Mutayoba, Paul Lyimo, Pantaleo Munishi, Christine Tam, Neil Burgess (2021). “Impact of Land Use and Land Cover Changes on Surface Runoff and Sediment Yield in the Little Ruaha River Catchmen,” Open Journal of Modern Hydrology, 2021, 11, 54-74. http:// doi.org/10.4236/ojmh.2021.113004
23. Nagraj S. Patil, Rohan S. Gurav , Rohit Reddy R., Nataraja M. (2019). "Study on impact assessment of climate change on watershed using hydrological model (SWAT)," Journal

of Spatial Hydrology: Vol. 15: No. 1, Article 4. Available at: https://scholarsarchive.byu.edu/josh/vol15/iss1/4.

24. Vose, R. S., Easterling, D. R., & Gleason, B. (2005). Maximum and minimum temperature trends for the globe: An update through 2004. Geophysical Research Letters, 32(23). doi:10.1029/2005gl024379Neitsch G J., Arnold S. L, Kiniry J. R. and Williams, J. R. (2001). "Soil and Water Assessment Tool Theoretical Documentation." Version 2000.
25. Abbaspour K, Johnson C, van Genuchten MT (2004) Estimating uncertain flow and transport parameters using a sequential uncertainty fitting procedure. Vadose Zone J 3:1340–1352
26. Abbaspour K, Vejdani M, Haghighat S (2007) SWAT-CUP calibration and uncertainty programs for SWAT. In: MODSIM 2007 International Congress on Modelling and Simulation, Modelling and Simulation Society of Australia and New Zealand, 2007
27. Arnold J, Allen P (1996) Estimating hydrologic budgets for three Illinois watersheds. J Hydrol 176:57–7
28. Santhi C, Srinivasan R, Arnold JG, Williams J (2006) A modeling approach to evaluate the impacts of water quality management plans implemented in a watershed in Texas. Environ Model Softw 21:1141–1157
29. Beck M (1987) Water quality modeling: a review of the analysis of uncertainty. Water Resour Res 23:1393–1442
30. Bekele EG, Nicklow JW (2007) Multi-objective automatic calibration of SWAT using NSGA-II. J Hydrol 341: 165–176
31. Srivastava PK, Han D, Ramirez MR, Bray M, Islam T (2012) Selection of classification techniques for land use/ land cover change investigation. Adv Space Res 50:1250–1265
32. Strayer DL, Ewing HA, Bigelow S (2003) What kind of spatial and temporal details are required in models of heterogeneous systems? Oikos 102:654–662

APPENDIX-A

LIST OF FIGURES

APPENDIX-B

LIST OF TABLES

APPENDIX-C

LIST OF ABBREVIATION

MRB	Mayurakshi River Basin
GIS	Geographical Information System
Hr	Hour
Km	Kilometer
m	Meter
mm	Millimeter
CV	Coefficient of Variation
PCI	Precipitation Concentration Index
SAI	Standardized Anomaly Index
MK	Mann-Kendall test
SSE	Sen's Slope Estimator
ITA	Innovative Trend Analysis
TP	Theissen Polygon
IDW	Inverse distance weighted
FAO	Food and Agriculture Organization
SWAT	Soil and Water Assessment Tool
Arc SWAT	ArcGIS interface Soil and Water Assessment Tool
HRU	Hydrological Response Unit
ET	Evapotranspiration
PREC	Precipitation
SURQ	Surface Runoff